Hydrodynamic and Sediment Transport Modeling Study Hopedale Harbour, Labrador

Newfoundland and Labrador
Department of Environment and Conservation
P.O. Box 8700
St. John's, NL A1B 4J6

Prepared by:
Stantec Consulting Ltd.
300-675 Cochrane Drive West
Markham ON L3R 0B8

Final Report

File No. 121411777

July 10, 2014

Table of Contents

LIST OF APPENDICES

LIST OF TABLES

LIST OF FIGURES

1.0 INTRODUCTION

The Inuit Community of Hopedale is located on the Labrador coast, 148 air miles to the north of Goose Bay, Newfoundland and Labrador (Figure 1-1). Between 1957 and 1969, a military and radar site was operated in Hopedale, Labrador by the United States government. The Hopedale site was a station on the United States Air Force Pinetree Line and was the most easterly site on the Mid-Canada Line of antennae stations which extended across the country. The Hopedale site was also one of a series of sites which functioned as a Ballistic Missile Early Warning System (BMEWS).

The base was closed down in 1969 and the radome and radar antennae were removed. Portions of the remaining site were operated by Canadian Marconi as a telecommunications site until 1972 and by ITT as a telecommunications site until 1975. The complex was finally closed in 1975. Most of the remaining aboveground structures were demolished and buried in several locations around the site in the mid-1980s. At that time, limited clean-up efforts were carried out and included the removal and disposal of polychlorinated biphenyl (PCB) containing transformers. With the exception of infrastructure at the Mid-Canada Line site, only the foundations and floor slabs of buildings currently remain on the former U.S. military site.

During the operation of the former military base, access to the site was largely via the sea. Therefore, the wharf located south of the site, in Hopedale Harbour, was likely used to dock, load and unload at that time. Fuel was also transferred from boats to an aboveground pipeline located near the wharf. The wharf is currently in use and there are various structures near the wharf approach including the community garage, a gas station, and the Newfoundland and Labrador Hydro Diesel Generating Plant.

Stantec (2012) conducted a marine sampling program at Hopedale Harbour to address data gaps in the 2011 sampling program. Forty-six sediment samples and thirty-two fish samples were collected throughout Hopedale Harbour. PCBs were detected in marine sediment and fish samples as well as from selected sediment samples collected from freshwater ponds and streams at the site.

Historically, an unknown quantity of PCBs (presently estimated to be less than 10 kg) has entered Hopedale Harbour, either by direct deposit, or via the small stream that enters the harbour near the wharf.

Aivek-Stantec Limited Partnership (Stantec) was retained by the Newfoundland and Labrador Department of Environment and Conservation (NLDEC) to conduct hydrodynamic and sediment transport modeling in Hopedale Harbour to assess sediment transport conditions in the harbour. The results from the sediment transport modeling will be used to inform future decisions about the management of PCB contamination at Hopedale.

The objectives of the present study are to:

- Develop a hydrodynamic and sediment transport model for Hopedale Harbour;
- Calibrate the hydrodynamic model using the field data collected from August 29 to September 2, 2012 in the project area;
- Study the sediment transport conditions in Hopedale Harbour using tidal and wind conditions;
- Identify conditions with the greatest potential to initiate sediment transport within Hopedale Harbour; and,
- Provide an estimate of the annual sediment transport out of Hopedale Harbour.

Figure 1-1 Site Location

2.0 SITE DESCRIPTION

The project area is Hopedale Harbour. The general configuration of the harbour is shown in Figure 2-1. Hopedale has a humid subarctic continental climate with cool summers and cold winters. Average daily temperatures range from -16.4 °C in January to 10.6 °C in August. The tides in the harbour are semi-diurnal. Neap tides are as low as 0.5 m and spring tides are up to 2.4 m. The harbour is protected from wave action by a number of islands including Ellen Island, Anniowaktook Island, Zacharias Island and Cross Island.

A field program was conducted in Hopedale Harbour in support of the hydrodynamic and sediment transport modeling study. NATECH, under contract to Stantec, conducted a field measurement program during a period of spring tides (2 m amplitude), between August 29 and September 2, 2012. The main components of the field program were:

- Record water level variations during the study;
- Survey the bathymetry of the Harbour, focusing on the Inner Harbour and the sill that separates the Inner Harbour basin from the deep waters of the Hopedale Run entering from the Labrador Sea;
- Measure current speeds and directions during different phases of the tide, and at different depths;
- Determine how the summer water column structure (temperature, salinity, density) varies throughout the area on both sides of the dividing sill and how the stratification responds to tidal water level changes; and
- Take sediment samples for analysis of PCB concentrations and grain-size distribution.

The field program and results are reported in the *Presentation of Field Test Results Hopedale Harbour, NL, September 2012* (NATECH, 2013). The relevant information is included herein.

2.1 Bathymetry

A Hopedale Harbour bathymetry survey was conducted using two echo sounders equipped with GPS and mounted on boats. The depth readings obtained were corrected for the tidal water level variation observed on the recording gauge. Figure 2-1 shows the bathymetry of the harbor and is relative to the gauge at the wharf. Two main basins are evident in the Inner Harbour, separated by a sill of variable depth (13 – 15 m). The innermost basin (B1) has an oval flat seabed with a maximum depth of approximately 16 m. B1 is surrounded on the west side by a comparatively steep shore. The slightly larger seaward basin (B2) is roughly circular in shape and has a maximum depth of 20 m. B2 is surrounded for the most part by more gradual bottom slopes. On the south-west side, the coastal slopes are less steep than around B1. Contours on the north side of B2 imply the presence of a rocky outcrop. B2 is separated by a broad sill from the outer deeper coastal waters. A definable channel is visible across the sill with water depths of around 7 m to 9 m at low tide. A sharp drop-off from this channel into B2 may be indicative of a rocky outcrop. A third basin (B3) is located south of B1 and B2. A high sill, partially exposed at low tide, separates B3 from B1.

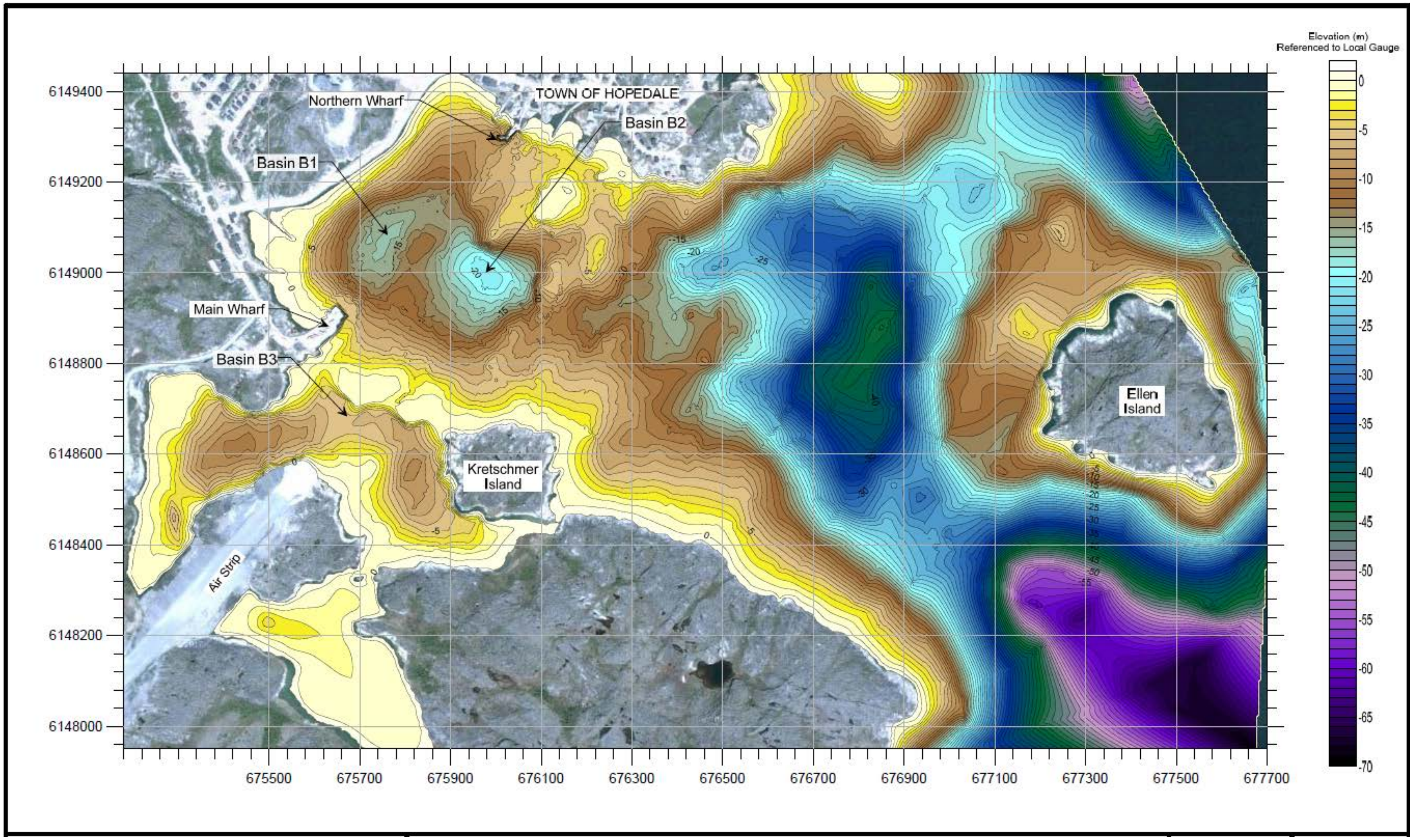

Figure 2-1 Hopedale Harbour Bathymetry

2.2 Wind

Monthly wind conditions at Hopedale are presented in Table 2.1 based on Hopedale Airport Environment Canada climate station data. Monthly mean wind speeds range from 17 km/h in May, June and July to 25 km/h in December. Winds are predominantly from the north from April to August, from the west from September to November, and from the southwest during winter months.

Table 2.1 Wind Conditions at Hopedale Harbour[1]

Month	Mean Wind Speed (km/h)	Most Frequent Direction
January	23	SW
February	22	SW
March	23	NW
April	20	N
May	17	N
June	17	N
July	17	N
August	18	N
September	20	W
October	22	W
November	24	W
December	25	SW

Note:
[1]Based on data from 1961 to 1990

2.3 Water Level

The nautical chart for the Hopedale area (#5047) from the Canadian Hydrographic Services (CHS) states that "the depths (shown on the chart) are reduced to Chart Datum (Lowest Normal Tide) which at Hopedale is at 1.2 m below the mean water level". Table 2.2 provides statistical water level information from the nautical chart for the Hopedale area. The CHS chart indicated tidal ranges for normal and large tides to be 1.5 m and 2.3 m respectively. Tidal ranges during the bathymetry survey varied from 1.9 m to 2.1 m. The water level variations measured in Hopedale Harbour from August 29 to September 1, 2012 are presented in Figure 2-2. The measured water levels were checked regularly using readings taken at the local gauge located on the northern wharf in the Harbour in front of the Amaguk Inn. The average of the measurements over the four day period was 0.84 m above the "0" of the local gauge. In comparison, the average of high and low levels predicted by CHS for the same period was 1.18 m. The average of all of the high and low water levels predicted by CHS for the year 2012 was also 1.18 m. Based on this observation, it is reasonable to assume that the 0.0 m level on the wharf gauge is 0.34 m above the chart datum. Table 2.3 compares the CHS predictions and the field measurements.

Table 2.2 Water Levels in Hopedale Harbour, NL

Tide	Large (Spring) Tide		Mean Tide	
Water Level	**Highest High Water**	**Lowest Low Water**	**High Water**	**Low Water**
Height[1] (m)	2.4	0.1	2.0	0.5

Note:
[1] Above chart datum

Table 2.3 Measured Water Level and CHS Predicted Water Level

Parameter	CHS Predictions (m)		Field Measurements (m)	Difference between CHS and Field Measurements (m)
Period	Year 2012	August 29 to September 2, 2012	August 29 to September 2, 2012	August 29 to September 2, 2012
Reference	CD	CD	Gauge at wharf	-
Minimum	-0.10	0.20	-0.23	0.43
Maximum	2.60	2.20	1.89	0.31
Average	1.18	1.18	0.84	0.34

Note:
CD = chart datum

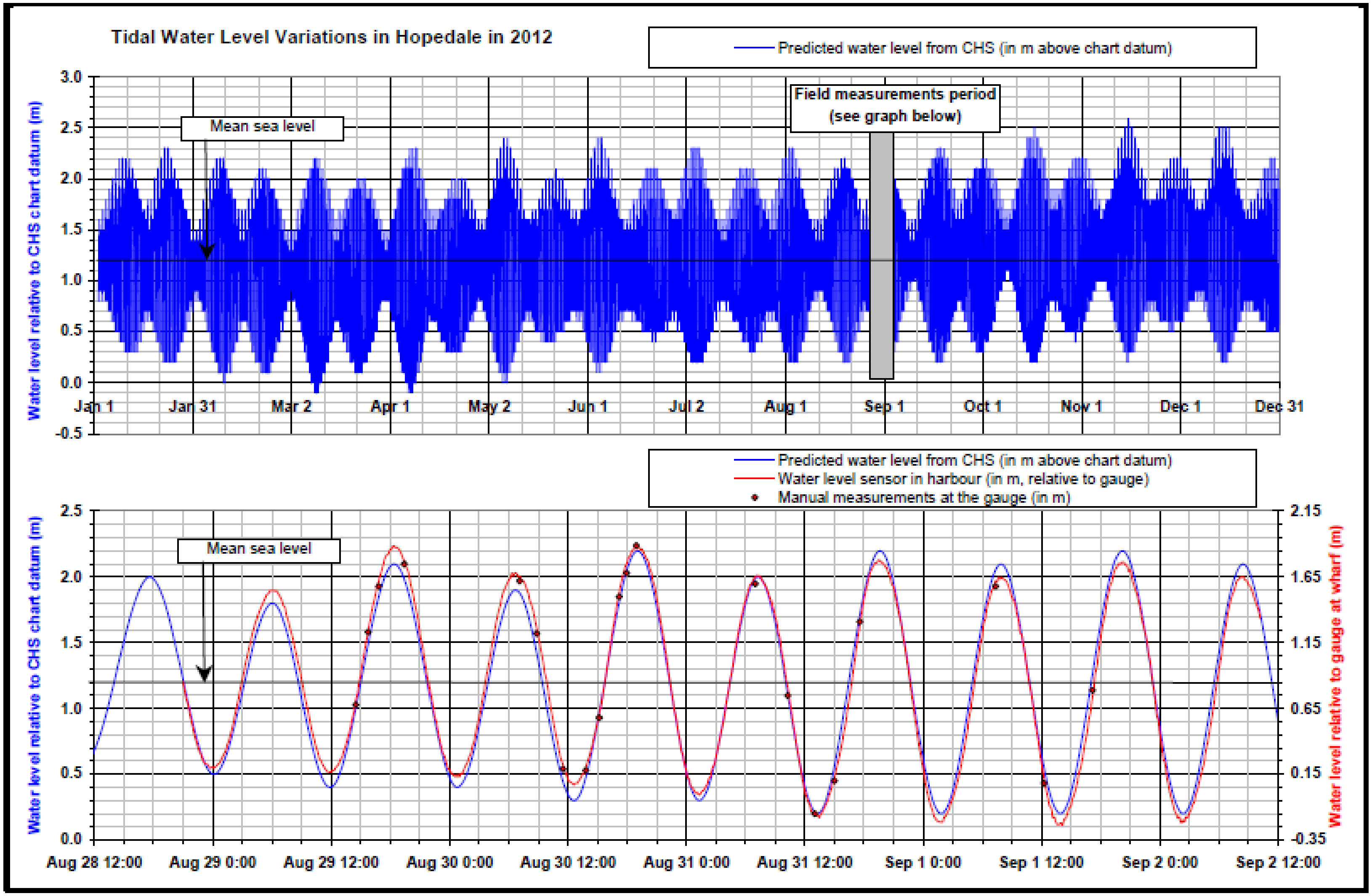

Figure 2-2 Water Level in Hopedale from August 29 to September 1, 2012

2.4 Current

2.4.1 ADCP Current Measurements

An Acoustic Doppler Current Profiler (ADCP) was used to measure currents in Hopedale Harbour between August 29 and September 2, 2012. The figures in Appendix A summarize the currents measured at the surface, at 5 m depth, and at the bottom, as well as cross-sections of the water column at key locations. The ADCP measurements show that during flood tide, incoming tidal waters flow into the Harbour from the north (Figure A5a, Appendix A). The major portion of this coastal tidal flow bypasses the mouth of the Harbour and continues south. Stronger currents are observed outside the inner harbour. The current direction within the harbor is highly variable, likely due to the smaller area, lower speeds, rugged shoreline and uneven bathymetry. During ebb tide, water from the Harbour drains toward the north-east, and merges with a current coming from the south, as shown in Figure A2a. Stronger bottom currents were observed in the inner harbour around low tide with the initiation of the flood tide, but no consistent direction could be observed (Figure A3a, Appendix A). Stronger currents were also observed around the inshore edge of Ellen Island, particularly during low tide (Figures A2a to A4a in Appendix A).

2.4.2 Drogues Current Measurements

Drogues were released several times per day from August 30 to September 1, 2012, with the underwater sails located at either 2 m or 5 m depth. The paths followed by the drogues are shown in Figures B-1 to B-4 in Appendix B. The drogues show low velocities in the inner harbour with no easily discernable pattern, largely similar to the ADCP records. During flood tide, the measurements suggest that the tide flows landward toward the west-north-west or north-west. During the falling tide, the currents in the inner harbour flowed toward the south-east or south. The current velocities were in the range of 2 cm/s to 4 cm/s in the inner harbour, and between 6 cm/s and 8 cm/s over the sill between the inner and the outer harbour. Velocities over 30 cm/s were observed in the large channel between the harbour and Ellen Island during flood tide. Currents at 2 m and 5 m depths were both observed to flow in the same general direction throughout the area, except at the end of the rising tide when the current at 5 m depth in the Harbour turned toward the south (Figure B-4).

2.4.3 Tilt Meter Measurements

Three current meters (tilt meters) were installed at the bottom of Hopedale Harbour. The meters are approximately 40 cm long, and therefore recorded the average current velocity for the first 0.4 m of the water column. Table 2.4 provides the current meter location details, average velocity and main current directions. The meter on the main sill and the meter further to the north-east were left in place for four days. Figure 2-3 shows the location of the tilt meters. Figure C-2 in Appendix C displays current roses and Figures C-3 to C-6 in Appendix C detail measured current velocities and directions over time. To the west of the inner harbour (tilt meter locations TM1 and TM2), the average velocity was 1.3 cm/s and the current flowed mainly toward the east or the west depending on the tidal stage. On the main sill (location TM3) the bottom current was faster, around 5.1 cm/s, and the predominant current directions were toward the north-west and the north-east. Further out (location TM4), the average velocity was 4.3 cm/s, and predominant flow directions were toward the east-north-east and south-south-west. Overall, it was found that the currents are slow in Basin B1, and are likely even slower in the deepest part of the basin. Faster currents occur over the sill between the inner and the outer harbour.

Table 2.4 Current Meter Details

Current Meter ID	Location		Depth at Meter Location (m)	Average Velocity (cm/s)	Main Current Directions
	Easting (m)	Northing (m)			
TM1	675,670	6,148,987	-12	1.3	E,W
TM2	675,781	6,148,880	-9	1.4	ESE
TM3	676,122	6,148,847	-9	5.1	NW, NE
TM4	676,495	6,149,027	-25	4.3	ENE, SSW

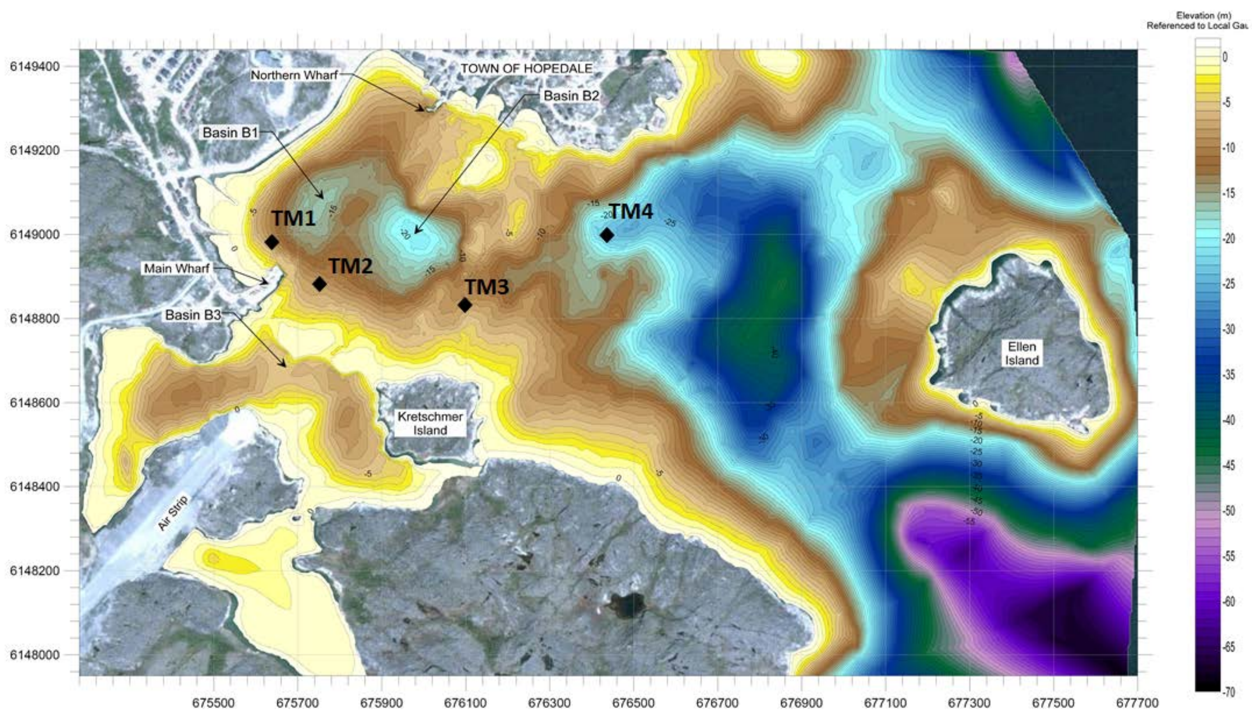

Figure 2-3 Tilt Meter Locations

2.5 Sediment

Sediment samples were collected in Hopedale Harbour in 2013 to characterize the sea bed sediment conditions. The grab sample locations are shown in Figure 2-4. Sediment composition and sediment particle sizes at the sampling locations are presented Tables 2.5 and 2.6, respectively. The harbour sediments are primarily composed of sand, silt and clay, except at two locations (13-SED3 and 13-SED14) where a higher portion of gravel is also present. Sample 13-SED3 was located near the east wharf area within the inner harbour and 13-SED14 was located outside the outer harbour as shown in Figure 2-4. The median sediment size (i.e., d50) ranges from 0.012 mm at 13-SED2 to 0.216 mm at 13-SED14.

Table 2.5 Sediment Composition at Sampling Locations

Sample ID	Gravel (%)	Sand (%)	Silt (%)	Clay (%)
13-SED1	1.1	21.0	41.5	36.4
13-SED2	1.0	21.3	40.4	37.4
13-SED3	38.6	31.1	13.6	16.7
13-SED4	0.3	58.7	21.6	19.4
13-SED5	1.3	64.8	16.6	17.4
13-SED6	17.5	56.7	12.3	13.5
13-SED7	3.4	20.1	41.5	35.0
13-SED8	8.8	71.1	8.7	11.4
13-SED11	0.0	86.6	6.9	6.5
13-SED14	27.4	48.0	8.9	15.6

Table 2.6 Sediment Locations and Particle Sizes

Sample ID	Sediment Particle Size		
	d_{90} (mm)	d_{50} (mm)	d_{10} (mm)
13-SED1	0.160	0.0145	< 0.002
13-SED2	0.139	0.0121	< 0.002
13-SED3	3.3	0.214	<0.002
13-SED4	0.224	0.076	<0.002
13-SED5	0.410	0.110	<0.002
13-SED6	2.7	0.157	<0.002
13-SED7	0.300	0.0143	<0.002
13-SED8	1.06	0.132	<0.002
13-SED11	0.248	0.107	0.034
13-SED14	3.1	0.216	0.002

Stantec conducted water sampling to characterize sediment transport over the sill that separates the inner harbour from the outer harbour. Water samples were collected at various depth intervals at three (3) locations above the sill (labelled Sill 1, Sill 2 and Sill 3). Sampling locations are shown in Figure 2-4. The sampling periods were as follows:

- September 23, 2013
  - Rising tide: 07h20 to 08h10
  - Falling tide: 13h00 to 13h30
- September 26, 2013
  - Rising tide: 09h15 to 10h00
  - Falling tide: 15h05 to 15h35

Details of the sampling program and results are reported in the *Freshwater and Marine Sampling in Support of the Marine Study – Years 2 and 3, Former U.S. Military Site, Hopedale, NL* report (Stantec 2014).

The concentration of total suspended solids (TSS) in water samples collected during the rising tide ranged from 1 to 13 mg/L. The concentrations of TSS in water samples collected during falling tide ranged from non-detect to 13 mg/L.

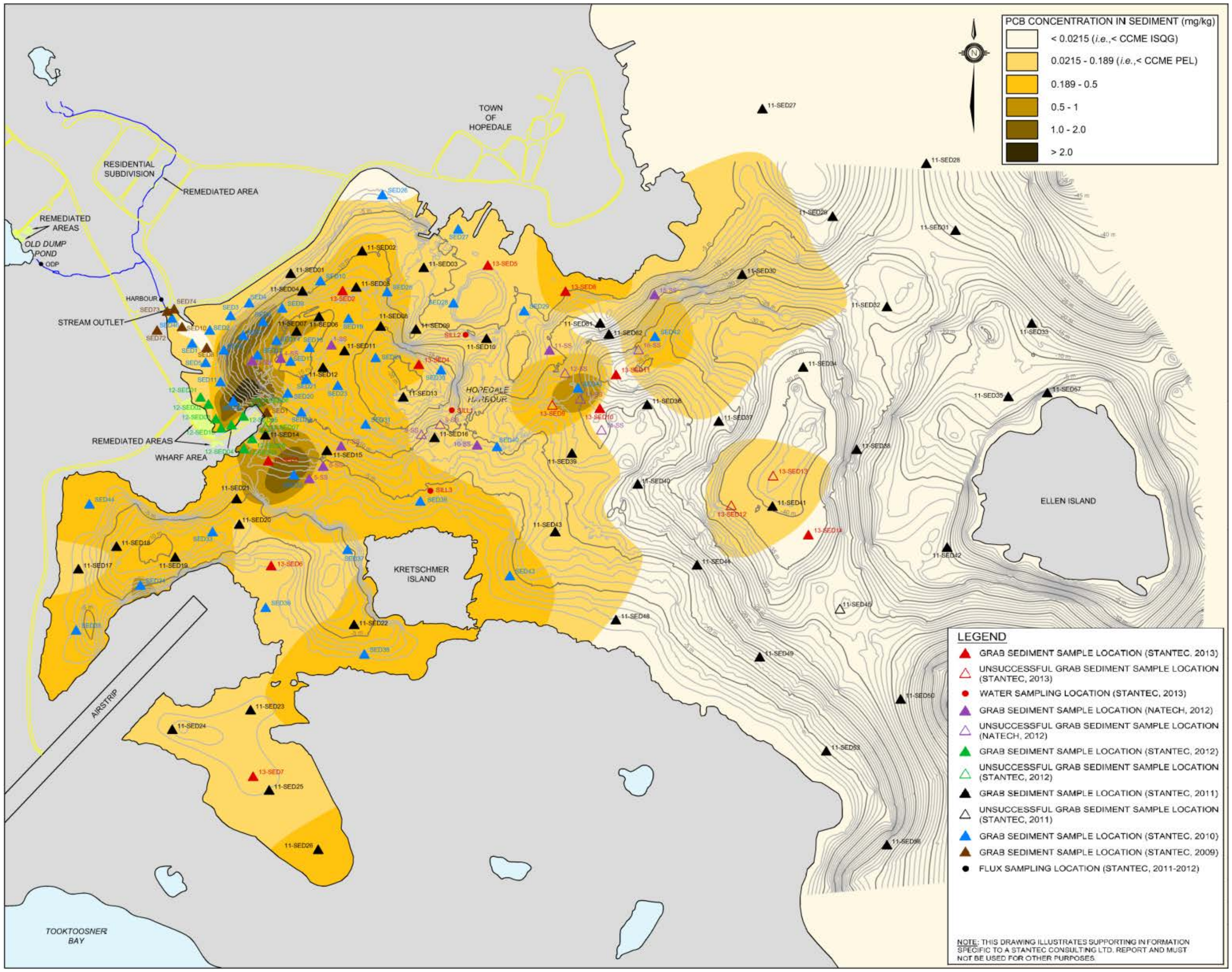

Figure 2-4 Sediment Sampling Locations

3.0 HYDRODYNAMIC AND SEDIMENT TRANSPORT MODELING

Hydrodynamic and sediment transport modeling was conducted using GEMSS® (Generalized Environmental Modeling System for Surface Waters) in order to study the movement of sediment in Hopedale Harbour. This section describes the GEMSS model, model set-up and model calibration using field data.

3.1 Model Description

A GEMSS® (Generalized Environmental Modeling System for Surfacewaters) model was used to predict the hydrodynamic and sediment transport conditions in Hopedale Harbour. GEMSS is an integrated system of 3-D hydrodynamic and transport models embedded in a geographic information and environmental data system (GIS) and includes a set of pre- and post-processing tools to support 3-D modeling. The GEMSS software uses GLLVHT (Generalized, Longitudinal-Lateral-Vertical Hydrodynamic and Transport) as the main kernel. GLLVHT is a three-dimensional numerical model that computes time-varying velocities, water surface elevations, and water quality constituent concentrations in rivers, lakes, reservoirs, estuaries, and coastal water bodies. The computations are done on a horizontal and vertical grid that represents the water body bounded by its water surface, shoreline, and bottom. The water surface elevations are computed simultaneously with the velocity components. The water quality constituent concentrations are computed from the velocity components and elevations. Included in the computations are boundary condition formulations for friction, wind shear, turbulence, inflow, outflow, surface heat exchange, and water quality kinetics. The model can be used to analyze system dynamics and predicts the effects of actual events or possible design or management alternatives. The theoretical basis of the three-dimensional GLLVHT model was first presented in Edinger and Buchak (1980) and subsequently in Edinger and Buchak (1985). GEMSS Hydrodynamic Module (HDM) and Sediment Transport Module (STM) were used in this study.

3.1.1 Hydrodynamic Module - HDM

The hydrodynamic and transport relationships used in GEMSS are developed from the horizontal momentum balance, continuity, constituent transport and the equation of state. These relationships have six unknowns (U, V, W – velocities in x, y and z directions, respectively, z' – water surface elevation, ρ – density, C_n – constituent n) in six equations with the momentum and constituent dispersion coefficients (A_x, A_y, A_z, D_x, D_y, D_z) evaluated from velocities and the density structure.

In the x and y momentum balances, the forcing terms are the barotropic or water surface slope, the baroclinic or density gravity slope, the Coriolis acceleration, the advection of momentum in each of the three coordinate directions, the dispersion of momentum in each of the coordinate directions and the specific momentum as would apply to a high velocity discharge. The baroclinic and barotropic slopes are arrived at from the hydrostatic approximation to vertical momentum and horizontal differentiation of the density-pressure integral by Leibnitz' rule. The baroclinic slope is seen to be the vertical integral of the horizontal density gradient and becomes the major driving force for density-induced flows due to discharge buoyancy.

The hydrodynamic equations use a semi-implicit integration procedure that has the advantage that computational stability is not limited by the Courant condition that $\Delta x/\Delta t$, $\Delta y/\Delta t<(gh_m)^{1/2}$ where h_m is the maximum water depth, which can lead to inefficiently small time steps of integration. Since the solutions are semi-implicit the stability is controlled by the Torrence condition ($U\Delta t/\Delta x$, $V\Delta t/\Delta y < 1$; Δx and Δy are grid sizes in x and y directions, respectively). Hence, the integration time step can be chosen to realistically represent the details of the boundary data, which are about 15 minutes for tides and up to one hour for meteorological data.

The vertical momentum dispersion coefficient and vertical shear is evaluated from a Von Karman relationship modified by the local Richardson number, Ri, which is defined as the ratio of vertical buoyant acceleration to vertical momentum transfer. The longitudinal and lateral dispersion coefficients are scaled to the dimensions of the grid cell using the dispersion relationships developed by Okubo (1971) and modified to include the velocity gradients of the velocity field using Smagorinsky relationship. The wind stress and bottom shear stress are computed using quadric relationships with appropriate friction coefficients.

A rectilinear (quasi-curvilinear) grid for mapping to different detail in different parts of a waterbody is used in GEMSS. Horizontal grid dimensions changing with depth are also used. The model domain is a space staggered finite difference grid with elevations and constituent concentrations computed at cell centers and velocities through cell interfaces. This scheme facilitates implementation of a control volume approach resulting in perfect water balance. A Z-level method is used for gridding in the vertical direction. Z-level allows the use of variable layer thicknesses in the vertical direction and facilitates implementation of the layer cell add and subtract algorithm for modeling tidal flats. It also allows the use of thick layers in deeper water.

Discharges and Intakes (e.g. river inflows, outfalls, marine disposals, thermal intakes and discharges etc.) are introduced as sources/sinks to the continuity and transport equations.

3.1.2 Sediment Transport Module - STM

The sediment Transport Module (STM) accounts for the movement of sediments in suspended and bed load form. The exchange of sediment between the two media is computed based on the local hydrodynamic conditions and bed properties. These exchanges take place in the form of differential settling and bed erosion. While the settling of particles depends on the fluid and sediment particle properties, bed erosion is quantified based on the bed/sediment properties and near bed hydrodynamic conditions. Figure 3-1 shows a schematic of these processes. These processes are parameterized based on the sediment characteristics, most importantly the cohesive/non-cohesive nature.

The suspended sediments are modeled under the assumption that they are essentially advected by the local velocities along with experiencing diffusive transport. The suspended sediment concentrations in the water column are solved using a mass balance equation. The source for sediments in the suspended column is the sediment erosion from bed, and the bed sediments are also a sink for the settling of the suspended sediments. Sediments, under the influence of lifting shear stress from moving water, can also move along the bed in the form of bed load. The accumulation and movement of sediments on the bed changes the elevation of the sediment bed. The bed load is calculated based on Van Rijn's (1984a) formulation and is given by:

$$Q_b = 0.053\, \rho_s\, [(S_s - 1) g D_s^3]^{0.4}\, \upsilon^{0.2}\, T_s^{2.1}$$

Where: ρ_s = sediment density

g = gravitational acceleration

v = kinematic viscosity of water

S_s = specific density of sediment

D_s = sediment particle size

T_s = transport stage parameter given by the following equation

$$T_s = \frac{u_*^2 - u_c^2}{u_c^2}$$

Where: u_* = shear velocity at the sediment-water interface

u_c = critical shear velocity for erosion

Settling

Sediment exchange between the suspended column and sediment bed takes place in the form of settling and erosion. The particle size influences the dominance of these two exchange processes to a great extent. While settling is dominant for large particle sizes, erosion is dominant for smaller size particles. For medium size particles these two processes remain in balance depending on the near bed velocity conditions.

Settling of non-cohesive particles is a function of the particle size and the fluid viscosity exerting surface drag against its movement under the influences of gravitational force. Cohesive particles in the suspended column tend to aggregate, thus affecting settling velocity. This aggregation is a function of the concentration in the suspended column and the shear stress effects due to the ambient flow.

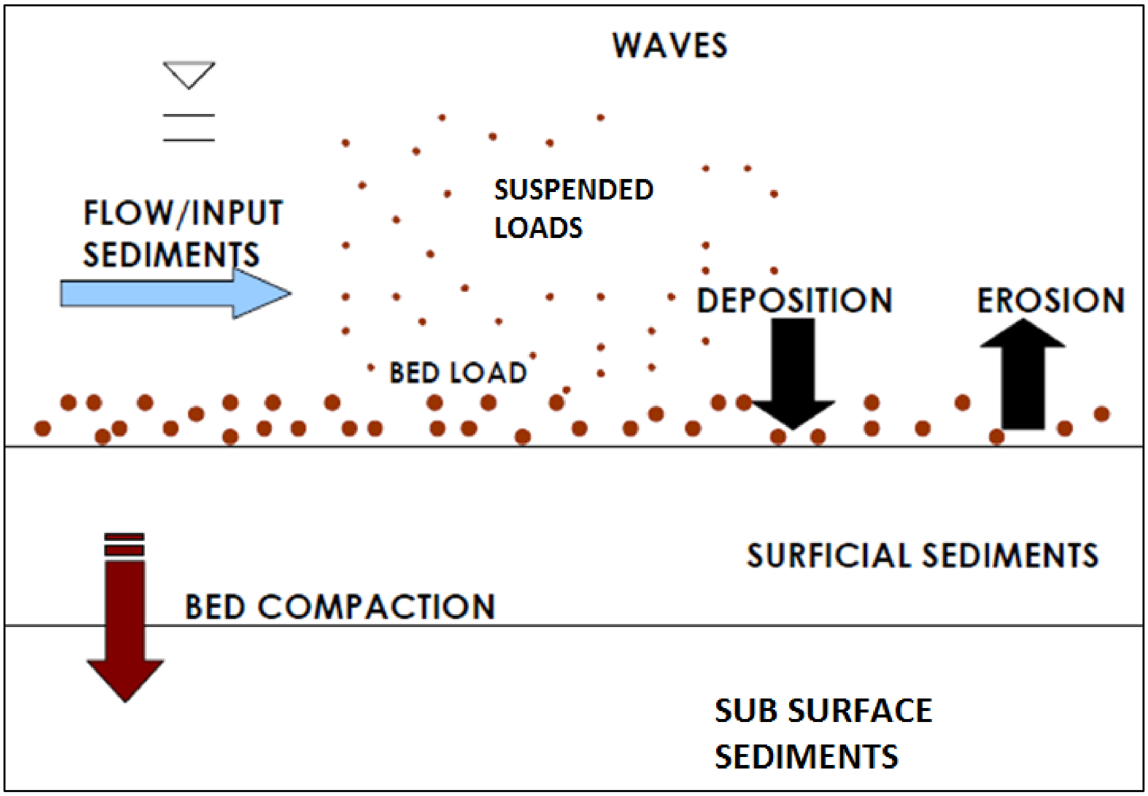

Figure 3-1 Sediment Transport Process in GEMSS-STM

Erosion

The non-cohesive sediment particles that settle from the suspended water column accumulate on the bed. Under the influence of moving water and its shear exerted on these bed sediments the particles experience uplifting force which, if greater than critical shear stress for erosion, move the particles back into the suspended water column. This movement of sediments back into the water column is called erosion. GEMSS-STM quantifies the sediment erosion based on the formulation of Van Rijn (1984 b).

Cohesive bed erosion occurs in two distinct modes, mass erosion and surface erosion. Mass erosion occurs rapidly when the bed stress exerted by the flow exceeds the shear strength of the bed. Surface erosion on the other hand occurs gradually when the flow-exerted bed stress is less than bed shear strength but greater than a critical erosion or resuspension stress, which is dependent on the shear strength and density of the bed. Typically under an accelerating flow resulting in an increase of bed stress first a gradual surface erosion starts to take place and is then followed by mass erosion. If the bed is well consolidated then only surface erosion will take place.

3.2 Model Set-Up

The hydrodynamic and sediment transport model set up involves discretizing the water body into computational grids, and specifying model parameters and boundary conditions that determine the hydrodynamic and sediment transport conditions in the water body.

3.2.1 Computational Grid

Hopedale Harbour shoreline and bathymetry data were used to develop the 3-D model grid for Hopedale Harbour using the automated grid generation module of GEMSS. The shoreline data for Hopedale Harbour was obtained by digitizing the Canadian Hydrographic Chart for Hopedale. Bathymetry data for Hopedale Harbour was obtained from the Canadian Hydrographic Chart and the field data collected during the field program in September 2012.

The model grid was constructed in a horizontal curvilinear and vertically variable z-level coordinate system and contains 2,304 cells at the maximum tidal elevation level in a horizontal plane. The model grid for GEMSS was configured as shown in Figure 3-2. The cell density of the computational grid generally increases in the vicinity of any abrupt changes in the bed geometry. The final computational grid configuration was derived after an iterative process of refining the cell density to ensure proper convergence of the numerical solution over the full ranges of water levels and wind speeds.

The grid cell size varies from 21.8 m to 115.5 m in the x direction and from 28.4 m to 53.0 m in the y direction. A total of 47 z-level layers were specified in the vertical direction. The vertical layer thickness ranges from 1 to 2 m.

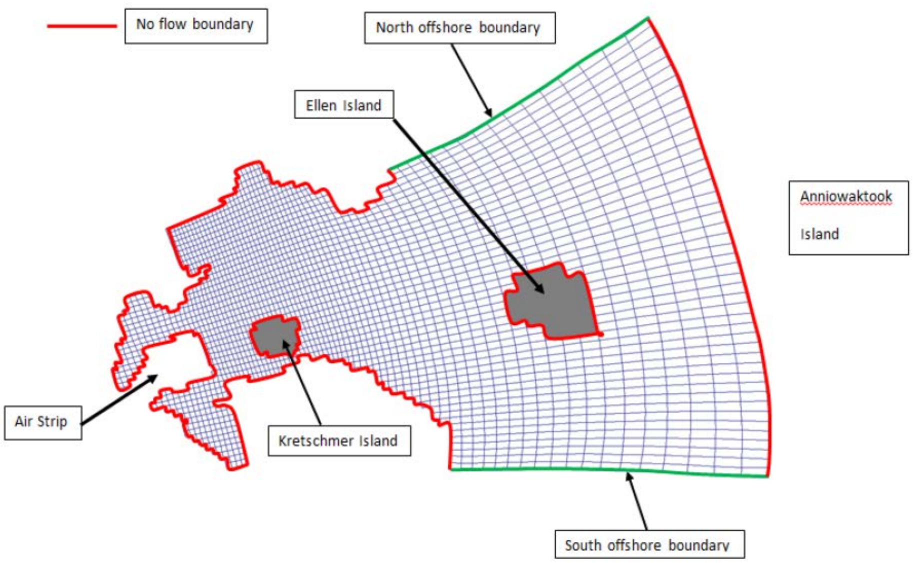

Figure 3-2 Computational Grid

3.2.2 Boundary Conditions

The following boundary conditions were specified for the GEMSS hydrodynamic module (HDM):

- A water level boundary condition was employed for the offshore boundaries. Tidal elevations from the Web Tide Tidal Prediction Model developed by the Ocean Science Division, Bedford Institute of Oceanography, Fisheries and Oceans Canada were used for the offshore boundaries.
- Wind speed and directions were specified at the water surface. Hourly wind speed and direction data from the Hopedale Airport climate station was used.
- A no-flow boundary condition that allows for lateral slip was employed for the coastline and island boundaries.

These boundary conditions are shown in Figure 3-2. Tidal elevations were specified in north and south offshore boundaries.

Wind-generated short waves will dominate the wave conditions in the study area. Swells (usually long waves) generated by distant storms will not reach the study area as it is protected by several islands located east of the study area. Short wave generated bottom currents are negligible in the sea bottom, except the nearshore area. Therefore, waves and breaking waves will affect the nearshore sediment transport conditions and most of the sediment moved by the waves will stay within the harbour area. Tidal currents will primarily determine the sediment transport in and out of the study area. Wave conditions in the harbour were not considered in the modeling study because they are expected to have minimal impact on sediment transport.

3.2.3 Model Parameters

Assigning model parameter values is a critical step in the modeling process. This section describes the considerations and process for estimating the various model parameters of GEMSS-HDM and GEMSS-STM.

3.2.3.1 Bottom Roughness Coefficient

The sea bed roughness affects the magnitude of simulated current speeds, particularly near the bottom. Chezy's friction coefficient (C) was used to specify the sea bottom roughness and was estimated using the following relationship:

$$C = 18 \log\left(\frac{12h}{r}\right)$$

$$r = 2.5\, d_{50}$$

Where C = Chezy's coefficient ($m^{1/2}/s$)

h = water depth (m)

r = roughness (m)

d_{50} = sediment size (m)

The Chezy's coefficient was estimated based on sediment particle sizes collected within Hopedale Harbour as discussed in Section 2.1.5. The estimated Chezy's coefficients range from 90 to 130 depending on sediment sizes and water depths as presented in Table 3.1. During model calibration it was found that the Chezy's coefficient is not a sensitive parameter within the range of 90 to 130. Therefore an average Chezy's coefficient of 100 was applied throughout the computational domain.

Table 3.1 Chezy's Coefficient for Hopedale Harbour

Location	Sediment Size, d50 (mm)	Roughness, r (mm)	Water Depth, h (m)					
			5	10	15	25	50	100
			Chezy's Coefficient					
13-SED1	0.0145	0.0363	112	117	121	125	130	135
13-SED2	0.0121	0.0303	113	119	122	126	131	137
13-SED3	0.214	0.5350	91	96	99	103	109	114
13-SED4	0.076	0.1900	99	104	108	112	117	122
13-SED5	0.110	0.2750	96	102	105	109	114	120
13-SED6	0.157	0.3175	95	100	104	108	113	118
13-SED7	0.0143	0.3925	93	99	102	106	111	117
13-SED8	0.132	0.0358	112	117	121	125	130	135
13-SED11	0.107	0.3300	95	100	103	107	113	118
13-SED14	0.216	0.2675	96	102	105	109	114	120

3.2.3.2 Dispersion Coefficient

The longitudinal and lateral dispersion coefficients are scaled to the dimensions of the grid cell using the dispersion relationships developed by Okubo (1971) and is given by:

$$D_i = 5.84 \times 10^{-4} \, (L_i)^{1.1}$$

Where D_i is the longitudinal or lateral dispersion coefficient in square meters per second and L_i is the longitudinal or lateral cell dimensions.

3.2.3.3 Wind Stress

Wind stress at the water surface was estimated using the following equation:

$$\tau_w = \rho_a C_D U_{10}^2$$

Where ρ_a is air density, C_D is surface drag coefficient and U_{10} is the wind velocity at 10 m. The wind velocities and directions at 10 m from Hopedale Airport Environment Canada climate station were used. The surface drag coefficient C_D was estimated using the Wu (1983) method as follows:

$$C_D = (0.8 + 0.065\, U^{10})\, 10^{-3}$$

3.2.3.4 Bottom Sediment Conditions

Ten sediment samples were collected in Hopedale Harbour and particle size analysis was conducted in the laboratory as discussed in Section 2.5. Based on the sea bottom sediment composition, the Hopedale Harbour area was divided into four classes as shown in Figure 3-3. Table 3.2 provides sediment composition details for each bottom class. The sediment in each region was modeled as a homogeneous mixture of clay, silt, sand and gravel with the composition as presented in Table 3.2.

The sediment thickness determines the sediment available for erosion in the study area. No data is available on sediment thickness in the study area. However, five (5) sediment core samples were collected at sediment depths ranged from 14 to 29 cm within the Inner Harbour (Basins 1 and 2, Figure 2-1). The core sediment samples were not terminated on rock. The cores were driven as deep as possible by a diver (by hand) and represent minimum sediment thickness in these areas. A uniform sediment thickness of 0.5 m was assumed for the model.

If the sea bottom has hard surfaces (e.g. rocky surfaces) in the Inner Harbour area, then the actual sediment load leaving the harbour area would be less than the predicted sediment load, depending on the percentage of hard surface in the Inner Harbour area and bottom currents. However, grab sediment sampling indicates that most of the study area is covered with sediments. It is expected that the selection of a modeled sediment thickness greater than 0.5 m would not affect the predicted annual sediment loading leaving the harbour. However, the sediment thickness will determine the long term sediment loads leaving the harbour.

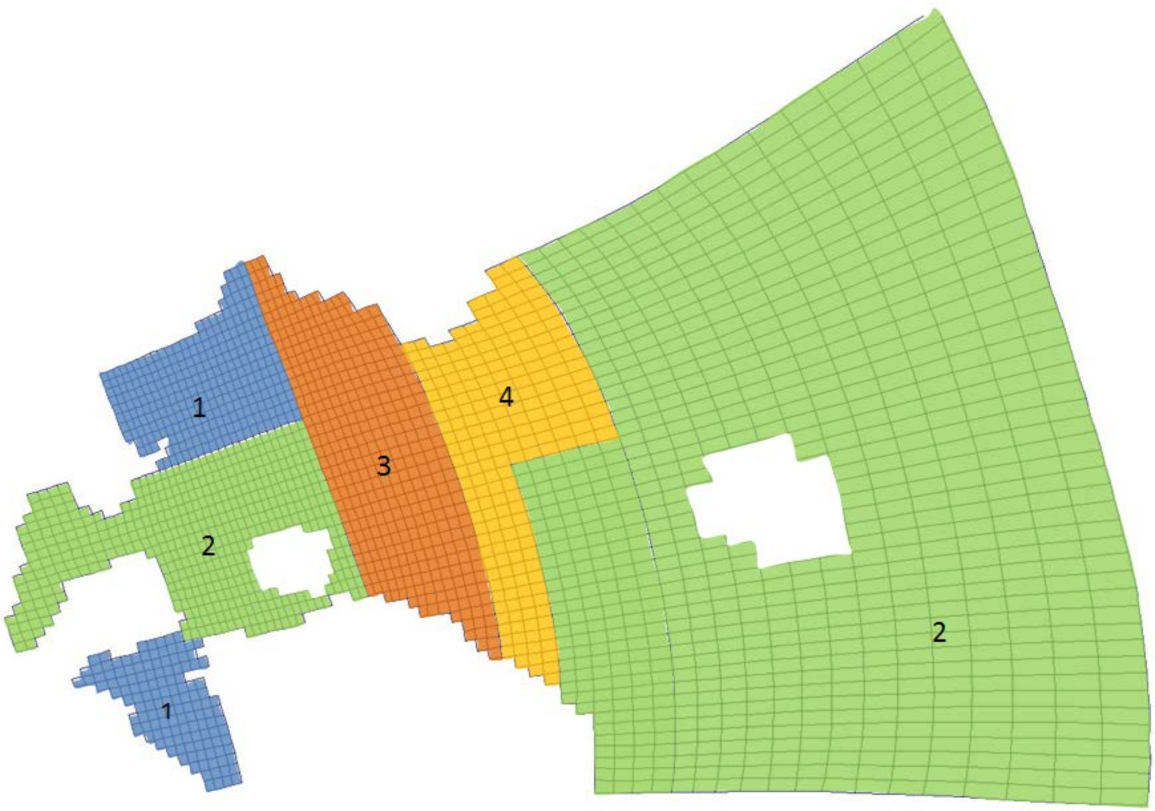

Figure 3-3 Sea Bottom Sediment Conditions

Table 3.2 Sediment Composition for Each Region

Bottom Class	% Sediment Composition			
	Clay	Silt	Sand	Gravel
1	37	41	21	1
2	15	12	45	28
3	18	19	62	1
4	9	8	79	4

3.2.3.5 Particle Settling Velocity

Settling velocity or fall velocity of a particle is defined as the terminal velocity when the particle is settling in an extended fluid under the action of gravity. The settling velocity of a particle in a fluid is governed by a number of factors including fluid viscosity (v), density (ρ), specific weight of the sediment, sediment type, salinity, turbulence, and other chemical and physical conditions.

Settling velocity (w_s) was estimated using the following formula recommended by Van Rijn (1984b). The formula is dependent on particle diameter (d).

$$\frac{w_s}{\sqrt{g'd}} = \begin{cases} \frac{R_d}{18} \quad for\ d \leq 100\mu m \\ \frac{10}{R_d}\left(\sqrt{1+0.01R_d^2}-1\right) \quad for\ 100\mu m < d \leq 1000\mu m \\ 1.1 \quad for\ d > 1000\mu m \end{cases}$$

Where:

$g' = g\left(\frac{\rho_s}{\rho_w} - 1\right)$ is the reduced gravitational acceleration

$R_d = \frac{d\sqrt{g'd}}{\nu}$ is the sediment grain densimetric Reynolds number

ν = viscosity

3.2.3.6 Critical Shear Stress/Velocity for Erosion and Deposition

Noncohesive sediment is transported as bed load and suspended load. The initiation of both modes of transport begins with erosion or resuspension of sediment from the bed when the bed stress, τ_b, exceeds a critical stress referred to as the Shield's stress, τ_{cs}. The Shield's stress depends on the density and diameter of the sediment particles and the kinematic viscosity of the fluid. It can be expressed in empirical dimensionless relationships of the form:

$$\theta_{cs} = \frac{\tau_{cs}}{g'd} = \frac{u_{*cs}^2}{g'd} = f(R_d)$$

The Shield's stress was determined using the relationships provided by Van Rijn (1984b), as presented below:

$$\theta_{cs} = \begin{cases} 0.24\left(R_d^{2/3}\right)^{-1} & for \quad R_d^{2/3} < 4 \\ 0.14\left(R_d^{2/3}\right)^{-0.64} & for\ 4 \leq R_d^{2/3} < 10 \\ 0.04\left(R_d^{2/3}\right)^{-0.1} & for\ 10 \leq R_d^{2/3} < 20 \\ 0.013\left(R_d^{2/3}\right)^{0.29} & for\ 20 \leq R_d^{2/3} < 150 \\ 0.055 & for\ R_d^{2/3} \geq 150 \end{cases}$$

3.3 Model Calibration

The hydrodynamic simulation period for calibration was from August 25, 2012 to September 2, 2012. The model simulation period includes the period of field data collection, which was from August 29, 2012 to September 2, 2012. The initial conditions for temperature and salinity were obtained from the field data. The model was calibrated by making minor adjustment to the model bathymetry and by adjusting Chezy's friction coefficient. The estimated Chezy's coefficients range from 90 to 130 depending on sediment sizes and water depths as presented in Table 3.1. During model calibration it was found that the Chezy's coefficient is not a sensitive parameter within the range of 90 to 130. Therefore an average Chezy's coefficient of 100 was applied throughout the computational domain.

3.3.1 Water Levels

Water levels were measured at the northern wharf in front of the Amaguk Inn for the period from August 29, 2012 to September 2, 2012. Figure 3-4 compares the model simulated and measured water levels at this location. The measured water levels and the model predicted water levels are in very good agreement except that;

- Predicted high water levels are slightly less than the observed water levels; and,
- Predicted low water levels are slightly higher than the observed water levels.

3.3.2 Tilt Meter Current

The tilt meter locations are shown in Figure 2-3 and are installed on the sea bed. Tilt meters TM1 and TM2 are located within the inner harbor and the tilt meters TM3 and TM4 are located in the outer harbor, as shown in Figure 2-3. The predicted and measured bottom currents at TM1, TM2, TM3 and TM4 are shown in Figures 3-5 and 3-12. The currents are presented in U and V components, which are in the east (positive) and north (positive) directions respectively. The predicted bottom U and V currents reasonably agree with the measured bottom currents at location TM1 and TM2, as shown in Figures 3-5 and 3-6. At TM3 it was found that the predicted bottom currents do not agree well with the observed values. At TM4 the predicted bottom current in the V direction (north-south) reasonably agrees with observed V direction currents. However, the predicted bottom currents in the U direction (east-west) do not agree well with the observed U direction currents. The tilt meter TM4 is located in the outer harbor in a deeper location (25 m depth). At this location it is expected that the currents will follow the tidal cycle. The predicted bottom currents at the TM4 location follow the tidal cycle very well but the observed bottom currents, particularly in the U direction, do not follow the tidal cycle very well.

The predicted and measured bottom currents indicate that the bottom currents within the inner harbour are much smaller than the bottom currents in the outer harbour. Average measured and predicted bottom currents at the tilt meter locations for the measurement period are presented in Table 3.3.

Table 3.3 Comparison of Predicted and Measured Average Tilt Meter Currents

Location	Measured Average Currents (cm/s)	Predicted Average Currents (cm/s)
TM1	1.3	0.40
TM2	1.4	1.12
TM3	5.1	2.21
TM4	4.3	6.91

The error statistics for modelled values and tilt meter observed values are presented in Table 3.4. The error statistics presented include Mean Error (ME), Mean Squared Error (MSE), Root Mean Squared Error (RMSE) and Mean Absolute Deviation (MAD). The definitions of these error statistics are provided below.

$$e_t = O_t - M_t$$

$$ME = \frac{1}{n}\sum e_t$$

$$MSE = \frac{1}{n}\sum e_t^2$$

$$RMSE = \sqrt{MSE}$$

$$MAD = \frac{1}{n}\sum |e_t|$$

Where: O_t = the observed value

M_t = the modelled value

n = number observations

Table 3.4 Modelled Error Statistics

Tilt Meter Location	Velocity Component	Mean Error (ME)	Mean Squared Error (MSE)	Root Mean Squared Error (RMSE)	Mean Absolute Deviation (MAD)
TM1	U	0.117	0.861	0.928	0.765
	V	0.303	0.272	0.521	0.428
TM2	U	0.725	2.41	1.55	1.27
	V	-0.093	0.575	0.758	0.605
TM3	U	-1.73	33.5	5.79	4.39
	V	1.64	14.9	3.86	2.74
TM4	U	-2.80	37.9	6.16	5.25
	V	0.043	14.3	3.79	3.03

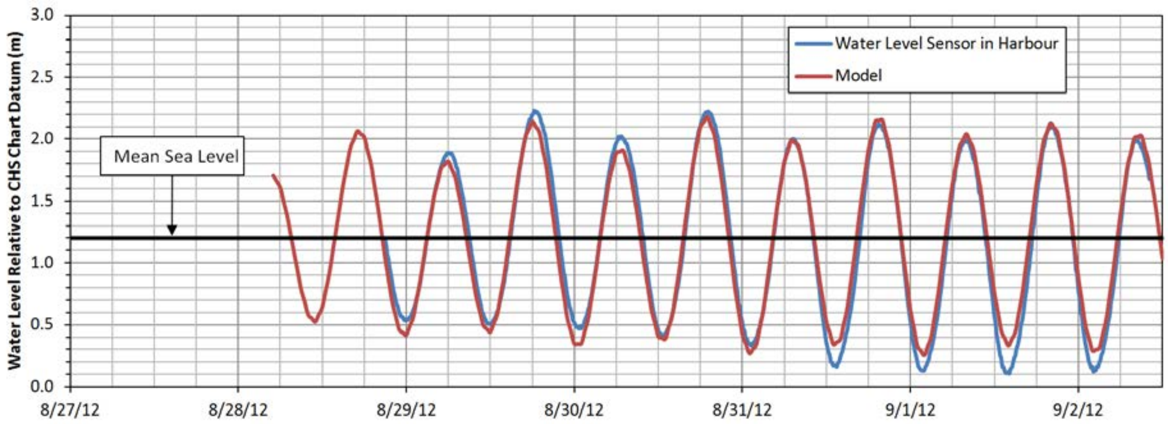

Figure 3-4 Comparison of Modeled and Measured Water Levels in the Harbour

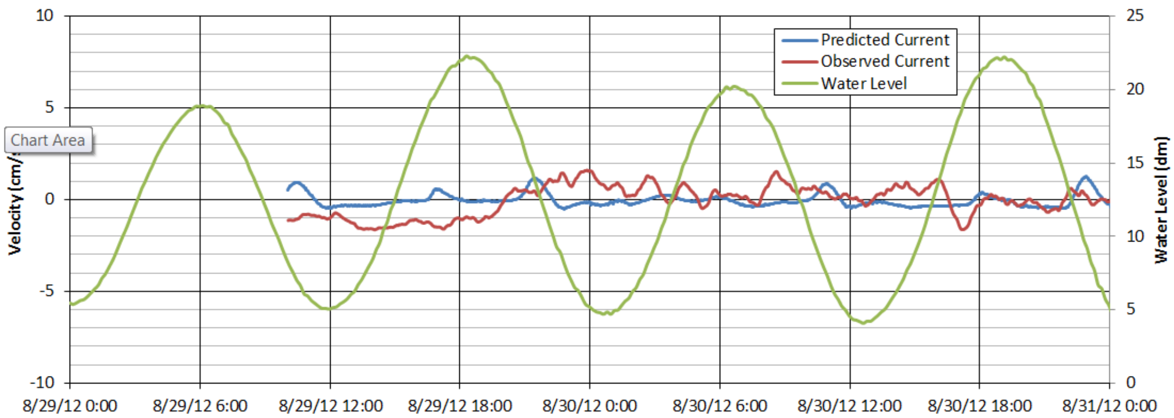

Figure 3-5 Comparison of Predicted and Observed U Velocity at TM1

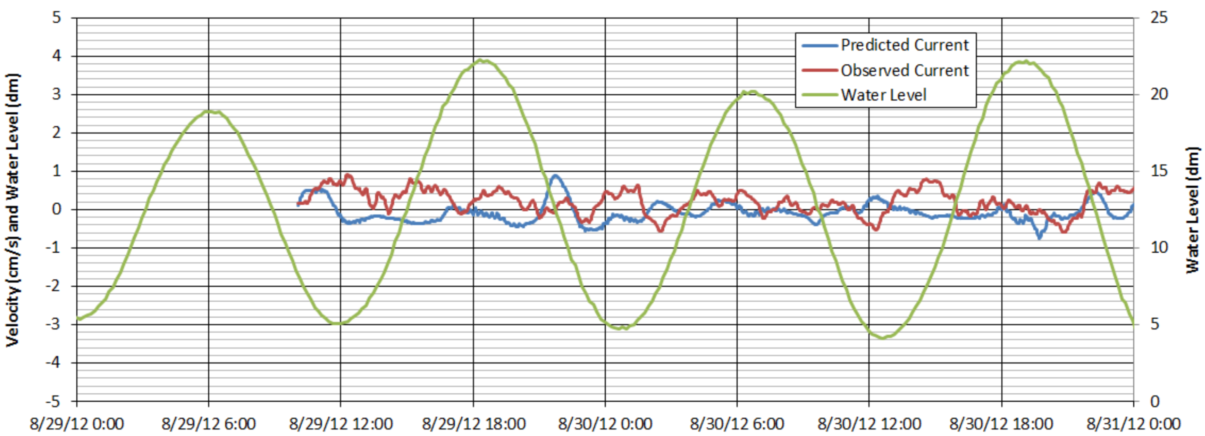

Figure 3-6 Comparison of Predicted and Observed V Velocity at TM1

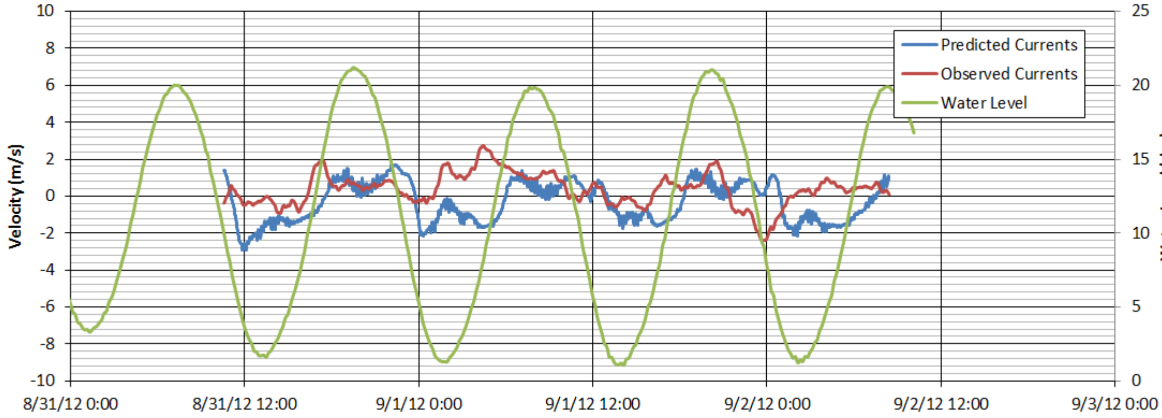

Figure 3-7 Comparison of Predicted and Observed U Velocity at TM2

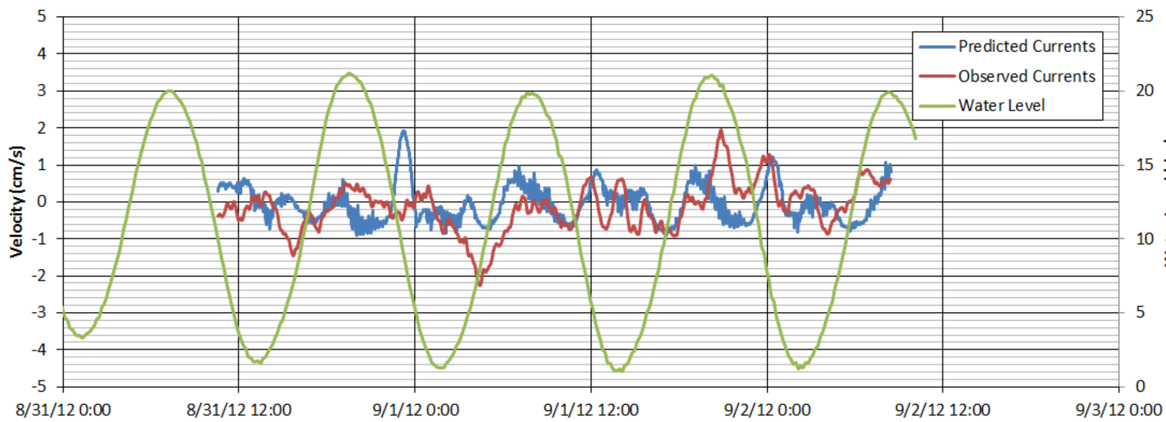

Figure 3-8 Comparison of Predicted and Observed V Velocity at TM2

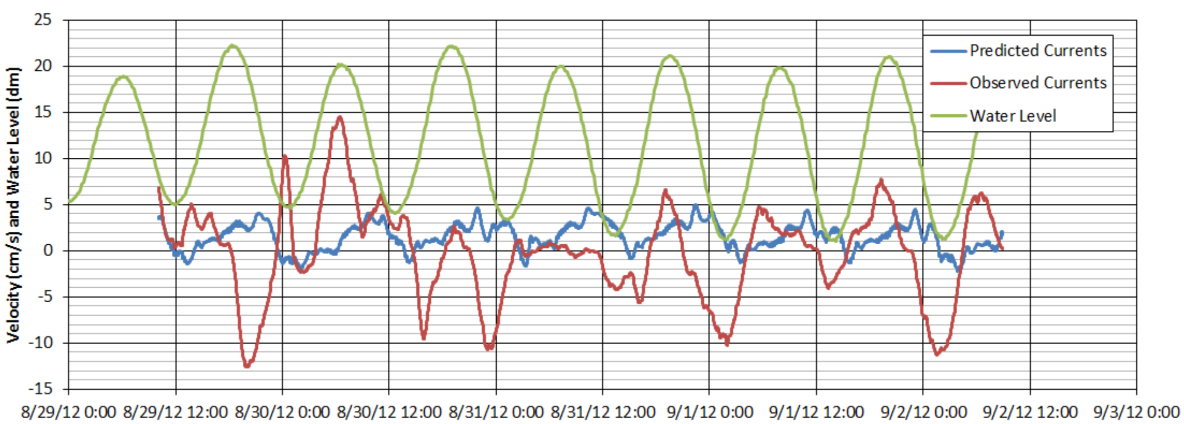

Figure 3-9 Comparison of Predicted and Observed U Velocity at TM3

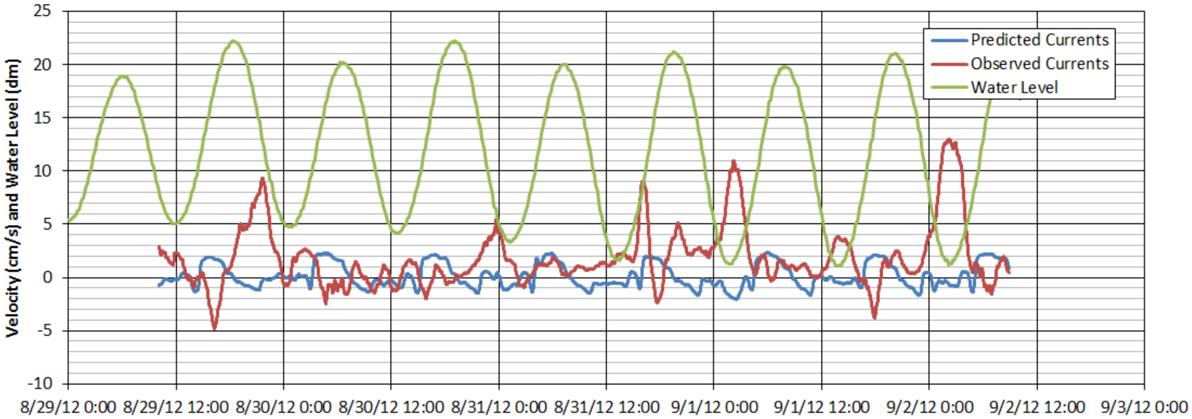

Figure 3-10 Comparison of Predicted and Observed V Velocity at TM3

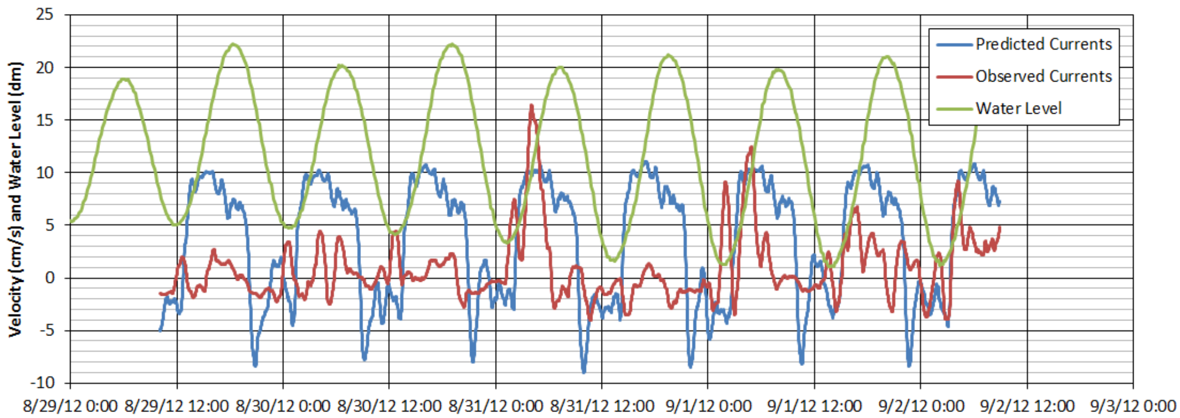

Figure 3-11 Comparison of Predicted and Observed U Velocity at TM4

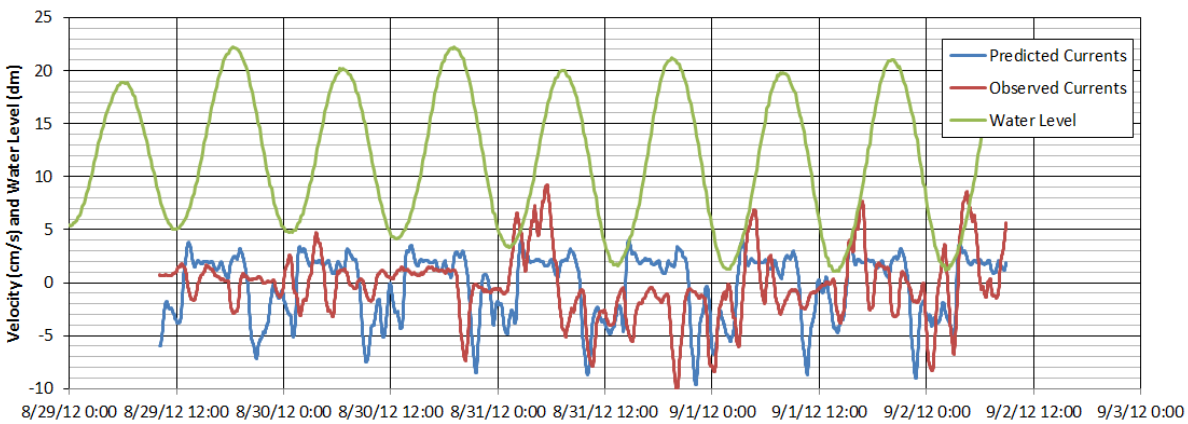

Figure 3-12 Comparison of Predicted and Observed V Velocity at TM4

3.3.3 ADCP Currents

As discussed in Section 2.4.1, the ADCP measurements show that during flood tide incoming tidal waters flow into the Harbour from the north and flow out to the south. During the ebb tide, water from the Harbour drains toward the northeast, and merges with a current coming from the south. The calibrated model simulates these major current patterns.

This is depicted in two figures, Figure 3-13 and Figure 3-14. Model predicted bottom currents and ADCP measured bottom currents are compared for ebb and flood tides. The bottom currents are compared as the sediment transport conditions primarily depend on the bottom currents.

Figure 3-13 shows the comparison of predicted and observed bottom currents during ebb tide on September 1, 2012. The ADCP measurements are depicted for transects which were taken from 10:29 am to 12:15 pm. During this period the water level varied from 1.32 m to 0.43 m. The predicted model results represent the conditions on September 1, 2012 at 11:00 am.

Figure 3-14 shows the comparison of predicted and observed bottom currents during flood tide on September 1, 2012. The ADCP measurements are depicted for transects which were taken from 16:25 pm to 18:05 pm. During this period water level varied from 0.74 m to 1.71 m. The predicted model results represent the conditions on September 1, 2012 at 17:30 pm.

The predicted and observed currents reasonably agree in magnitude and direction for both the ebb and flood tide conditions. The field data has significant variation both in magnitude and direction. The model results correlate well with the main current directions to the northeast during ebb tide and to the south during flood tide. It must be noted that model results are shown at one time and the ADCP transect data was gathered over a period of time with varying tidal elevations and wind conditions as mentioned above. In the inner harbor it is difficult to discern current patterns based on the field data. However, model results appear well correlated in areas where the field data are consistent. The current magnitudes are also generally consistent with field data but with overall less variation.

Based on specifications from Teledyne RD Instruments for the ADCP unit used in the study, velocity accuracy for the measured currents is 0.3% of water velocity relative to the ADCP ±0.3 cm/s. The unit used was a 600 KHz Workhorse ADCP unit.

Overall the hydrodynamic model correlates reasonably well with field data from the calibration period, with the exception of differences in modeled and observed currents at TM3 and TM4. The hydrodynamic model reproduces the following observations:

- Water level in the harbour;
- Currents at tilt meter locations TM1 and TM2 in the inner harbour;
- Current patterns in the inner and outer harbor;
- Stronger currents along the mouth of the harbour; and
- Major portion of the tidal flow bypassing the inner harbour.

The differences in modeled and observed currents at TM3 and TM4 may be due to the following:

- Errors in the TM3 and TM4 tilt meter observations;
- Simplifications in the model's representation of physical processes; and,
- Assumptions in the values of model parameters in these locations.

Further investigation is needed to find out the causes of the differences between modeled and observed currents at TM3 and TM4.

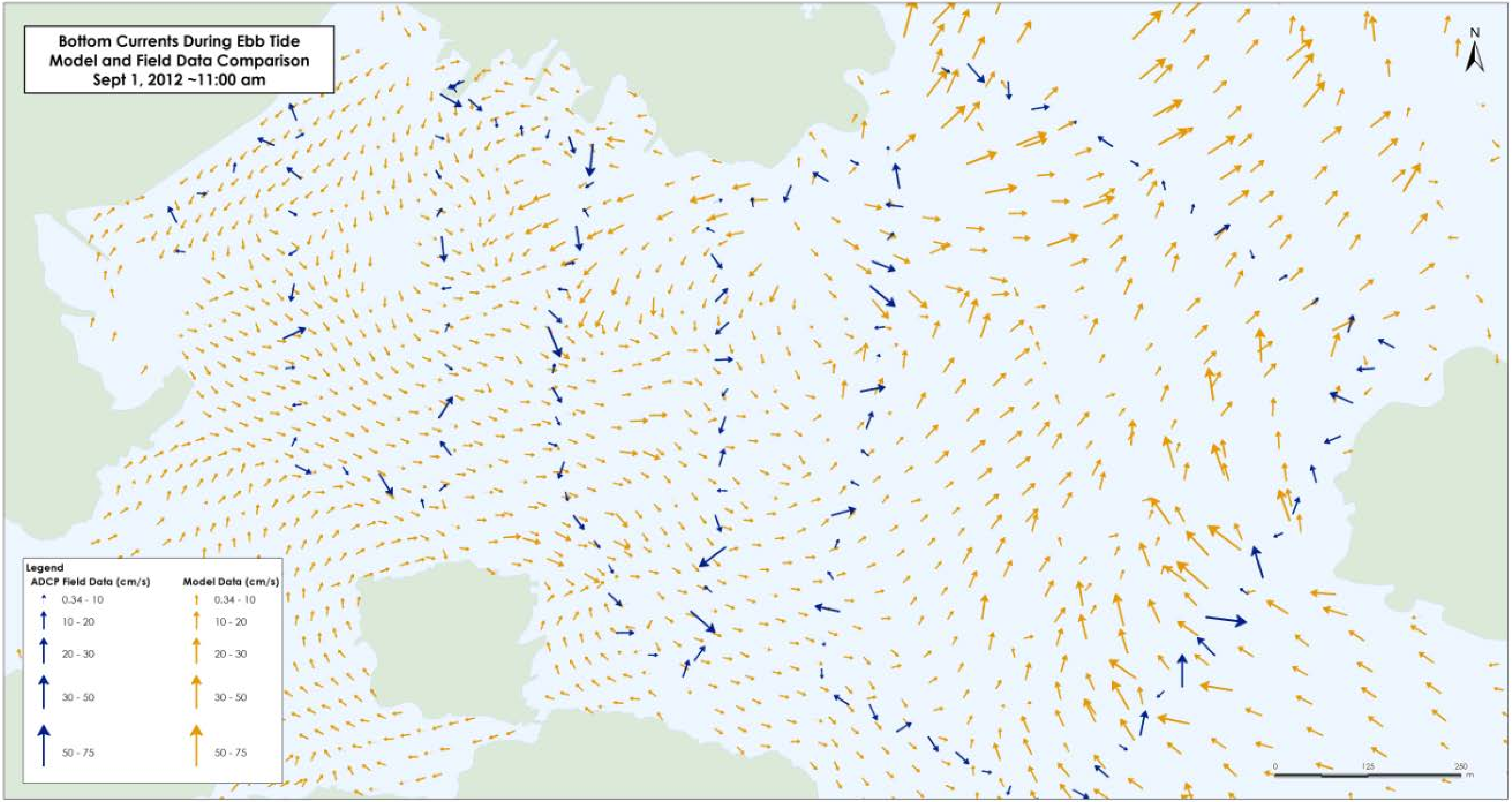

Figure 3-13 ACDP Measured Bottom Currents During the Ebb Tide September 1, 2012 Time: ~11:00 am

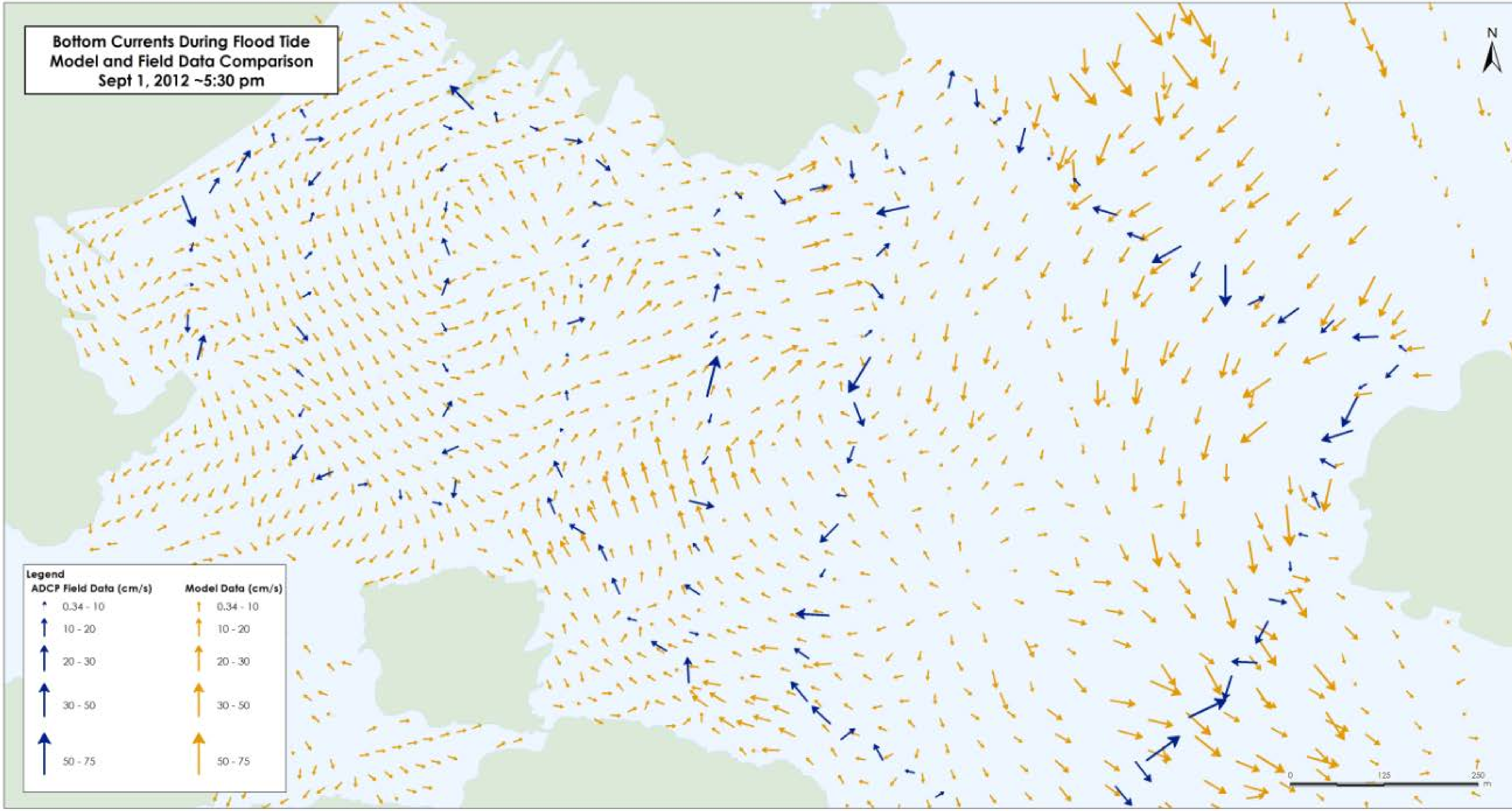

Figure 3-14 ACDP Measured Bottom Currents During the Flood Tide September 1, 2012 Time: ~5:30 pm

3.3.4 Total Suspended Sediment (TSS) Concentration

A hydrodynamic and sediment transport model run was completed from September 18, 2013 to September 26, 2013 to assess the sediment transport model results against the observed TSS concentration at three locations (Sill 1 to Sill 3, Figures 3-15 to 3-18) over the sill that separates the inner harbour and outer harbour. The water samples were collected during rising and falling tides on September 23, 2013 and September 26, 2013 as discussed in Section 2.5. The sampling periods were as follows:

- September 23, 2013
  - Rising tide: 07h20 to 08h10
  - Falling tide: 13h00 to 13h30
- September 26, 2013
  - Rising tide: 09h15 to 10h00
  - Falling tide: 15h05 to 15h35

Modeled depth-averaged TSS concentrations at the inner harbour are presented in Figures 3-15 and 3-16 for rising and falling tides on September 23, 2013. Modeled depth-averaged TSS concentrations at the inner harbour are presented in Figures 3-17 and 3-18 for the rising and falling tides on September 26, 2013. Modeled and observed TSS over the sill is compared in Tables 3.5 to 3.8.

The modeled depth-averaged TSS and observed depth-averaged TSS concentrations compare reasonably well as shown in Tables 3.5 to 3.8 except at Sill 1 on September 23 during the rising tide. It must be noted that model results are shown at one time and the TSS data was gathered over a period of time with varying tidal elevations and wind conditions as mentioned above.

Table 3.5 Comparison of Modeled and Observed TSS on September 23 during the Rising Tide

Location	Observed TSS (mg/L)		Modeled Depth-Averaged TSS (mg/L)
	TSS Range	Depth-Averaged	
Sill 1	1.6 – 13.0	4.06	12.0 – 14.0
Sill 2	1.0 – 3.4	2.33	4.0 – 6.0
Sill 3	< 1 – 4.0	2.60	2.0 – 4.0

Table 3.6 Comparison of Modeled and Observed TSS on September 23 during the Falling Tide

Location	Observed TSS (mg/L)		Modeled Depth-Averaged TSS (mg/L)
	TSS Range	Depth-Averaged	
Sill 1	1.4 – 13.0	4.43	2.0 -4.0
Sill 2	< 1.0 – 7.8	3.40	2.0 – 4.0
Sill 3	< 1.0 – 1.8	1.33	2.0 – 4.0

Table 3.7 Comparison of Modeled and Observed TSS on September 26 during the Rising Tide

Location	Observed TSS (mg/L)		Modeled Depth-Averaged TSS (mg/L)
	TSS Range	Depth-Averaged	
Sill 1	1.8 – 4.4	3.50	2.0 – 4.0
Sill 2	2.0 – 4.2	2.93	0.0 – 2.0
Sill 3	1.0 – 5.0	3.47	0.0 – 2.0

Table 3.8 Comparison of Modeled and Observed TSS on September 26 during the Falling Tide

Location	Observed TSS (mg/L)		Modeled Depth-Averaged TSS (mg/L)
	TSS Range	Depth-Averaged	
Sill 1	< 1.0 – 2.2	1.13	0.0 – 2.0
Sill 2	2.6 – 5.8	4.27	0.0 – 2.0
Sill 3	<1.0 – 2.4	1.93	2.0 – 4.0

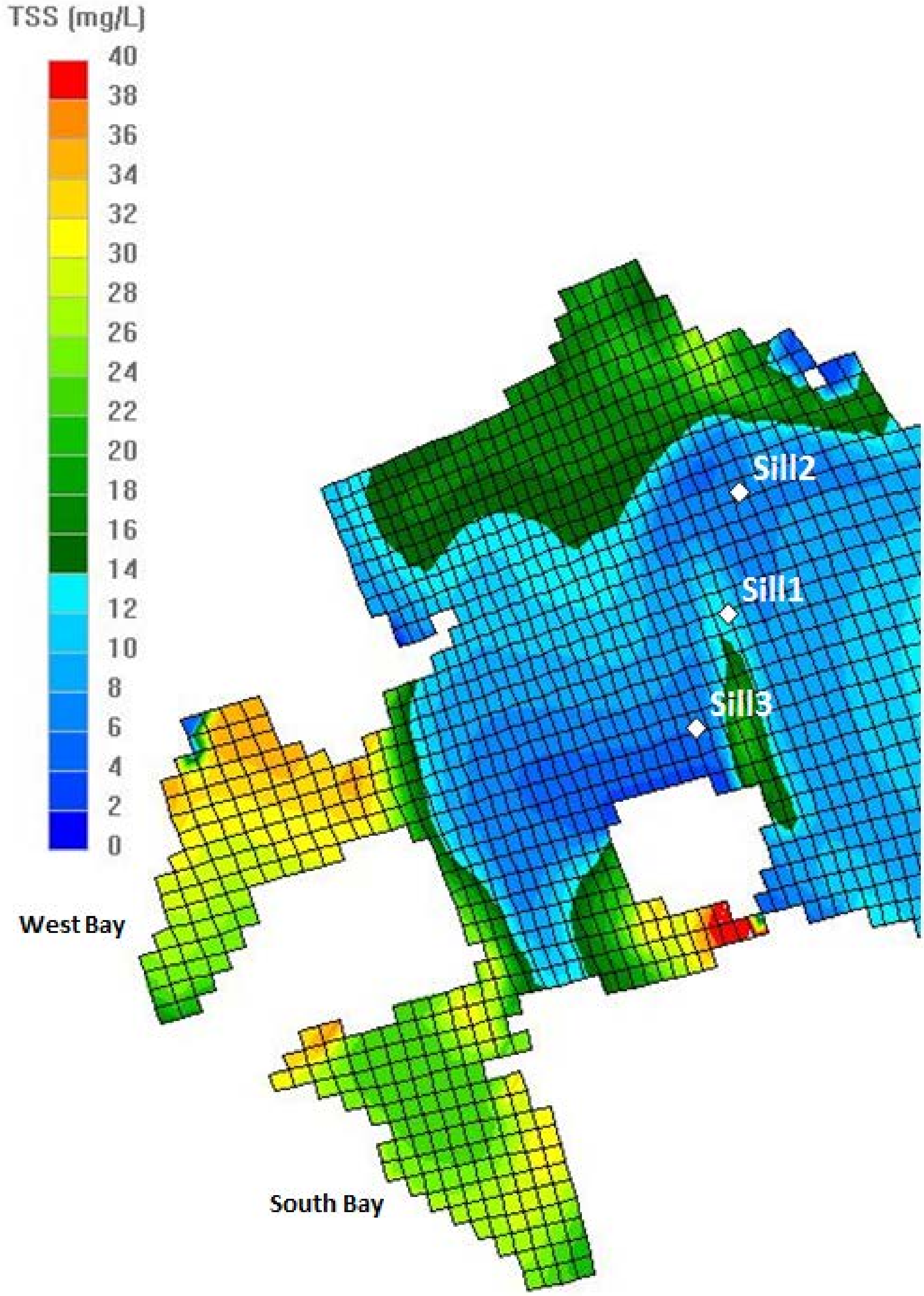

Figure 3-15 Modeled Depth-Averaged TSS Concentrations on September 23 during the Rising Tide at 7:30 hrs

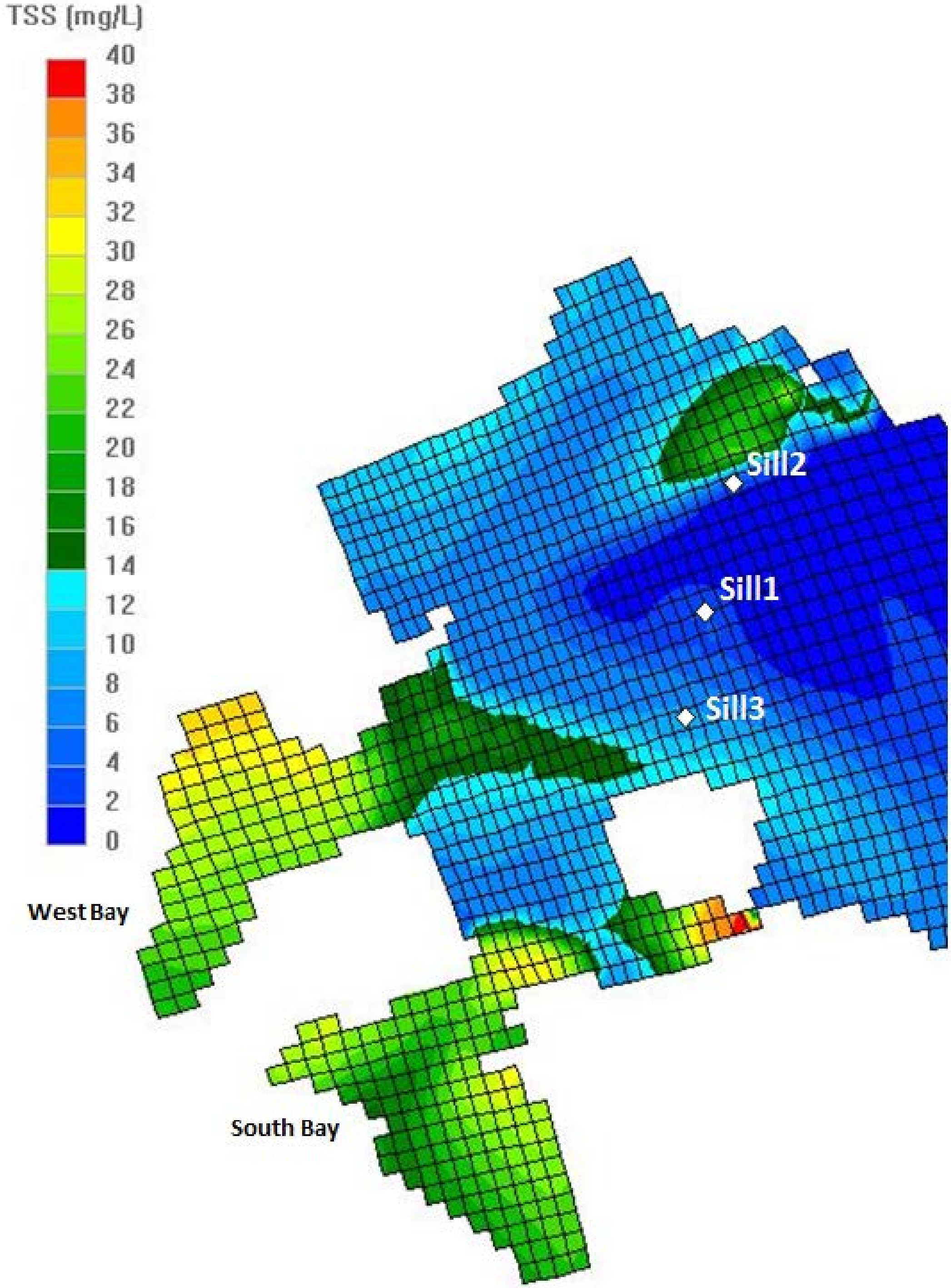

Figure 3-16 Modeled Depth-Averaged TSS Concentrations on September 23 during the Falling Tide at 13:00 hrs

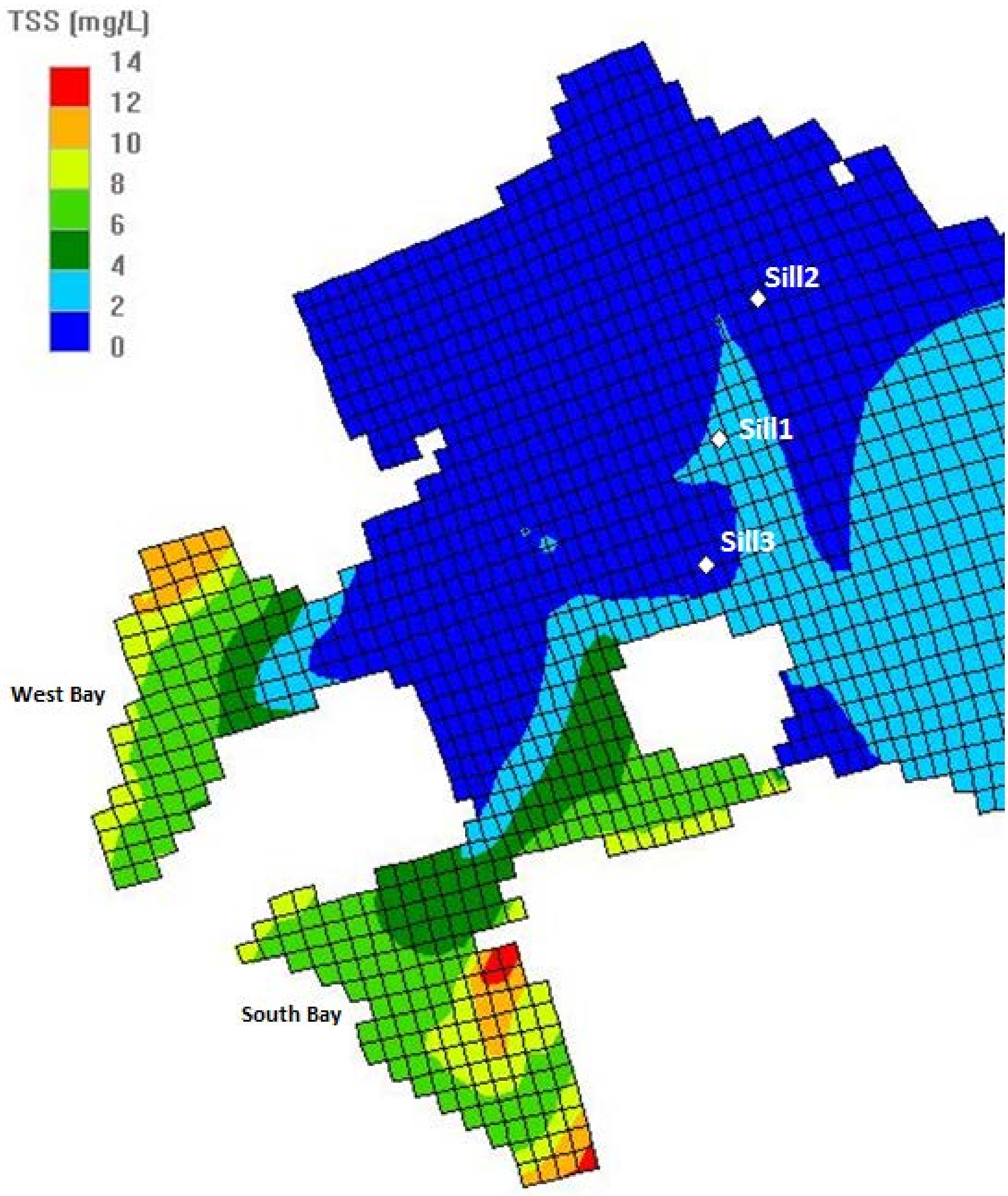

Figure 3-17 Modeled Depth-Averaged TSS Concentrations on September 26 during the Rising Tide at 9:30 hrs

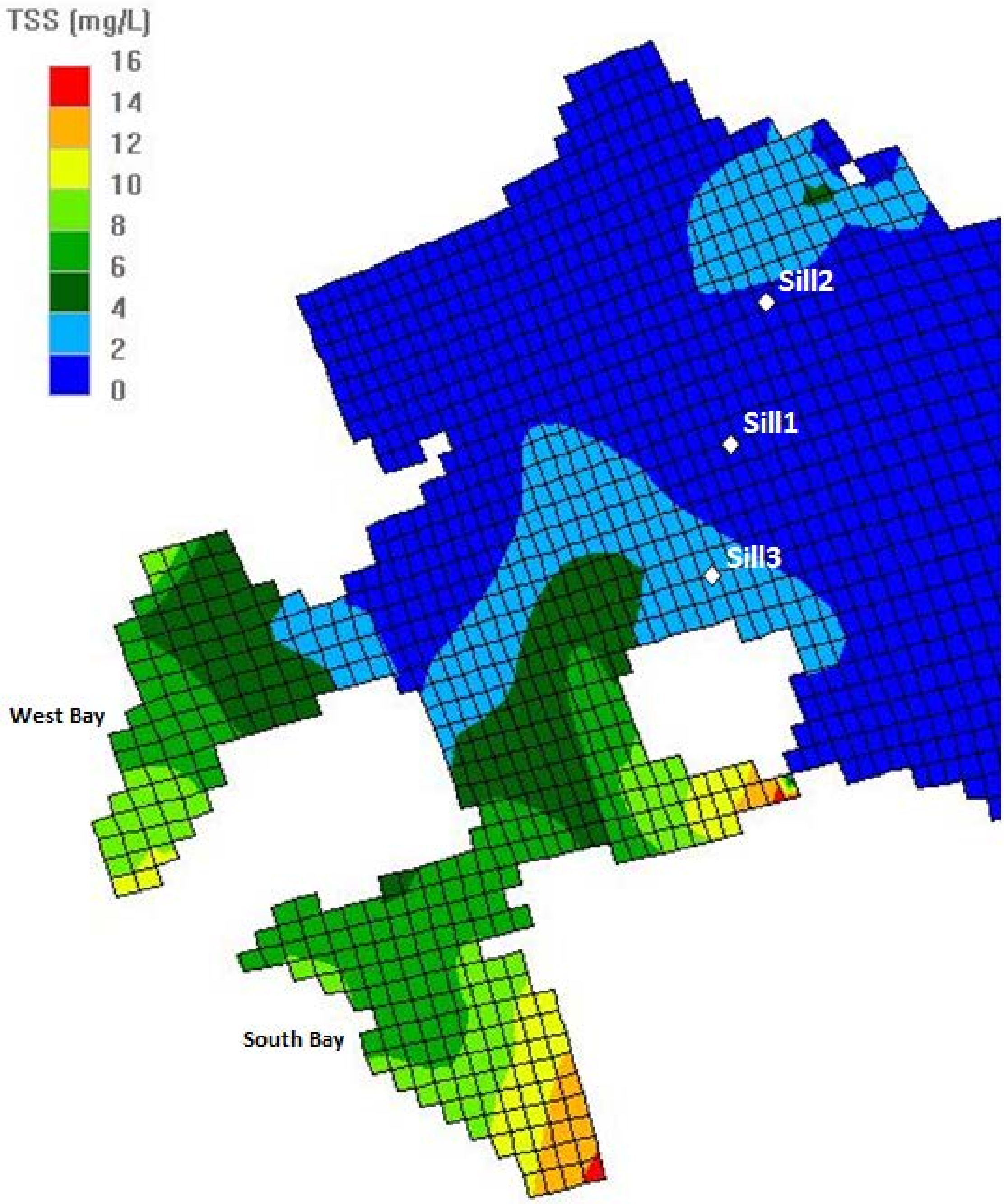

Figure 3-18 Modeled Depth-Averaged TSS Concentrations on September 26 during the Falling Tide at 15:30 hrs

4.0 MODELING RESULTS

The hydrodynamic model results include the water level and currents in Hopedale Harbour due to tidal and wind conditions. Tidal conditions for 2012 in Hopedale Harbour are shown in Figure 4-1. The tides in Hopedale Harbour are semi-diurnal and there are 730 tidal cycles per year, consisting of neap, average and spring tidal conditions. After the hydrodynamic calibration was completed, the hydrodynamic and sediment transport models for Hopedale Harbour were simulated for the period of July 12, 2012 to July 20, 2012 to predict the hydrodynamic and sediment transport conditions. The model simulation period of July 12, 2012 to July 20, 2012 was selected as this period includes typical neap tide, average tide and spring tide conditions. Annual sediment load leaving Hopedale Harbour was estimated by extrapolating the sediment load for spring, neap and average tidal conditions. The following sections discuss the hydrodynamic and sediment transport modeling results.

4.1 Hydrodynamic modeling results

The following hydrodynamic modeling results for the spring, average and neap tidal conditions are presented in this section:

- Depth-averaged currents and current directions in the Hopedale Bay;
- U, V and depth averaged currents along the cross section V1 (Figure 4-2) in the west-east direction running through the harbour sill; and,
- U, V and depth averaged currents along the cross section V2 (Figure 4-2) in the south-north direction running along the harbour sill.

The currents are presented in U and V components, which are in the east (positive) and north (positive) directions respectively.

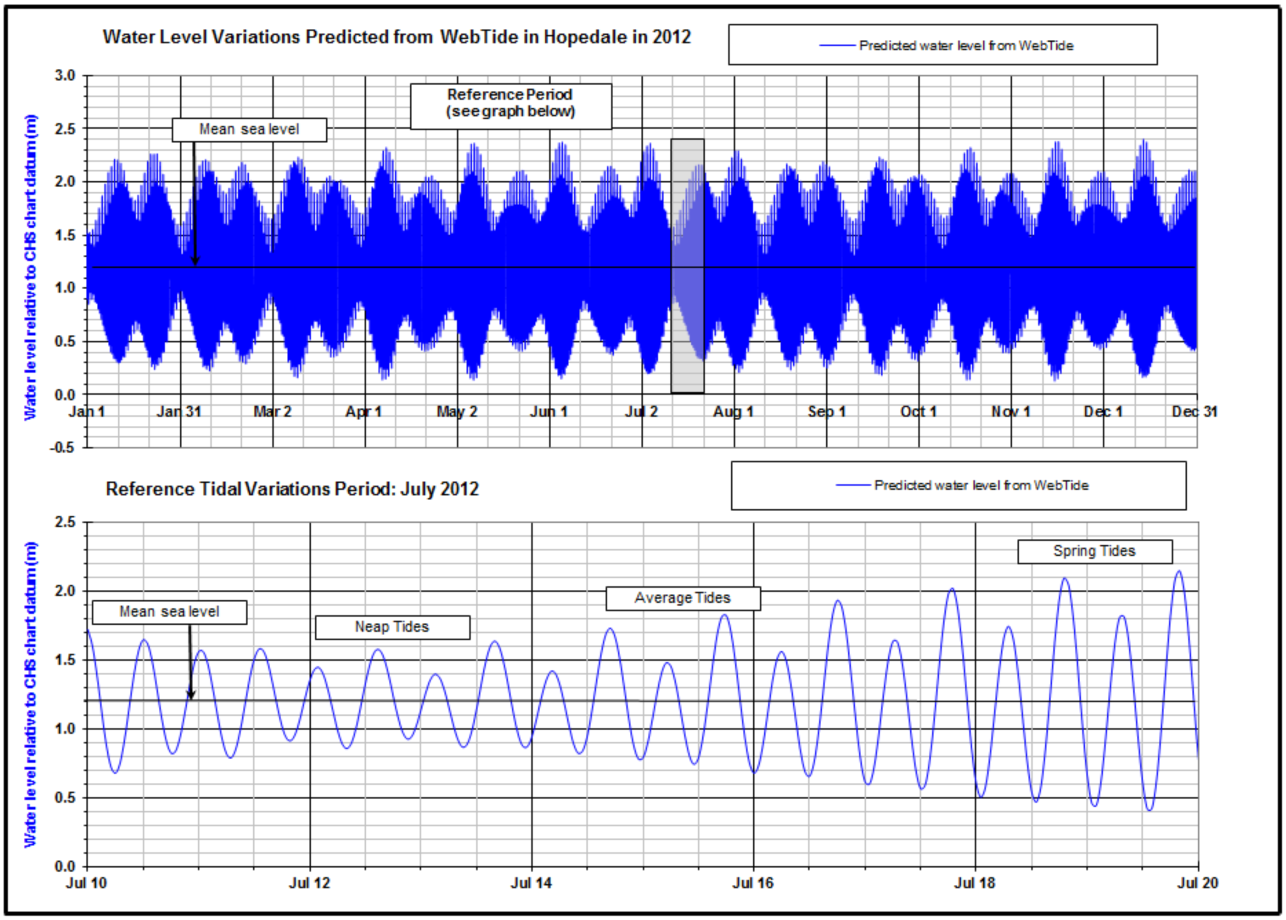

Figure 4-1 Tidal Conditions for Hydrodynamic Simulations

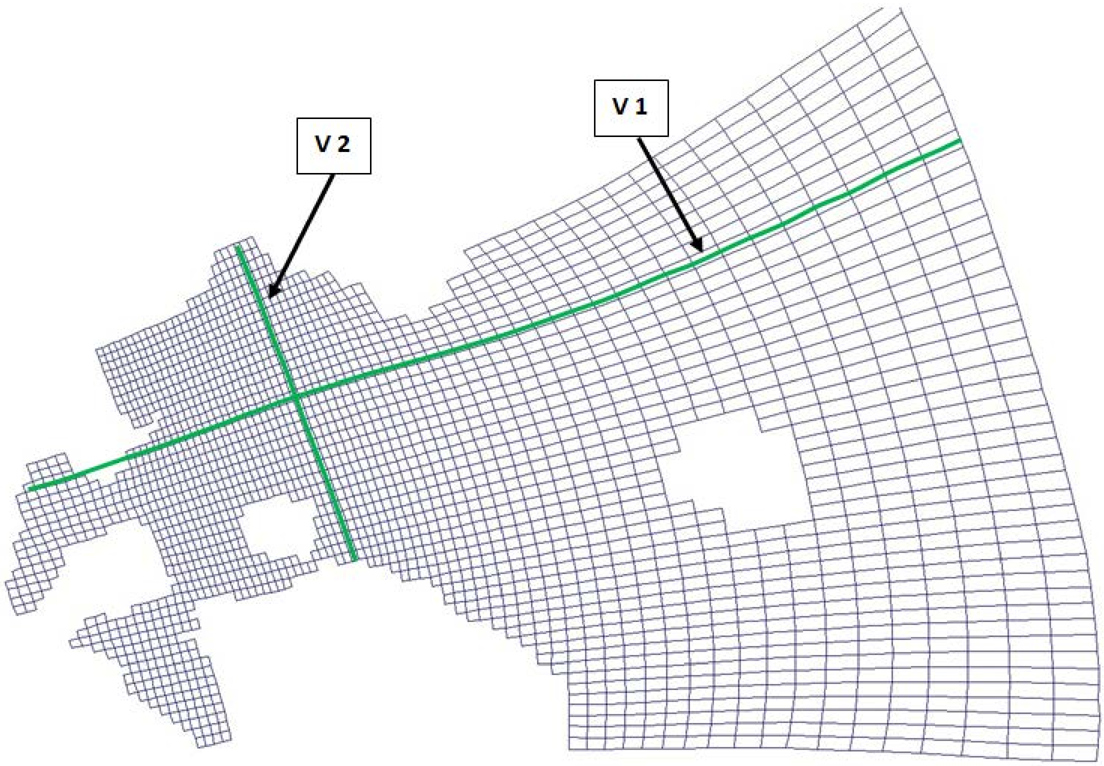

Figure 4-2 Velocity Cross Sections V1 and V2

4.1.1 Spring Tidal Conditions

Depth-averaged currents and current directions in Hopedale Harbour are shown in Figure 4-3 for July 18, 2012 at 18:00 hrs corresponding to flood conditions during a spring tide. Figure 4-4 shows the current patterns within the inner harbour. The modeling results indicate that current velocities are higher along the mouth of the harbour and behind Ellen Island. The major portion of the tidal flow passes by the mouth of the harbour and continues toward the south as observed in the field ADCP measurements. The water depths behind Ellen Island are very shallow (about 20 m) compared to water depths (about 60 to 70 m) to the north and south of the shallow area. The shallow area behind Ellen Island causes the higher current velocities behind Ellen Island as seen in Figure 4-3. The current velocities in the harbour are relatively much smaller than the velocities outside of the harbour area.

Figure 4-5 shows U, V and depth-averaged currents variation in a vertical plane at cross section V1 on July 18, 2012 at 18:00 hrs. The V current plot indicates that the current direction is towards the south outside the harbour area and that higher velocities were observed at the surface. V currents are towards the north inside the harbour and higher velocities were observed over the sill and east of the sill. The U currents are higher in the harbour mouth and a circulation pattern is observed in the mouth. The depth-averaged velocities are smaller at the inner harbour and increasing towards the harbour mouth with peak values at the mouth of the harbour.

Figure 4-6 shows U, V and depth-averaged current variation in a vertical plan at cross section V2 on July 18, 2012 at 18:00 hrs. The velocities are relatively much smaller towards north in the sheltered area and increasing towards the south with a maximum value at the shallowest location on the sill.

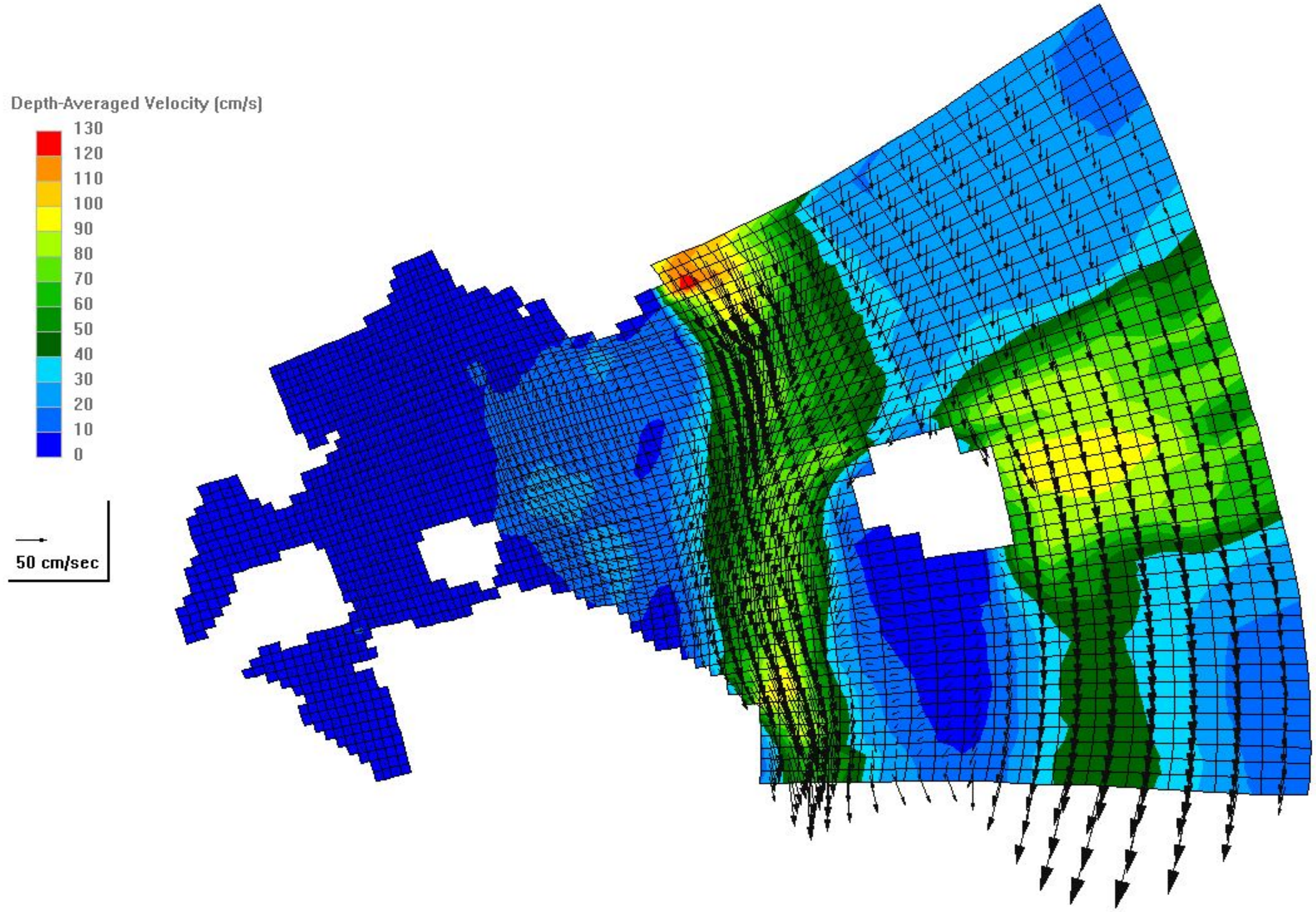

Figure 4-3 Depth-Averaged Currents on July 18, 2012 18:00 hrs

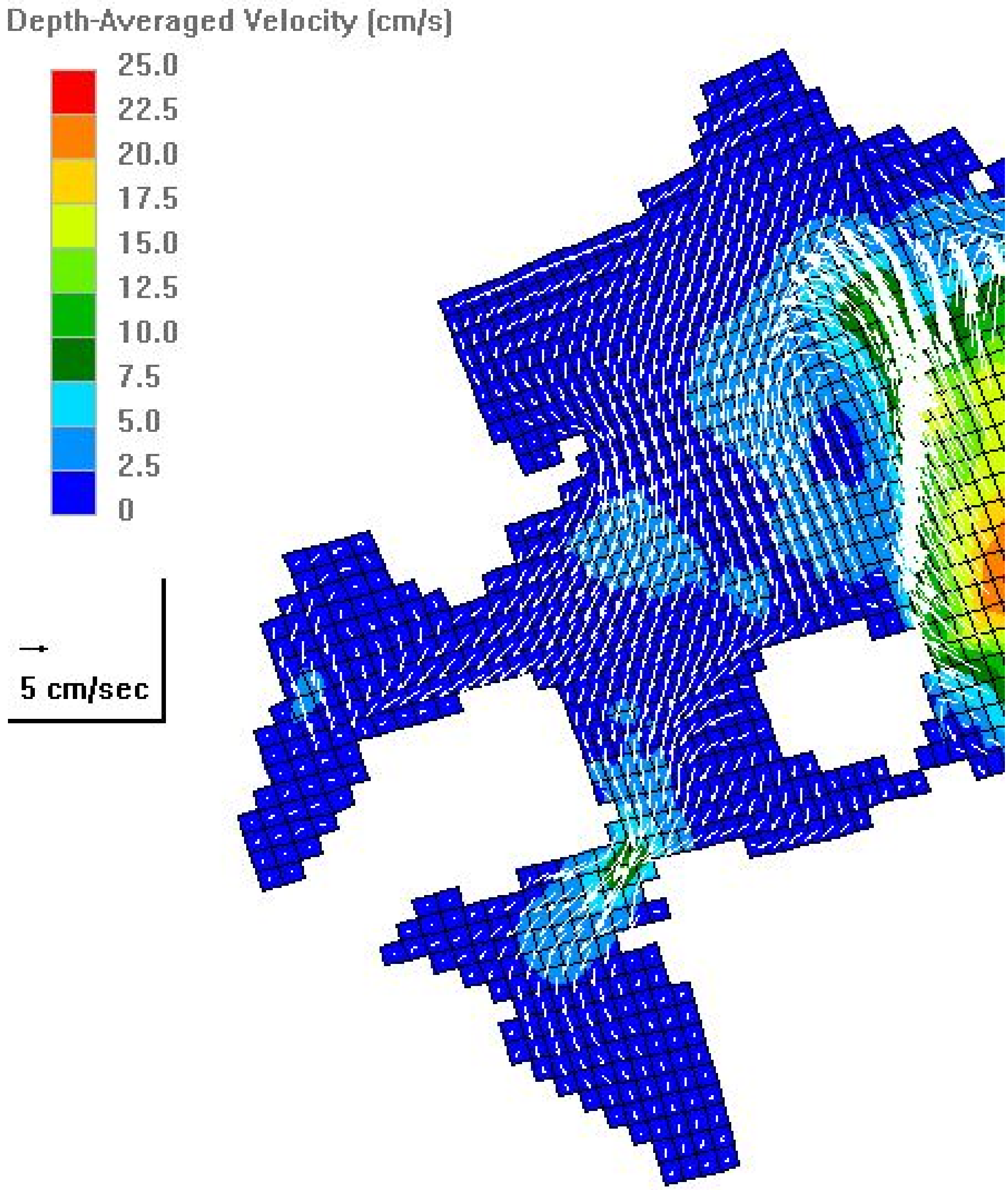

Figure 4-4 Depth-Averaged Currents in the Inner Harbour on July 18, 2012 18:00 hrs

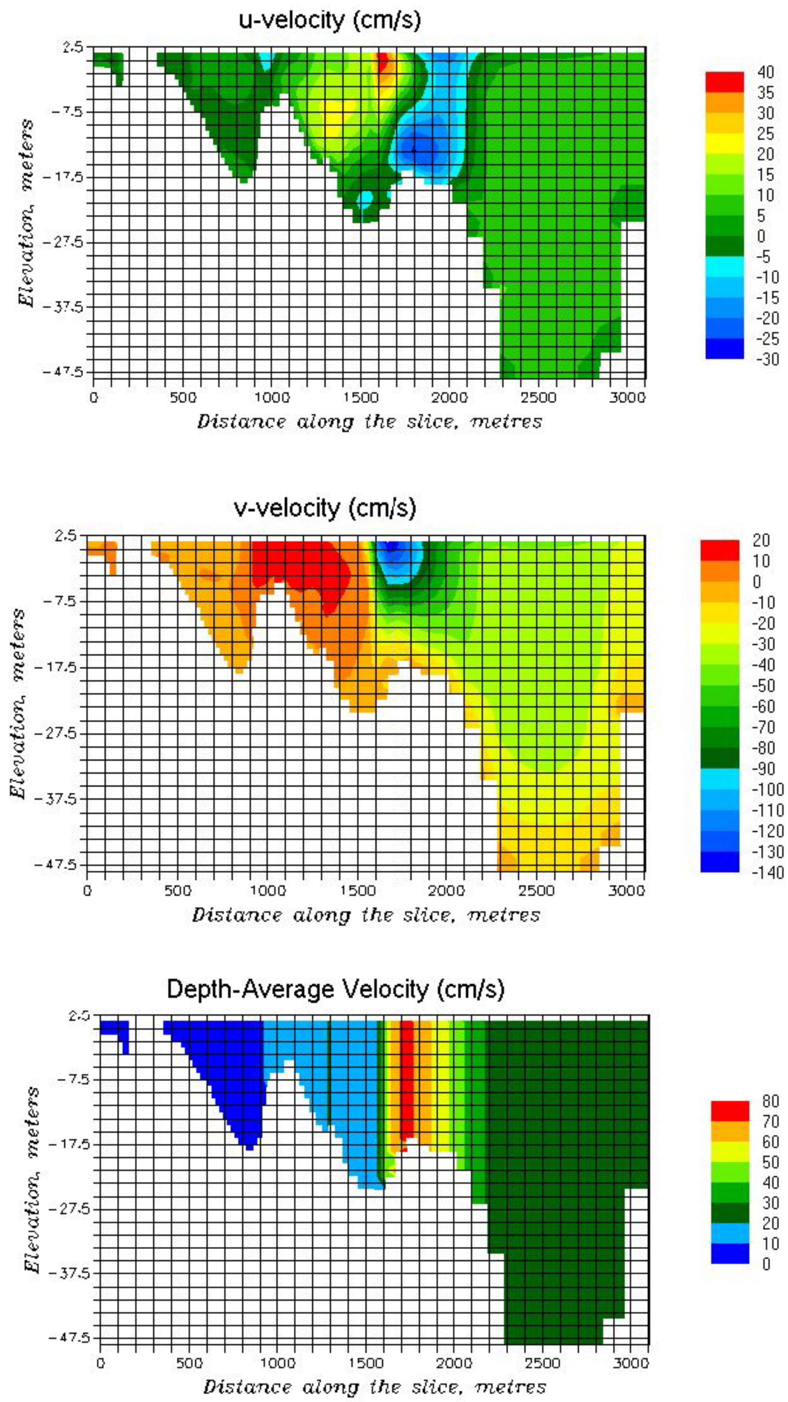

Figure 4-5 U, V and Depth-Averaged Currents at Cross Section V1 (West- East Direction)

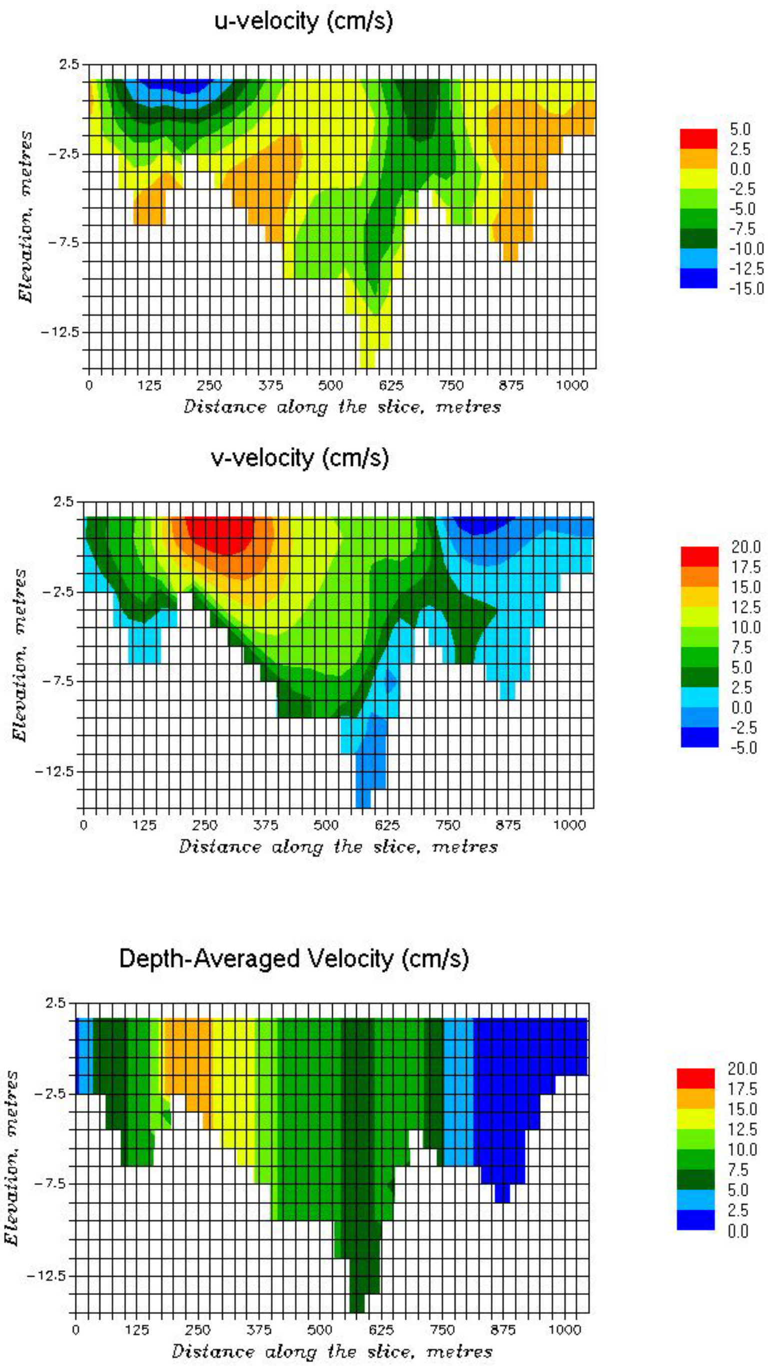

Figure 4-6 U, V and Depth-Averaged Currents at Cross Section V2 – Sill (South – North Direction)

4.1.2 Neap Tidal Conditions

Depth-averaged currents and current directions in Hopedale Harbour are shown in Figure 4-7 for July 13, 2012 17:00 hrs, just after high water levels. Figure 4-8 shows the current patterns within the inner harbour. Results indicate that current velocities are higher along the mouth of harbour and behind Ellen Island as observed during the spring tides. The current velocities in the harbour are relatively much smaller than the velocities outside of the harbour area, as observed during the spring tides. The current magnitudes are generally smaller during the neap tides, as expected.

Figure 4-9 shows U, V and depth-averaged currents at the cross section V1 on July 13, 2012 at 17:00 hrs. Figure 4-10 shows U, V and depth-averaged currents at the cross section V2 on July 13, 2012 at 17:00 hrs. These figures show similar current patterns and directions in comparison with the spring tide but the velocities are smaller.

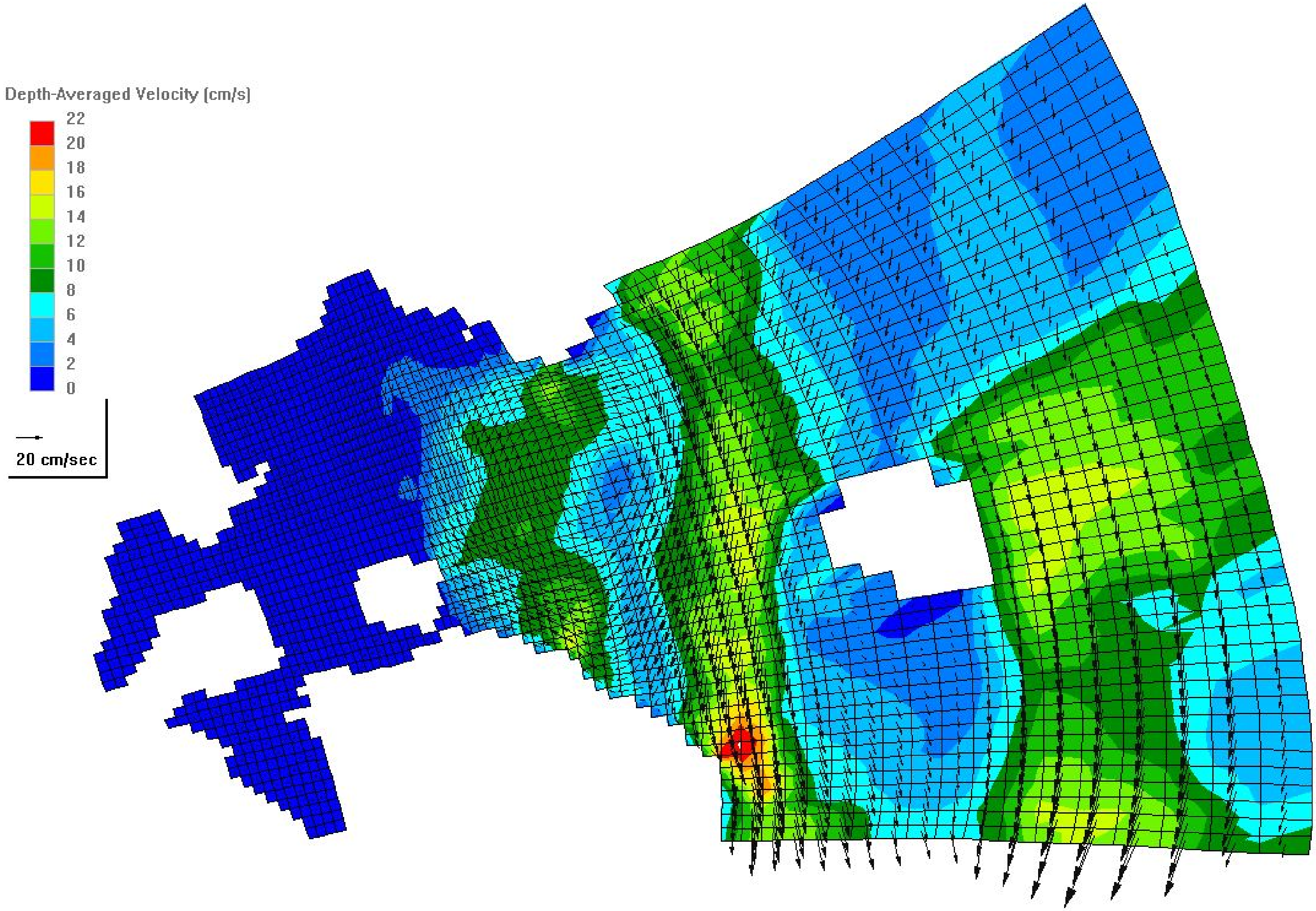

Figure 4-7 Depth-Averaged Currents on July 13, 2012 17:00 hrs

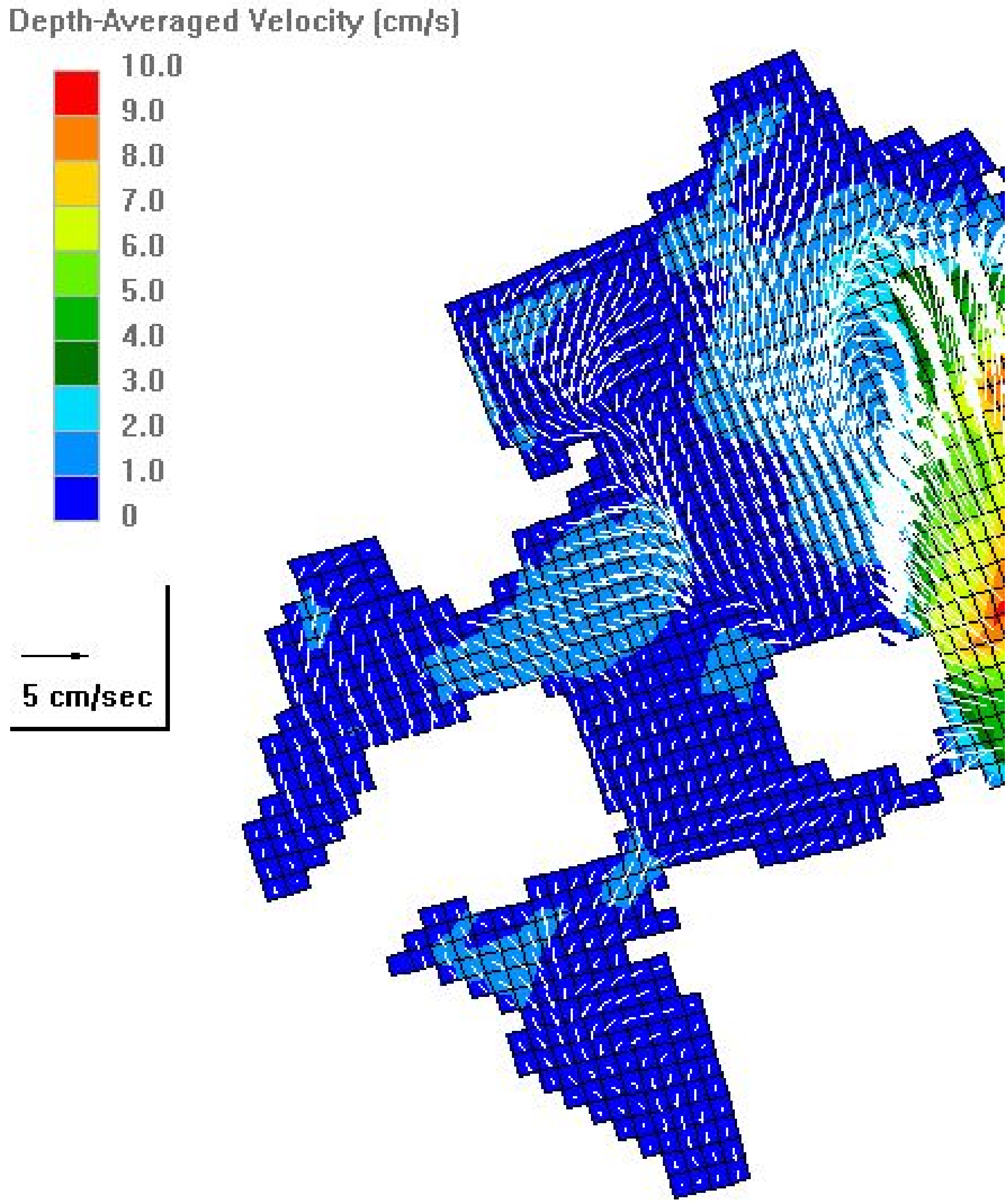

Figure 4-8 Depth-Averaged Currents in the Inner Harbour on July 13, 2012 17:00 hrs

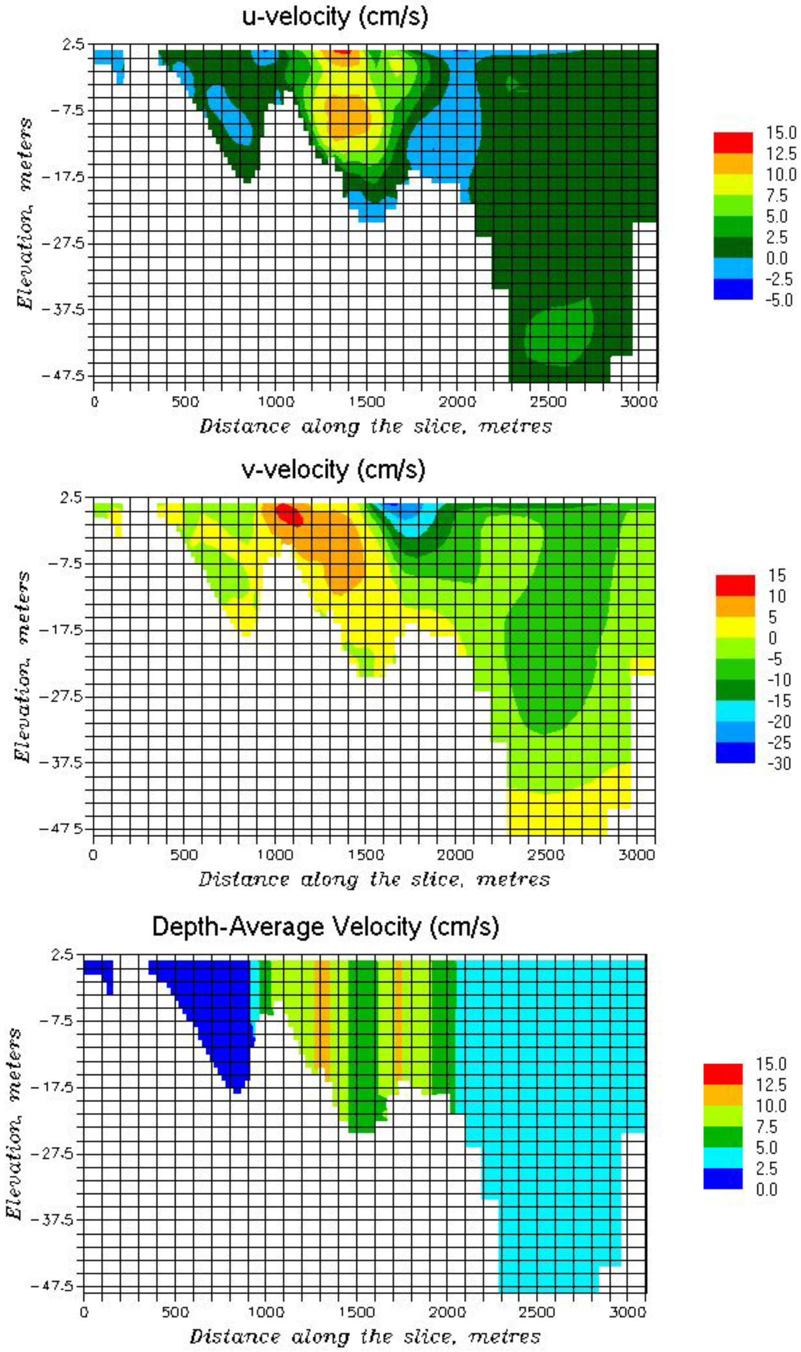

Figure 4-9 U, V and Depth-Averaged Currents at Cross Section V1 (West- East Direction)

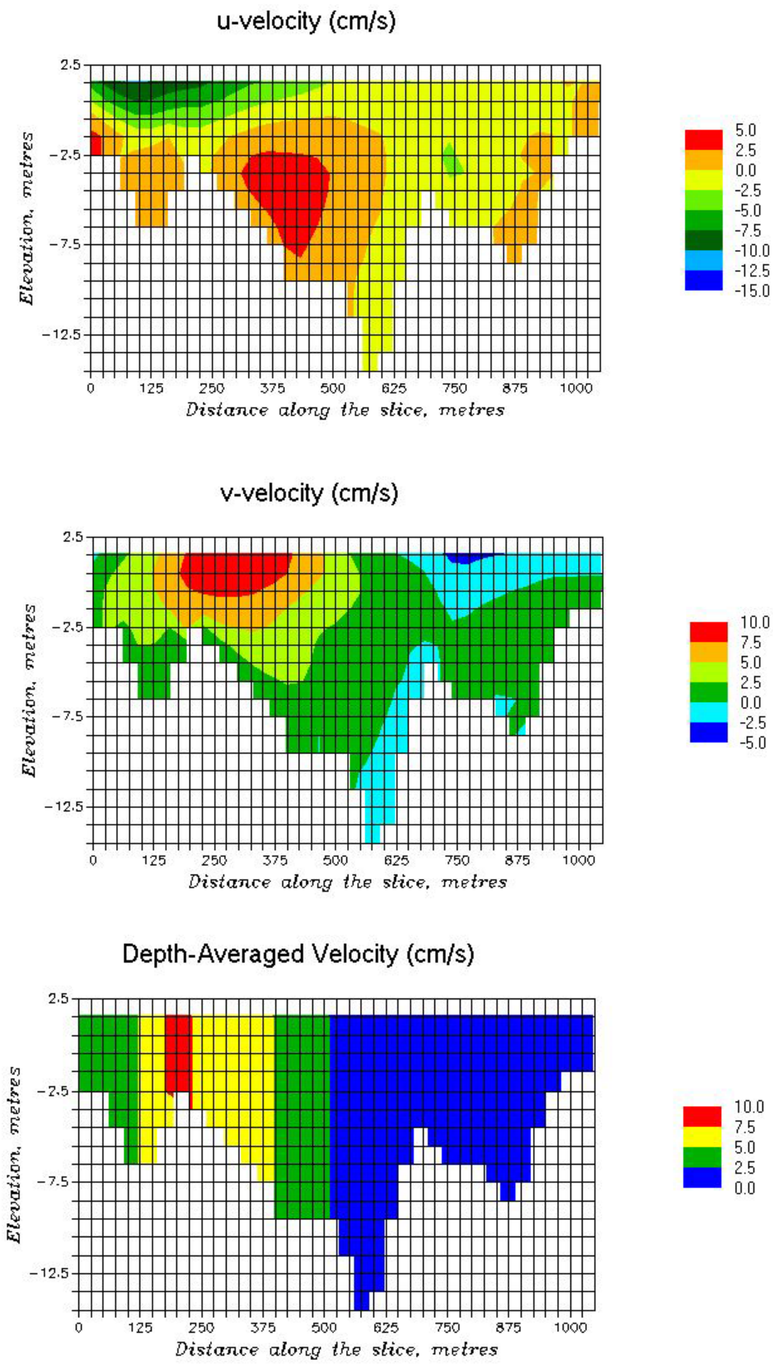

Figure 4-10 U, V and Depth-Averaged Currents at Cross Section V2 – Sill (South – North Direction)

4.1.3 Average Tidal Conditions

Depth-averaged currents and current directions in Hopedale Harbour are shown in Figure 4-11 for July 15, 2012 at 20:00 hrs, corresponding to ebb tide conditions. Figure 4-12 shows the current patterns within the inner harbour. The modeling results indicate that current velocities are higher along the mouth of harbour and behind Ellen Island as observed during spring and neap tides. The major portion of the tidal flow bypasses the mouth of the harbour and continues toward the north as observed in the field ADCP measurements for ebb tide conditions. The current velocities in the harbour are relatively much smaller than the velocities outside of the harbour area as observed in flood tide conditions; however, their directions have been reversed.

Figure 4-13 shows U, V and depth-averaged currents at the cross section V1 on July 15, 2012 at 20:00 hrs. Figure 4-14 shows U, V and depth-averaged currents at the cross section V2 on July 15, 2012 at 20:00 hrs. These figures show the currents are reversed in direction from generally southward to generally northward across V1 and that there is a circulation through the inner harbour across V2.

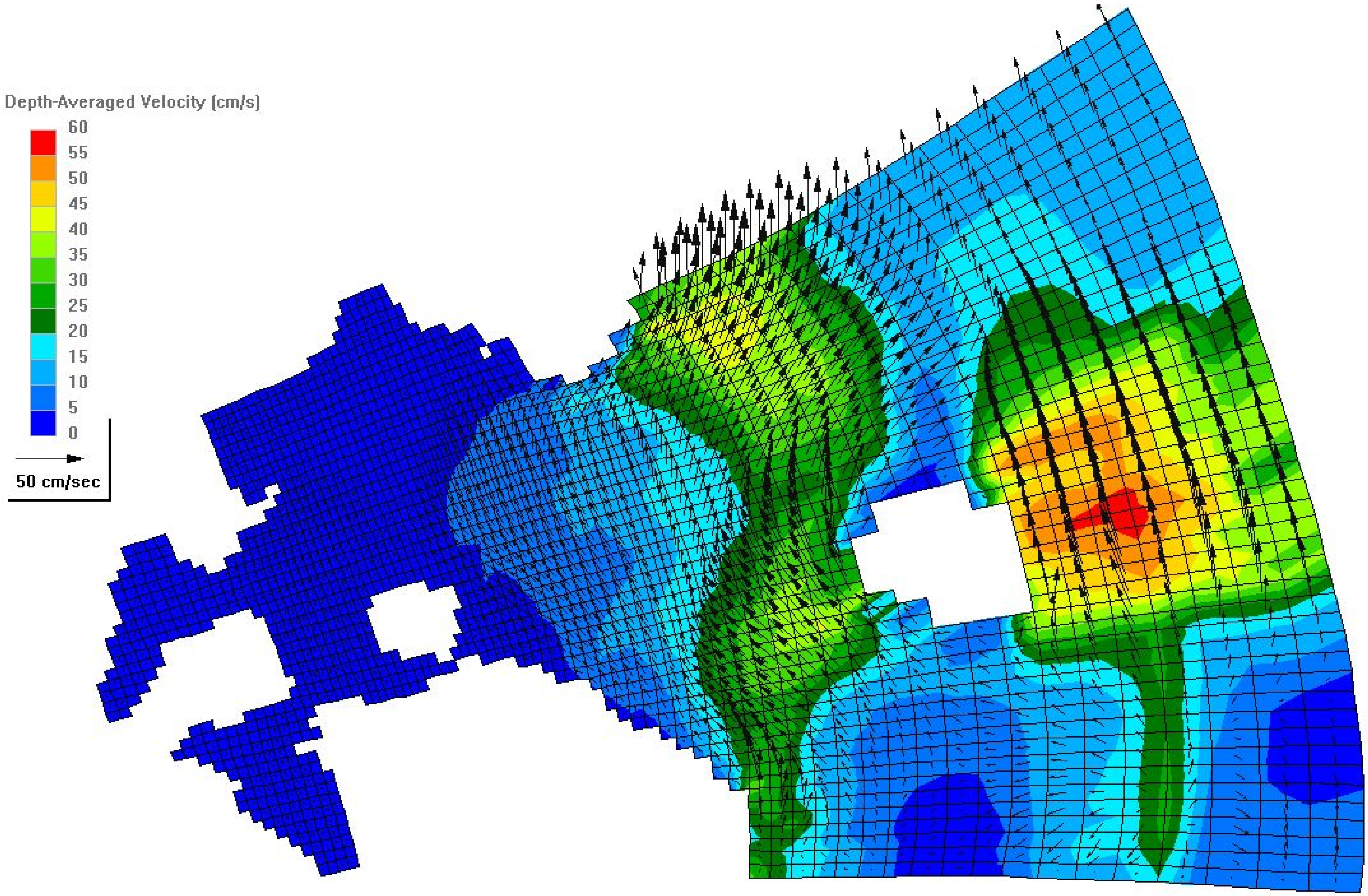

Figure 4-11 Depth-Averaged Currents on July 15, 2012 20:00 hrs

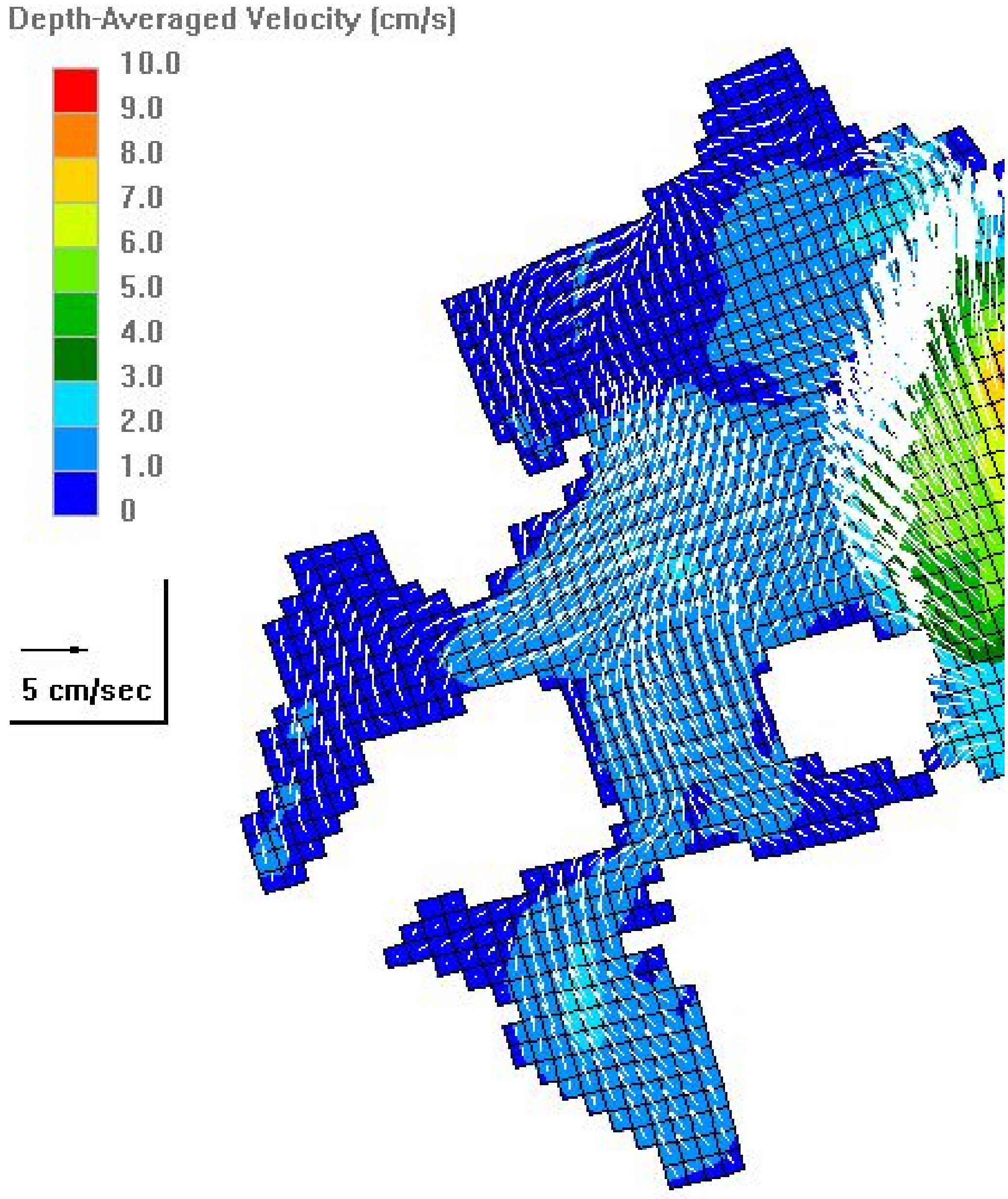

Figure 4-12 Depth-Averaged Currents in the Inner Harbour on July 15, 2012 20:00 hrs

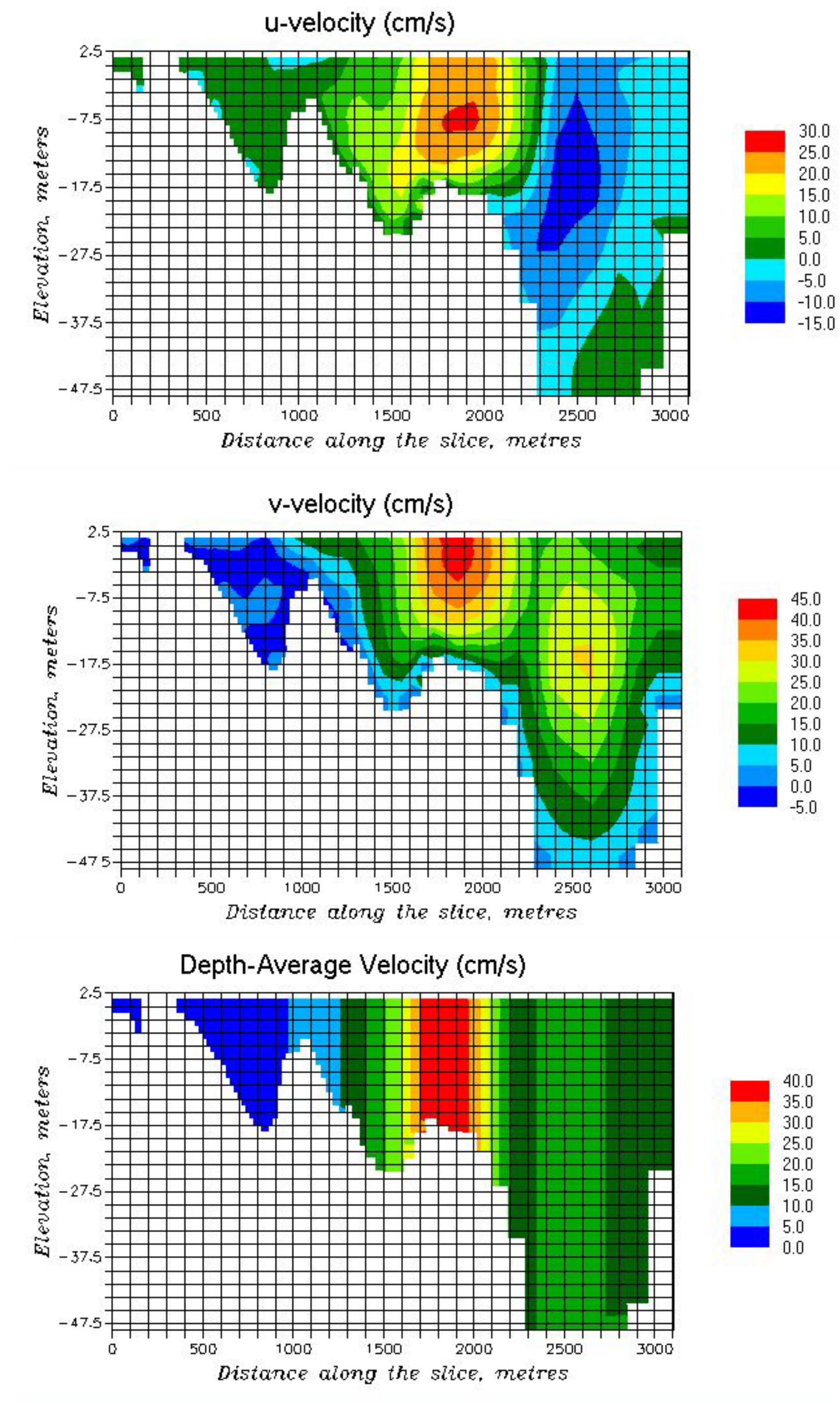

Figure 4-13 U, V and Averaged Currents at Cross Section V1 (West- East Direction)

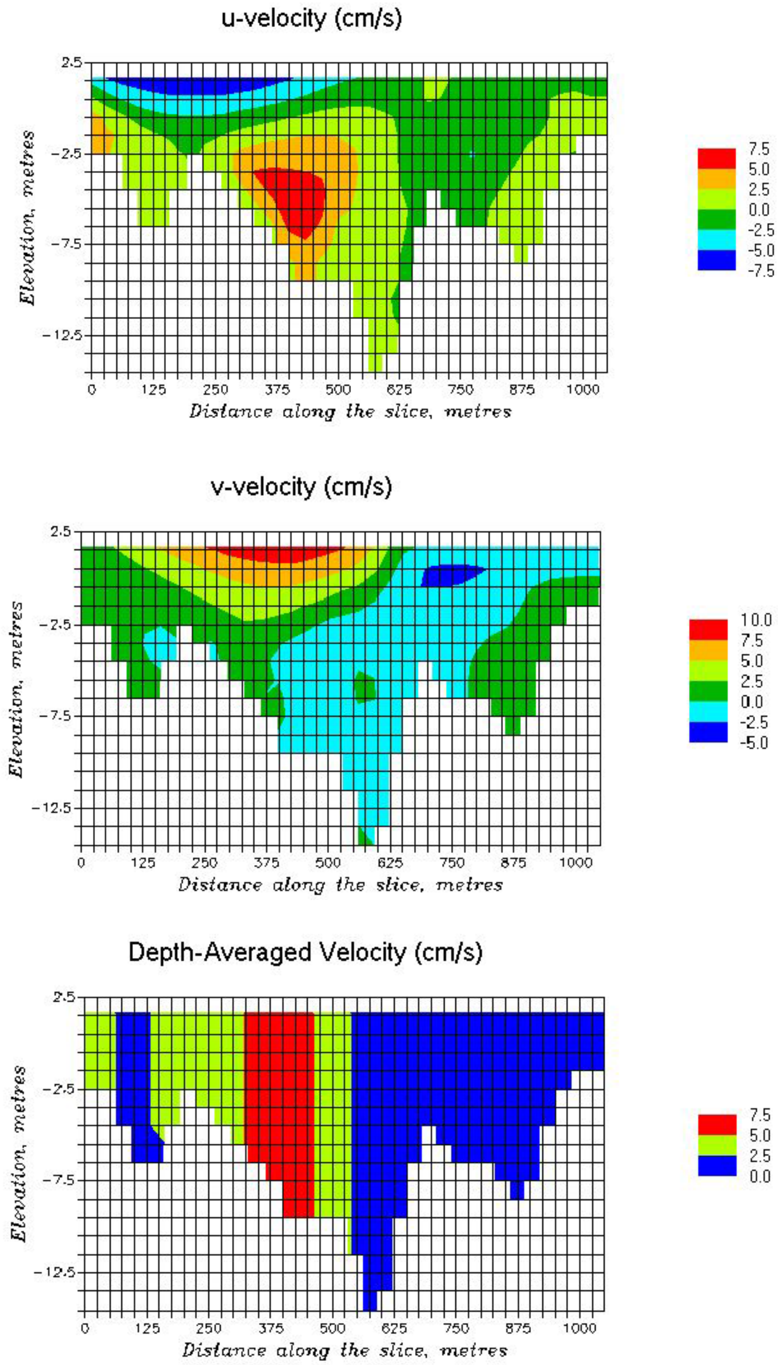

Figure 4-14 U, V and Depth-Averaged Currents at Cross Section V2 – Sill (South – North Direction)

4.2 Sediment Transport Modeling Results

Sediment transport modeling was carried out for neap, average and spring tidal conditions to estimate annual sediment transport from the harbour area. The simulation period chosen is from July 12, 2012 to July 20, 2012, which covers spring, neap and average tidal conditions as illustrated in Figure 4-1. The Hopedale Harbour area is divided into four classes (Figure 3-3) to characterize the bottom sediment conditions based on the field data. These four classes are specified in the Hopedale Harbour sediment transport model with corresponding sediment characteristics as discussed in Section 3.2.3. A 0.5 m thick bed of homogeneous sediment was applied with the sediment consisting of clay, silt, sand and gravel with compositions specified for each class (Table 3.2). The sediment transport simulations were conducted for three Hopedale Harbour sediment conditions, Scenarios 1, 2 and 3, to estimate the expected range of sediment transport from Hopedale Harbour. Scenario 1 assumes that the sediment particle sizes fall in the lower end of the range of sediment particle sizes based on field data for each sediment composition. Scenario 2 represents the median sediment particle sizes based on field data for each composition. Scenario 3 assumes that the sediment particle sizes fall in the upper end of the range of sediment particle sizes based on field data for each sediment composition. The selected sediment particle sizes for the three scenarios are presented in Table 4.1.

Scenario 2 is presented in detail in Sections 4.2.1 and 4.2.2 as it represents the actual bottom sediment characteristics based on the available field data. Scenario 1 and Scenario 3 were considered to determine the sensitivity to sediment size and present the possible range of sediment loads.

Table 4.1 Sediment Particle Sizes Used in the Sediment Transport Modeling

Sediment Conditions	Description	Particle Size (mm)			
		Clay	Silt	Sand	Gravel
Scenario 1	Fine	0.001	0.004	0.062	2.00
Scenario 2	Medium	0.002	0.016	0.300	4.00
Scenario 3	Coarse	0.005	0.062	2.00	8.00

4.2.1 Sediment Concentration (Scenario 2)

The predicted TSS concentration in Hopedale Harbour is presented in Figure 4-15 for ebb spring tide conditions (July 18, 2012 9:00 hrs). Higher TSS concentrations are observed outside the inner harbour towards the north as expected in ebb tide conditions. The tidal flows in the mouth of the harbour are from south to north during the ebb tide conditions.

Figure 4-16 shows the predicted TSS concentration in Hopedale Harbour for neap tide conditions during the high water level. The TSS concentrations are higher over the sill that separates the inner and outer harbour.

Figure 4-17 shows the predicted TSS concentration in Hopedale Harbour for flood average tide conditions (July 16, 2012, 14:00 hrs). Higher TSS concentrations are observed outside the inner harbour towards the south as expected in flood tide conditions. The tidal flows in the mouth of the harbour are from north to south during flood tide conditions.

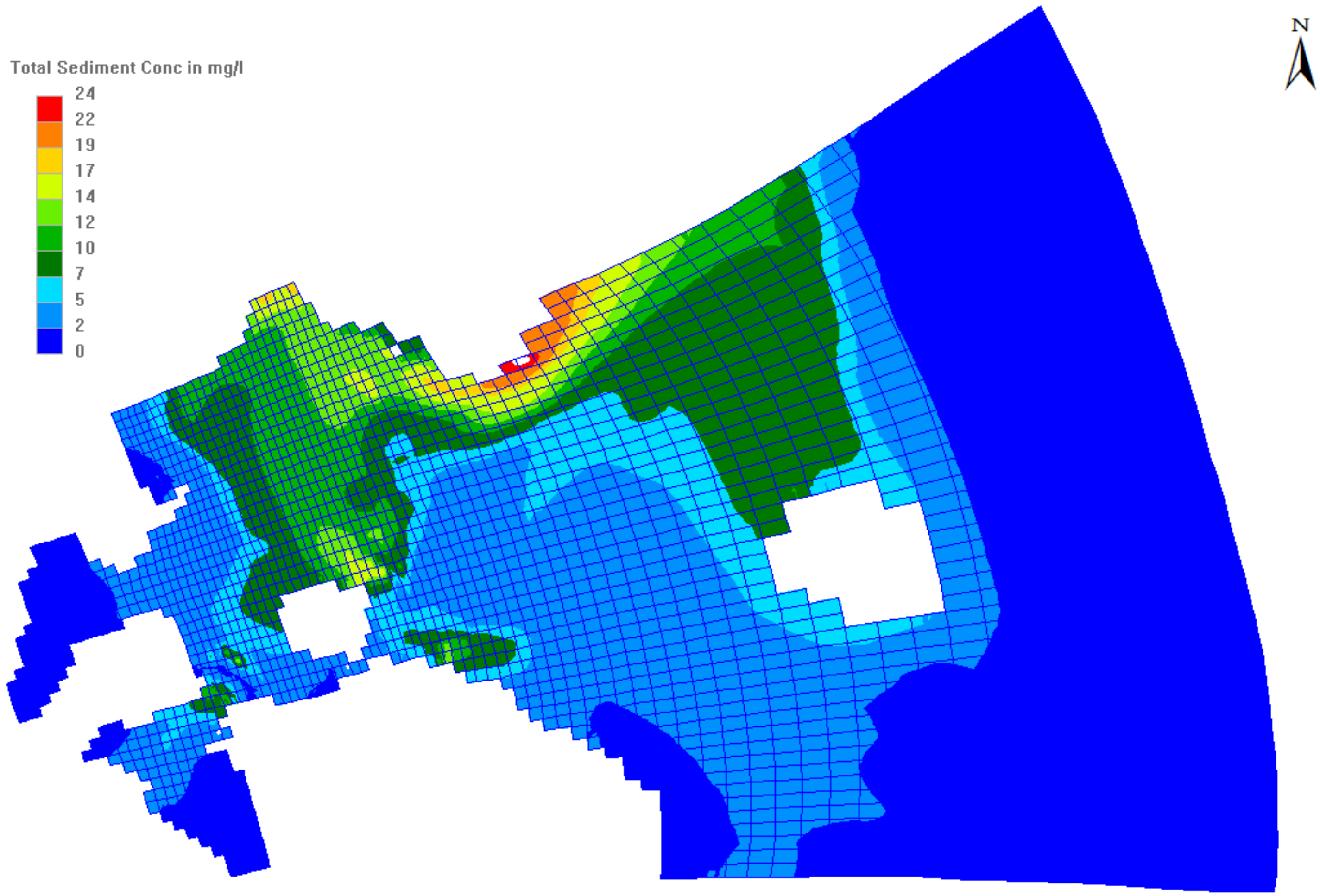

Figure 4-15 Modeled Depth-Averaged TSS Concentrations on July 18, 2012 9:00 hrs (Ebb Spring Tide)

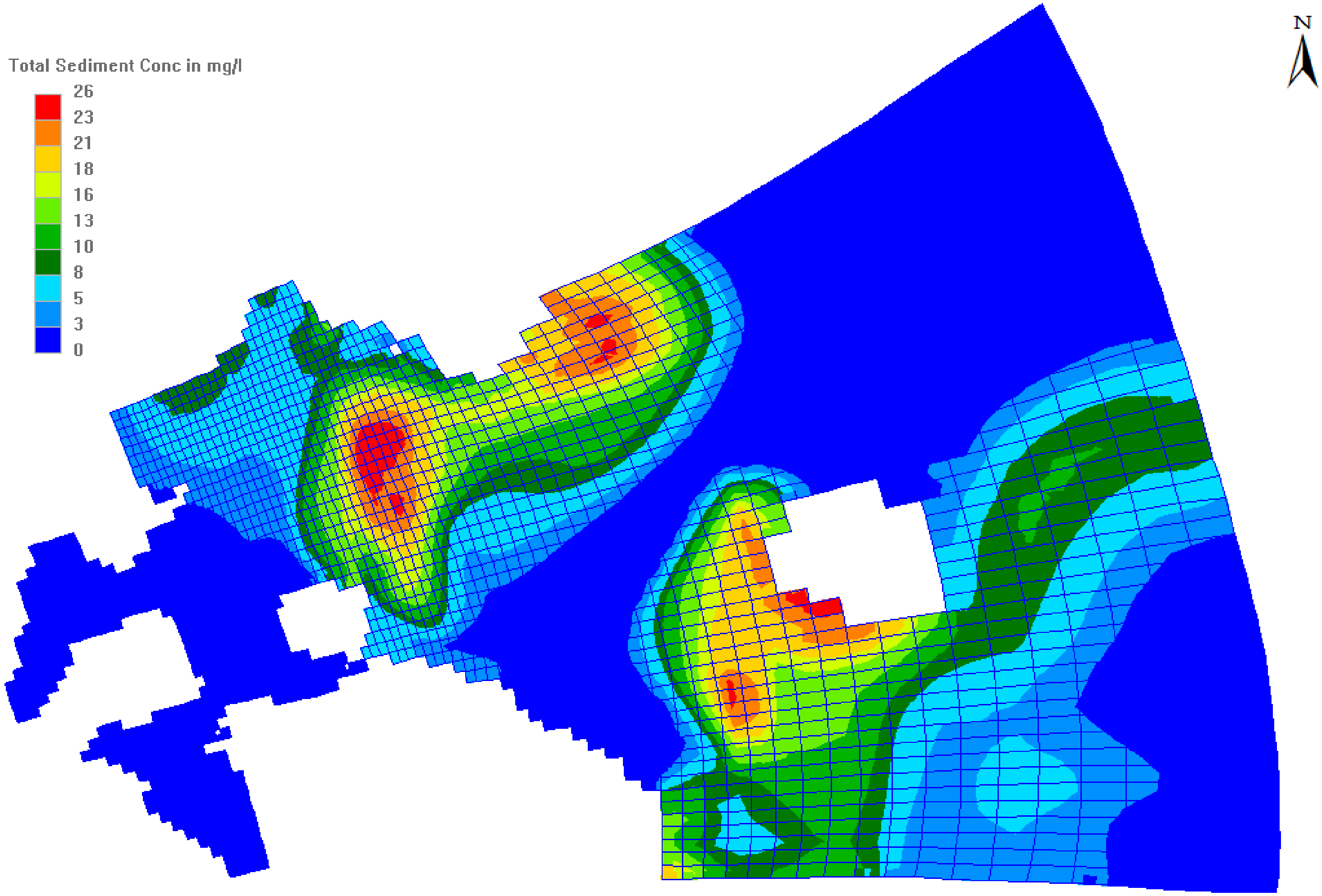

Figure 4-16 Modeled Depth-Averaged TSS Concentrations on July 13, 2012 17:00 hrs (Neap Tide at High Water Level)

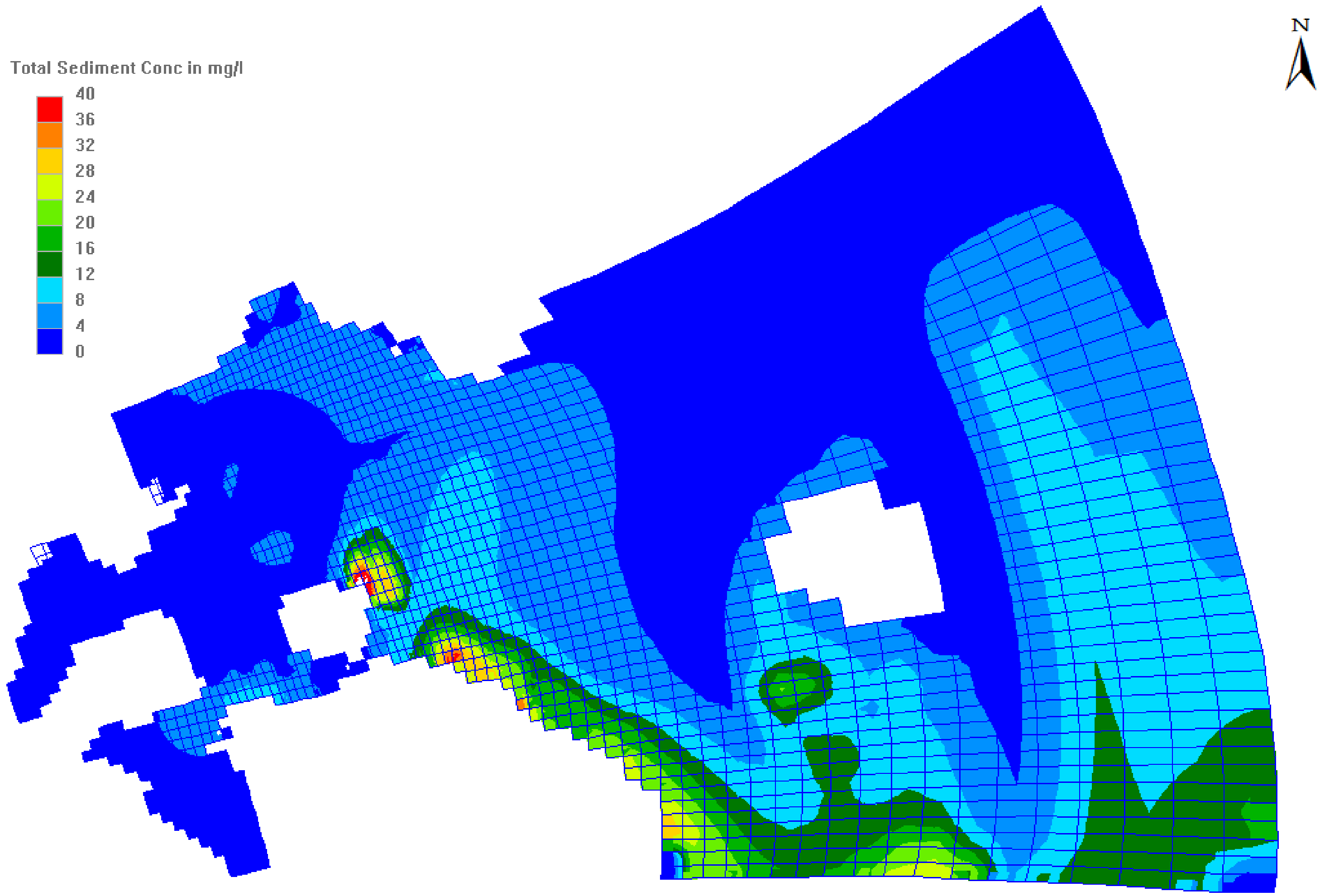

Figure 4-17 Modeled Depth-Averaged TSS Concentrations on July 16, 2012 14:00 hrs (Average Flood Tidal Conditions)

4.2.2 Sediment Flux (Scenario 2)

Sediment flux was estimated at two cross sections as shown in Figure 4-18, one at the inner harbour eastern boundary (S1) and one at the outer harbour eastern boundary (S2). The predicted silt, clay, sand, gravel and total sediment fluxes at cross section S1 over the simulation period are presented in Figures 4-19 to 4-23, respectively. The predicted silt, clay, gravel and total sediment fluxes at cross section S2 over the simulation period are presented in Figures 4-24 to Figures 4-27, respectively. Water levels in Hopedale Harbour are also superimposed in the Figures.

The predicted sediment flux at S1 indicates that the highest amount of silt is leaving from the inner harbour, followed by sand and clay. Gravel is not predicted to leave from the inner harbour. A similar sediment flux trend was observed at the outer harbour boundary except that gravel can also be transported at the outer harbour boundary, S2 due to the stronger currents.

Sediment flux and direction varies with the tidal conditions in the harbour. In addition to tidal conditions, the sediment flux will also be affected by the wind conditions in the harbour. Sediment fluxes are leaving the harbour during ebb tidal conditions and entering the harbour during the flood tide conditions as can be observed from Figures 4-19 to 4-27. Sediment flux is higher for the spring tide conditions and lower for the neap tide conditions.

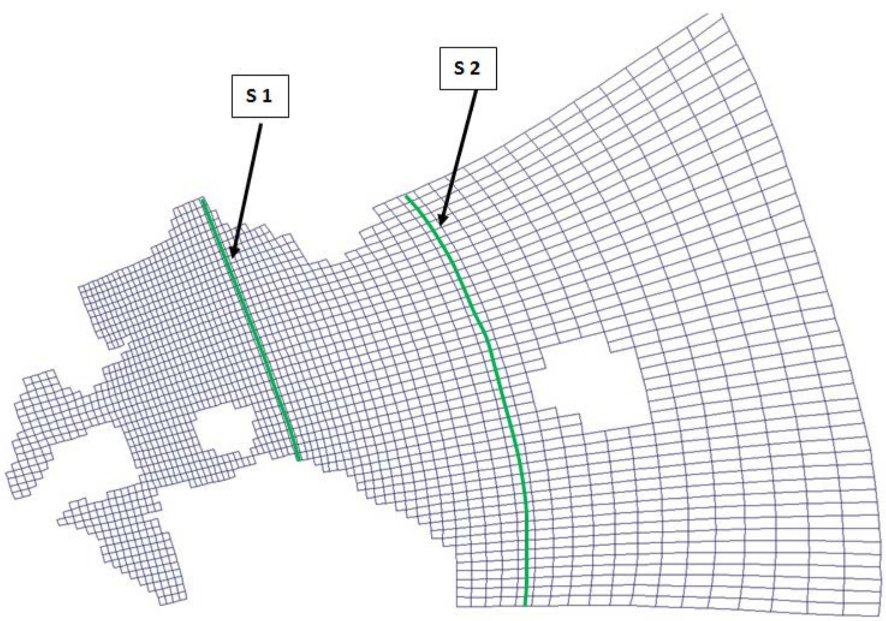

Figure 4-18 Sediment Flux Cross Sections at Inner Harbour and Outer Harbour Boundaries

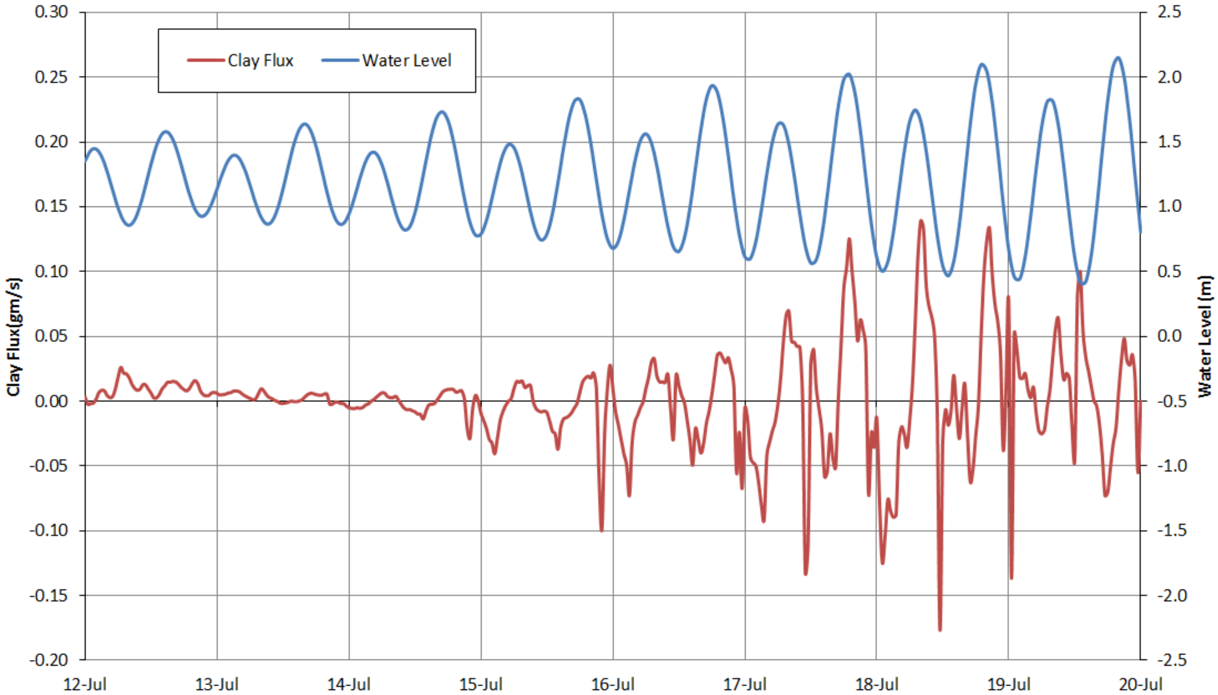

Figure 4-19 Clay Flux at S1 (Inner Harbour)

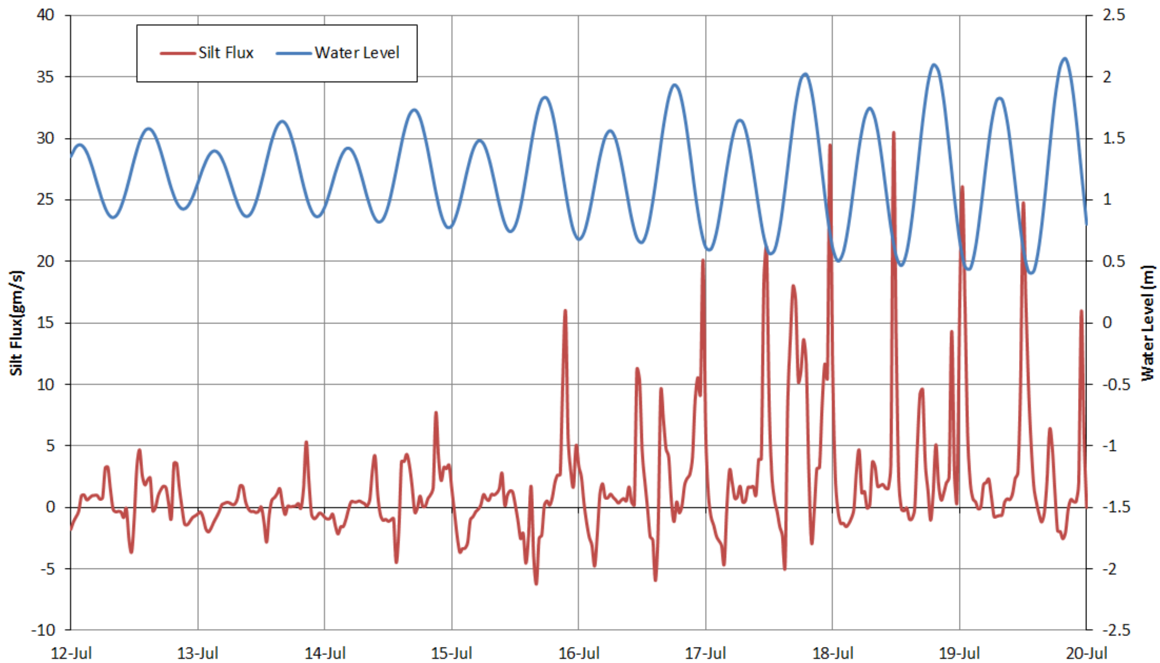

Figure 4-20 Silt Flux at S1 (Inner Harbour)

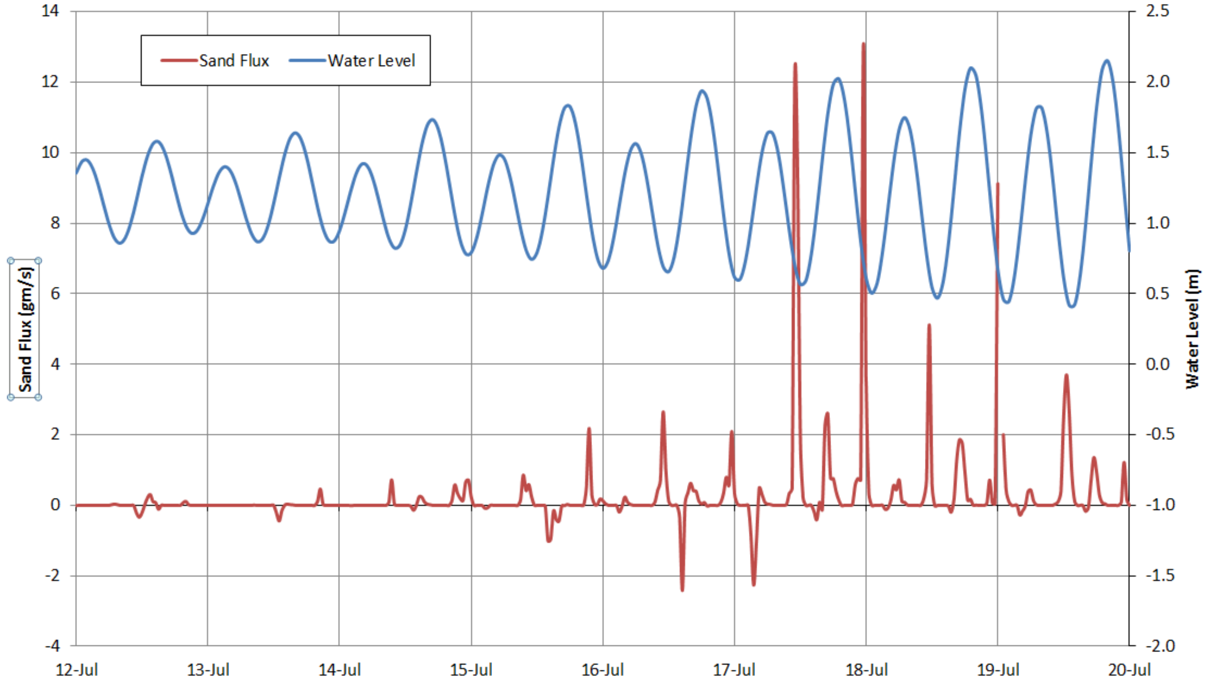

Figure 4-21 Sand Flux at S1 (Inner Harbour)

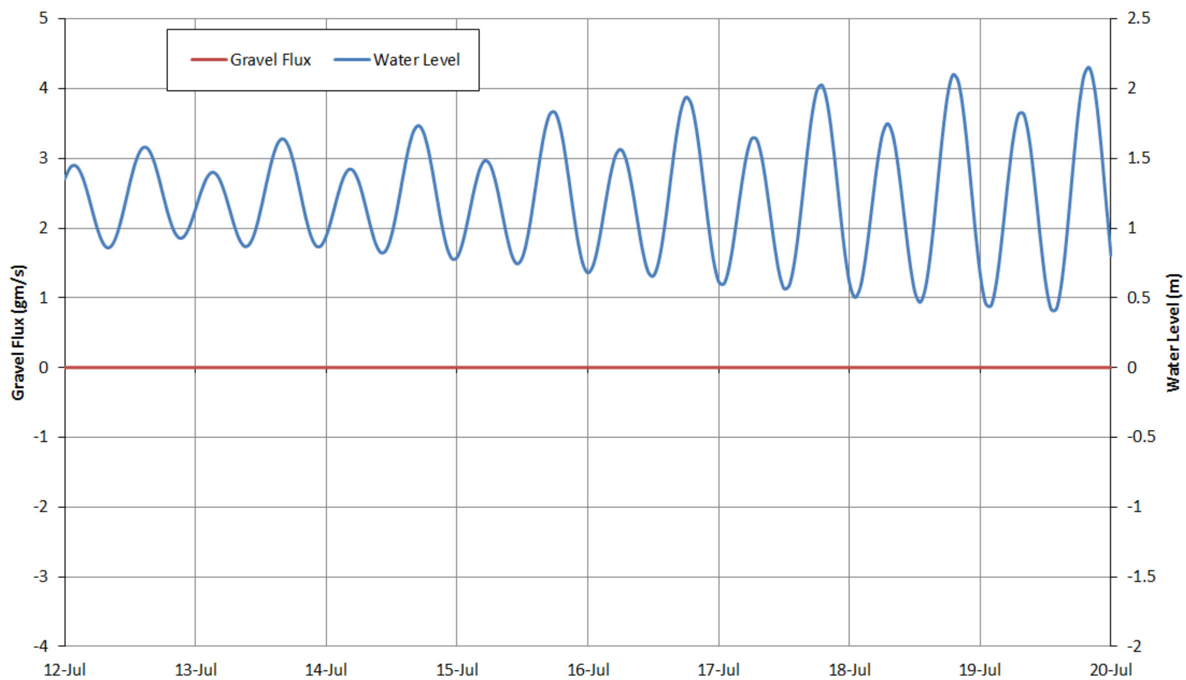

Figure 4-22 Gravel Flux at S1 (Inner Harbour)

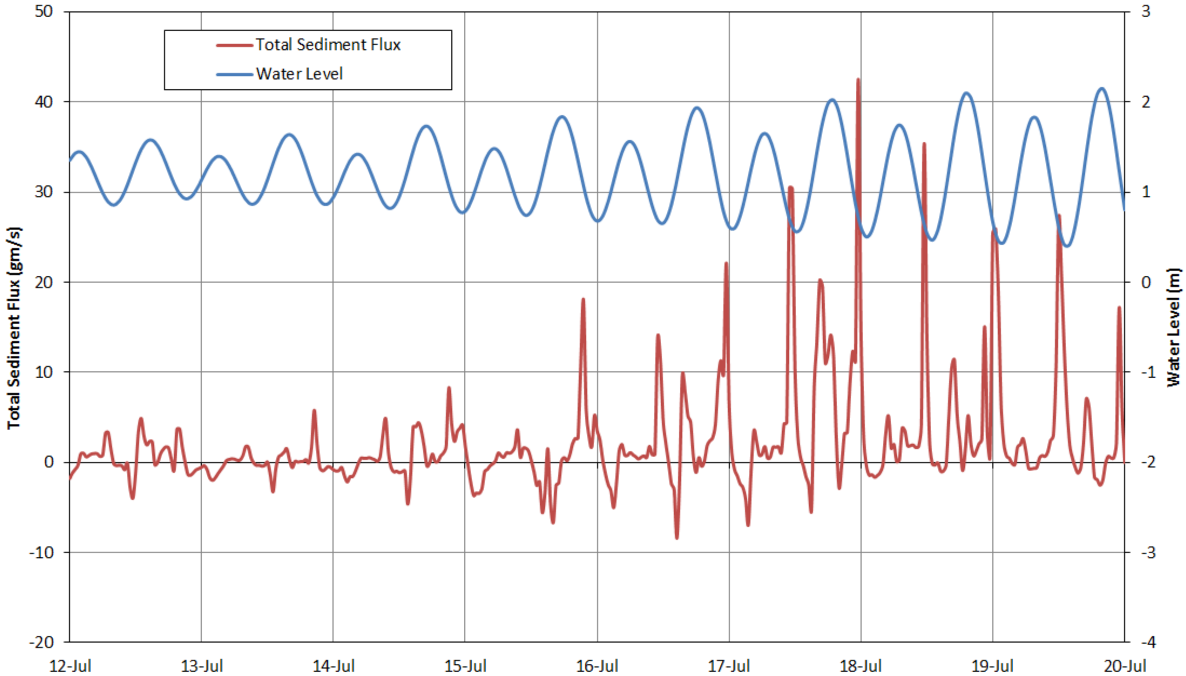

Figure 4-23 Total Sediment Flux at S1 (Inner Harbour)

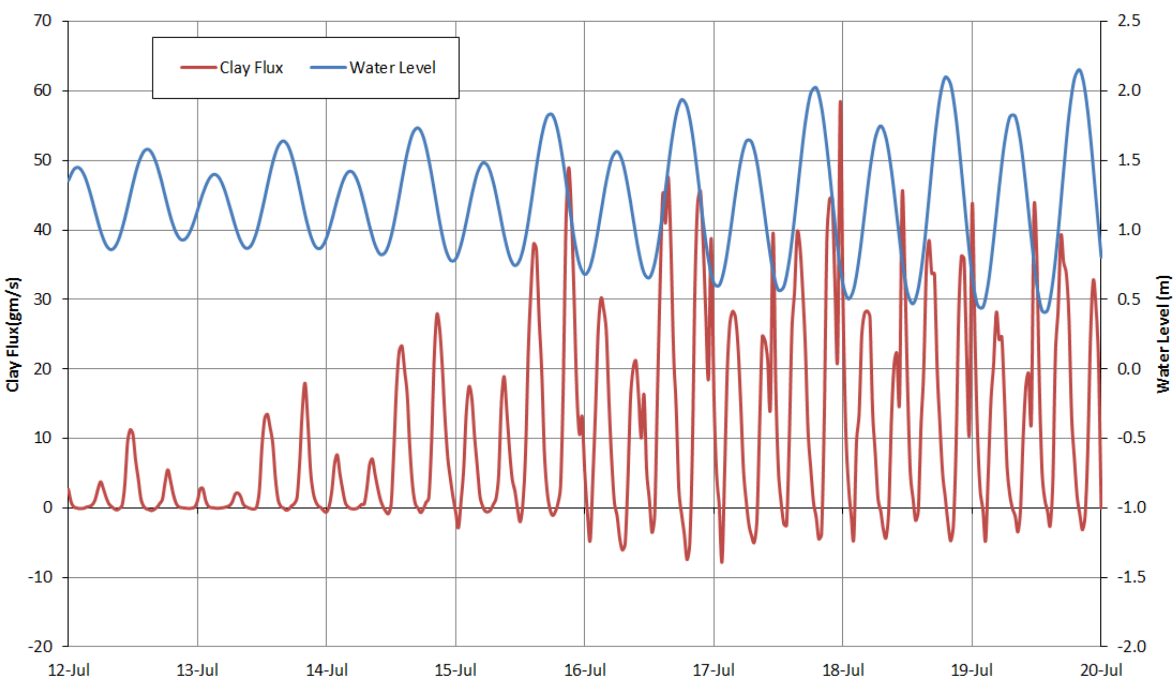

Figure 4-24 Clay Flux at S2 (Outer Harbour)

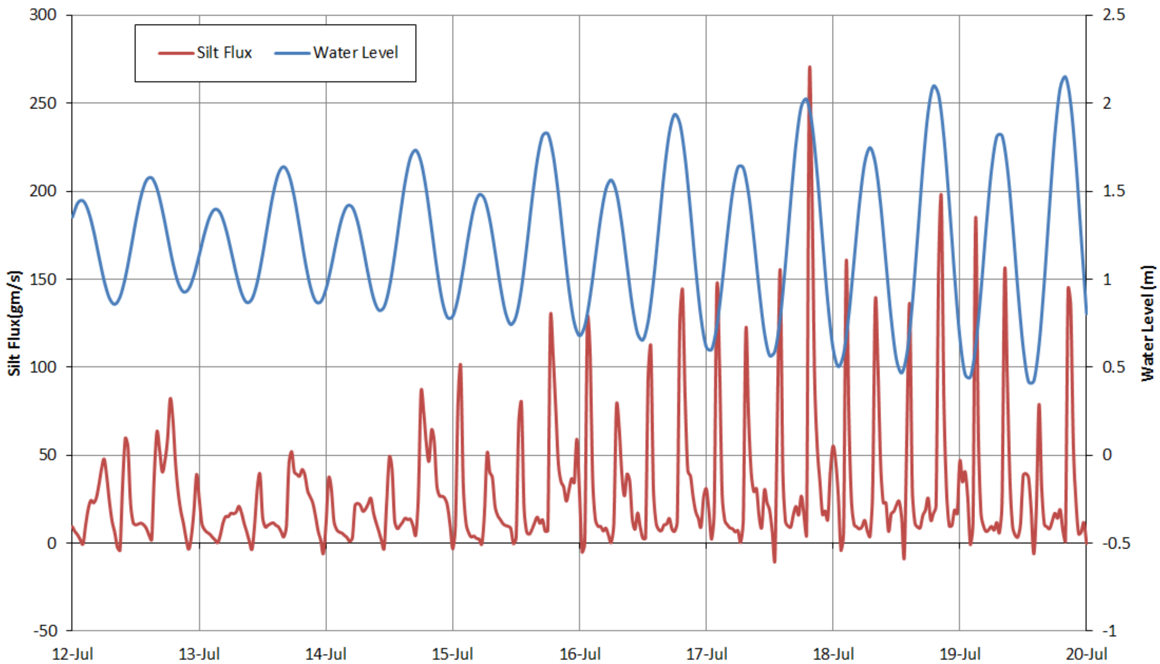

Figure 4-25 Silt Flux at S2 (Outer Harbour)

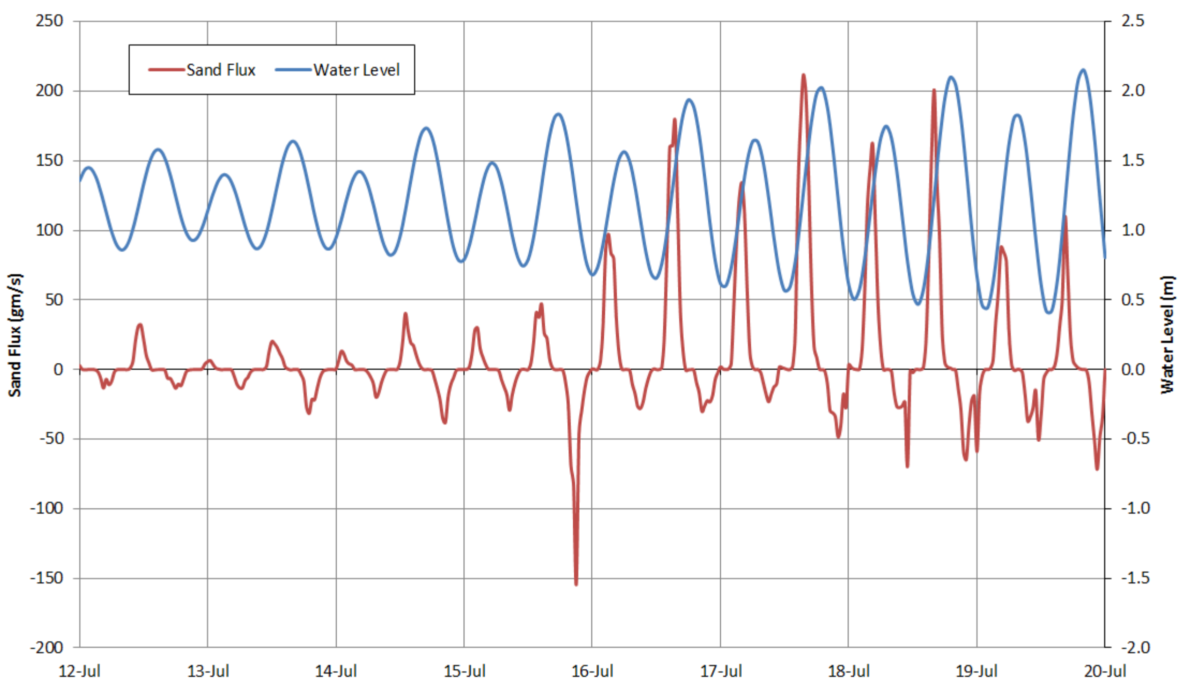

Figure 4-26 Sand Flux at S2 (Outer Harbour)

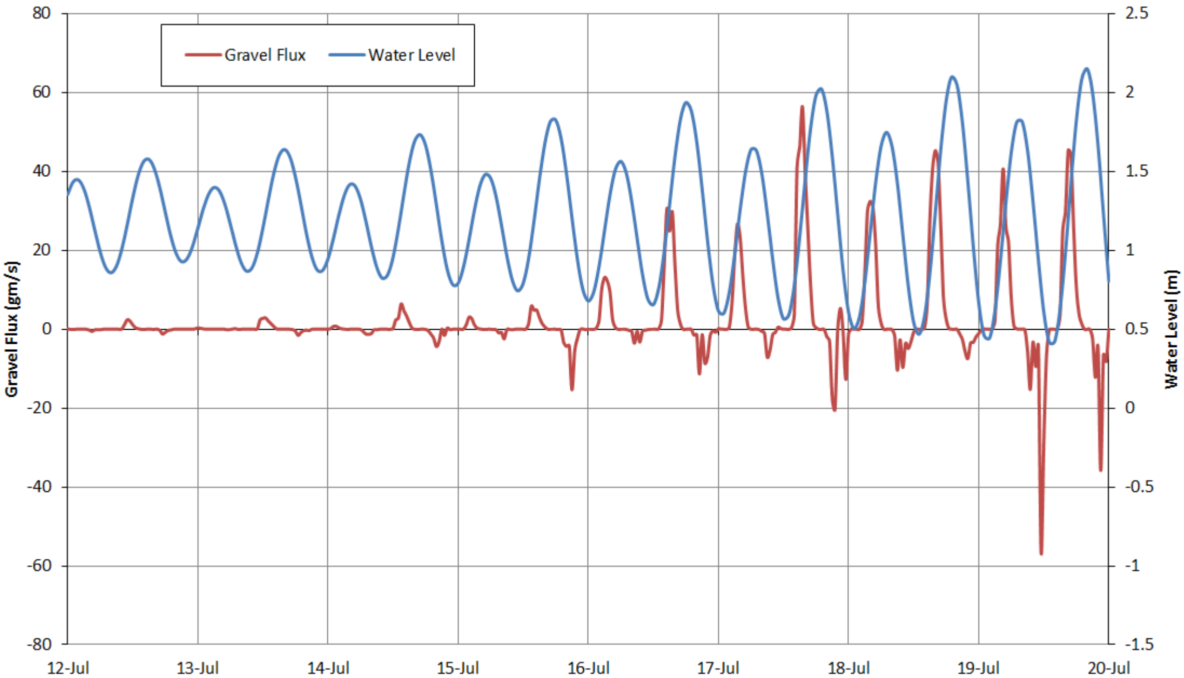

Figure 4-27 Gravel Flux at S2 (Outer Harbour)

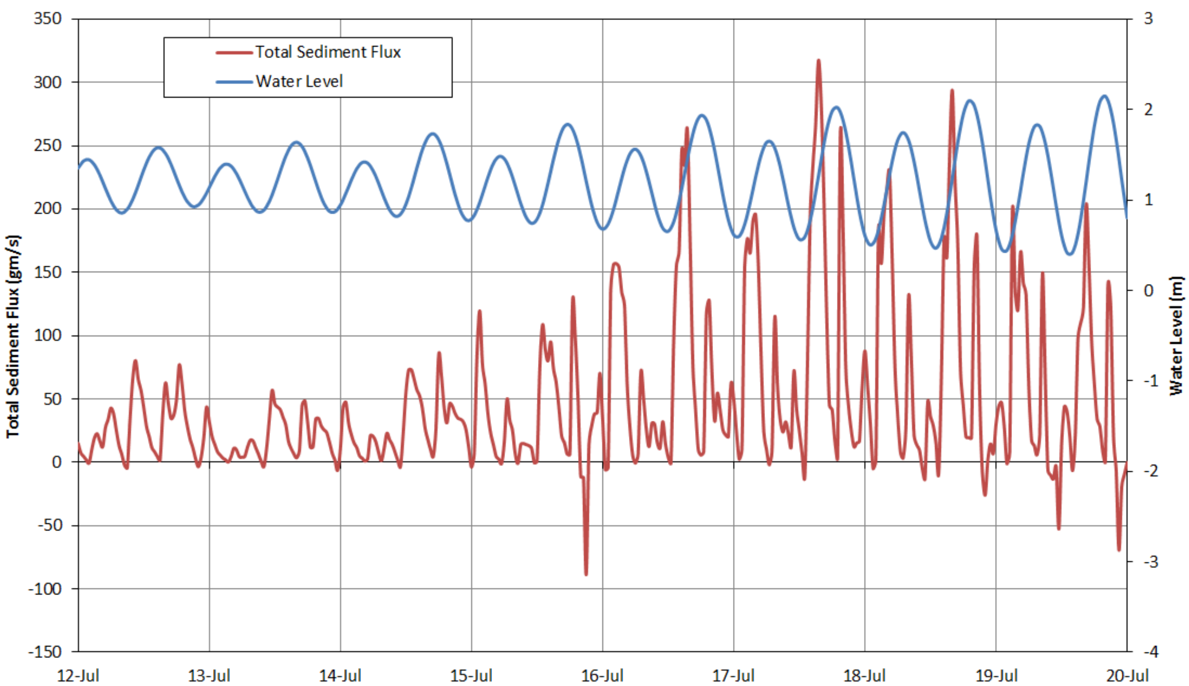

Figure 4-28 Total Sediment at S2 (Outer Harbour)

4.2.3 Sediment Load

Sediment loads leaving from the Hopedale inner and outer harbour areas were estimated for neap, average and spring tidal conditions. The time periods used to estimate the sediment loads for the neap, average and spring tidal conditions are presented in Table 4.2.

Table 4.2 Tidal Conditions

Tidal Conditions	Period			No. of Tidal Cycles
	Start	End	Total Time (hrs)	
Neap Tide	7/12/2012 9:00	7/14/2012 9:00	48	4
Average Tide	7/15/2012 12:00	7/17/2012 12:00	48	4
Spring Tide	7/17/2012 12:00	7/19/2012 12:00	48	4

Scenario 1

Predicted sediment loads transported across the cross sections S1 and S2 are presented in Tables 4.3 and 4.4 respectively for Scenario 1. The predicted total sediment load leaving from the inner harbour area is 0.270 g/sec, 2.95 g/sec and 5.54 g/sec for neap, average and spring tidal conditions respectively. The predicted total sediment load leaving from the outer harbour areas is 34.4 g/sec, 73.5 g/sec and 85.1 g/sec for neap, average and spring tidal conditions respectively. The total sediment mass leaving from inner harbour area is much smaller than the total sediment mass leaving from the Hopedale Harbour area. This is due to the significantly smaller current in the inner harbour area in comparison to the outer harbour area.

Table 4.3 Sediment Loads Leaving from Inner Harbour Area (Cross Section S1)

Sediment Constituent	Sediment Load (g/sec)		
	Neap Tide	Average Tide	Spring Tide
Clay	0.005	-0.001	0.004
Silt	0.250	2.71	5.34
Sand	0.015	0.24	0.200
Gravel	0.000	0.000	0.000
Total	**0.270**	**2.95**	**5.54**

Table 4.4 Sediment Loads Leaving from Hopedale Bay (Cross Section S2)

Sediment Constituent	Sediment Load (g/sec)		
	Neap Tide	Average Tide	Spring Tide
Clay	2.66	14.0	17.5
Silt	26.8	36.8	42.6
Sand	4.90	21.69	22.4
Gravel	0.069	1.03	2.52
Total	**34.4**	**73.5**	**85.1**

Scenario 2

Predicted sediment loads transported across the cross sections S1 and S2 are presented in Tables 4.5 and 4.6 respectively for Scenario 2. The predicted total sediment load leaving from the inner harbour area is 0.200 g/sec, 2.27 g/sec and 5.08 g/sec for neap, average and spring tidal conditions respectively. The predicted total sediment load leaving from the outer harbour areas is 22.1 g/sec, 62.6 g/sec and 78.0 g/sec for neap, average and spring tidal conditions respectively. The total sediment mass leaving from inner harbour area is much smaller than the total sediment mass leaving from the Hopedale Harbour area similar to Scenario 1.

Table 4.5 Sediment Loads Leaving from Inner Harbour Area (Cross Section S1)

Sediment Constituent	Sediment Load (g/sec)		
	Neap Tide	Average Tide	Spring Tide
Clay	0.005	-0.008	0.009
Silt	0.188	1.97	4.41
Sand	0.007	0.309	0.657
Gravel	0.000	0.000	0.000
Total	**0.200**	**2.27**	**5.08**

Table 4.6 Sediment Loads Leaving from Hopedale Bay (Cross Section S2)

Sediment Constituent	Sediment Load (g/sec)		
	Neap Tide	Average Tide	Spring Tide
Clay	2.61	15.1	15.6
Silt	20.0	33.2	39.4
Sand	-0.477	12.2	18.1
Gravel	0.013	2.07	4.89
Total	**22.1**	**62.6**	**78.0**

Scenario 3

Predicted sediment loads transported across the cross sections S1 and S2 are presented in Tables 4.7 and 4.8 respectively for Scenario 3. The predicted total sediment load leaving from the inner harbour area is 0.423 g/sec, 1.94 g/sec and 2.51 g/sec for neap, average and spring tidal conditions respectively. The predicted total sediment load leaving from the outer harbour areas is 15.8 g/sec, 26.4 g/sec and 28.7 g/sec for neap, average and spring tidal conditions respectively. The total sediment mass leaving from inner harbour area is much smaller than the total sediment mass leaving from the Hopedale Harbour area similar to Scenarios 1 and 2.

Table 4.7 Sediment Loads Leaving from Inner Harbour Area (Cross Section S1)

Sediment Constituent	Sediment Load (g/sec)		
	Neap Tide	Average Tide	Spring Tide
Clay	0.002	0.003	0.004
Silt	0.410	1.43	2.27
Sand	0.011	0.510	0.240
Gravel	0.000	0.000	0.000
Total	**0.423**	**1.94**	**2.51**

Table 4.8 Sediment Loads Leaving from Hopedale Bay (Cross Section S2)

Sediment Constituent	Sediment Load (g/sec)		
	Neap Tide	Average Tide	Spring Tide
Clay	2.42	8.35	8.07
Silt	13.1	15.0	16.1
Sand	0.230	2.50	3.28
Gravel	0.033	0.55	1.24
Total	**15.8**	**26.4**	**28.7**

4.3 Annual Sediment Transport from the Harbour

Annual sediment load leaving Hopedale Harbour was estimated using the simulation results from July 12, 2012 to July 20, 2012. The sediment flux was averaged over the period of July 12, 2012 to July 20, 2012. Annual sediment loads were estimated using the average sediment fluxes for each sediment constituent. The estimated annual sediment load leaving from the Hopedale inner harbour (at cross section S1) and the Hopedale outer harbour (at cross section S2) were presented in Tables 4.9 and 4.10, respectively.

The sediment leaving from inner harbour primarily consists of silt at about 90%. As expected, sediment loads are higher for finer bottom sediments (Scenario 1) and lower for coarser bottom sediments (Scenario 3). The predicted gravel transport is zero from the inner harbour. The predicted total annual sediment load leaving from the inner harbour ranges from 44,057 kg to 72,317 kg.

Table 4.9 Annual Sediment Loads Leaving from Inner Harbour (Cross Section S1)

Sediment Constituent	Scenario 1		Scenario 2		Scenario 3	
	Average (g/s)	Annual Load (kg/Year)	Average (g/s)	Annual Load (kg/Year)	Average (g/s)	Annual Load (kg/Year)
Clay	0.002	69	0.001	43	0.0015	48
Silt	2.14	67,593	1.93	60,747	1.18	37,176
Sand	0.18	5,667	0.274	8,641	0.217	6,834
Gravel	0.000	0.000	0.000	0.000	0.000	0.000
Total	**2.29**	**72,317**	**2.20**	**69,430**	**1.40**	**44,057**

The sediments leaving from the outer harbour consist of clay, silt, sand and gravel as outer harbour area currents are much higher than the currents in the inner harbour area. As expected, sediment loads are higher for finer bottom sediments (Scenario 1) and lower for coarser bottom sediments (Scenario 3). The predicted total annual sediment load leaving from the inner harbour ranges from 0.7 million kg to 1.8 million kg.

Table 4.10 Annual Sediment Loads Leaving from Hopedale Bay (Cross Section S2)

Sediment Constituent	Fine Sediments		Medium Sediments		Coarse Sediments	
	Average (gm/s)	Annual Load (kg/Year)	Average (gm/s)	Annual Load (kg/Year)	Average (gm/s)	Annual Load (kg/Year)
Clay	10.6	332,805	10.3	326,087	6.13	193,198
Silt	29.9	944,473	29.3	923,218	13.9	438,882
Sand	15.9	501,995	7.94	250,346	1.6	50,668
Gravel	1.01	31,987	2.12	66,706	0.6	17,734
Total	**57.4**	**1,811,260**	**49.7**	**1,566,356**	**22.2**	**700,482**

Larger sediment particles leaving the inner harbour will settle quickly, but silt and clay may not be deposited for days or months due to their smaller settling velocity and ocean turbulence. A major portion of the sediment transport from the inner harbour is silt. These fine particles are likely to remain suspended in the water and therefore most of the exported sediment load would be transported far away from Hopedale Harbour by tidal and ocean currents.

The predicted sediment loads are based on model parameters such as settling velocity, critical shear stress/velocity for erosion, characterization of bottom sediments and hydrodynamic conditions in the harbour. There are uncertainties associated with estimating settling velocities, critical shear stress/velocity for erosion, sediment characterization and modeled hydrodynamic conditions in the harbour.

Due to the number of parameters and the model run time it was necessary to be selective in conducting uncertainty analyses. No uncertainty analysis was conducted for the sediment transport modeling apart from the sediment particle sizes. Due to the lack of widespread sediment data, scenarios with fine, medium and coarse bottom sediments were run to determine the model sensitivity. For all other model parameters reasonable values were selected based on theoretical basis and previous studies.

Although there are inherent uncertainties associated with sediment transport modeling, model results have aided our understanding of the sediment transport in Hopedale Harbour. It was found that sediment transport during the neap tides is negligible and a large fraction of total sediment transport typically occurs during the spring tide conditions. In addition it was found that the majority of the sediment transported from the harbour is silt.

5.0 CONCLUSIONS

Hydrodynamic and Sediment transport modeling was conducted for Hopedale Harbour to predict the sediment transport conditions in the harbour using GEMSS® (Generalized Environmental Modeling System for Surface waters). The results from the modeling study will be used to inform future decisions about the management of PCB contamination at Hopedale. A field program was conducted to collect the field data in support of hydrodynamic and sediment transport modeling. The data was collected from August 29, 2012 to September 2, 2012. Hydrodynamic and sediment transport models were set up using harbour bathymetry data, Hopedale Airport wind data, tidal elevations predicted by Web Tide Tidal Prediction Model and bottom sediment characteristics based on field data. The wave conditions in the harbour were not considered in the modeling study and are expected to have minimal impact on the sediment transport.

The hydrodynamic model was calibrated using water level data, tilt meter current data and ADCP current data collected at various transects in the harbour. The predicted and observed water levels at the wharf agree very well. The predicted currents reasonably agree with the tilt meter current data and ADCP current data, with the exception of tilt meters TM3 and TM4 in the outer harbor area. These differences at TM3 and TM4 would not impact the predicted sediment load leaving from the Inner Harbour area.

Sediment transport conditions were assessed for spring, average and neap tide conditions. Results were used to estimate the annual sediment transport from Hopedale Harbour. The sediment loads leaving from the Hopedale inner and outer harbour areas were estimated for finer, medium and coarser sediment particle sizes. As expected, the finer bottom sediment conditions produce higher sediment loads and the coarser bottom sediment conditions produce lower sediment loads. The sediment loads leaving from the inner harbour are much smaller than the total sediment loads leaving from the outer harbour area.

Total sediment transport from inner harbour is likely to be ± 70,000 kg/year, of which most (±90%) will be silt-sized particles. These particles are likely to remain suspended in the outer harbour where current velocities are greater, and upon leaving the outer harbour will be dispersed over a larger area by the higher current fields outside the harbour.

When using the sediment transport loads presented in this report, the following limitations must be taken into consideration:

- The hydrodynamic and sediment transport modeling results are based on methods and assumptions discussed in Section 3.0, and the selected model parameters (i.e. wind drag coefficient, bottom roughness coefficient, and sediment characteristics);
- The hydrodynamic model was calibrated using data over a limited period, during the spring tide conditions;

- Harbour bottom sediment was characterized using sediment samples data from ten locations;
- A homogenous sediment thickness of 0.5 m, consisting of clay, silt, sand and gravel was assumed in the model for the harbour area;
- Annual sediment loads were estimated by extrapolating sediment transport from short-term simulation period results; and,
- Sensitivity and uncertainty analysis was conducted for sediment particle sizes.

The level of certainty required depends on the proposed use of the model results. In order to reduce the uncertainty in sediment transport prediction, it is recommended that:

- A long-term simulation be carried out to estimate the sediment loads;
- Further sensitivity and uncertainty analysis be conducted for particle settling velocity, critical shear stress/velocity for erosion and sediment thickness;
- Additional characterization of bottom sediments be conducted using an appropriate number of sediment samples to reduce the uncertainties in the modeled sediment loads;
- A harbour sediment map be developed delineating areas of fine-grained material, coarse-grained material, and hard bottom along with sediment thickness in order to refine the sediment transport model; and,

  Additional water sampling be conducted to estimate spatial TSS concentration variation and to calibrate sediment transport model.

6.0 CLOSURE

This report documents work that was performed in accordance with generally accepted professional standards at the time and location in which the services were provided. No other representations, warranties or guarantees are made concerning the accuracy or completeness of the data or conclusions contained within this report, including no assurance that this work has uncovered all potential liabilities associated with the identified property.

This report provides an evaluation of selected environmental conditions associated with the identified portion of the property that was assessed at the time the work was conducted and is based on information obtained by and/or provided to Stantec at that time. There are no assurances regarding the accuracy and completeness of this information. All information received from the client or third parties in the preparation of this report has been assumed by Stantec to be correct. Stantec assumes no responsibility for any deficiency or inaccuracy in information received from others.

The opinions in this report can only be relied upon as they relate to the condition of the portion of the identified property that was assessed at the time the work was conducted. Activities at the property subsequent to Stantec's assessment may have significantly altered the property's condition. Stantec cannot comment on other areas of the property that were not assessed.

Conclusions made within this report consist of Stantec's professional opinion as of the time of the writing of this report, and are based solely on the scope of work described in the report, the limited data available and the results of the work. They are not a certification of the property's environmental condition. This report should not be construed as legal advice.

This report has been prepared for the exclusive use of the client identified herein and any use by any third party is prohibited. Stantec assumes no responsibility for losses, damages, liabilities or claims, howsoever arising, from third party use of this report.

The locations of any utilities, buildings and structures, and property boundaries illustrated in or described within this report, if any, including pole lines, conduits, water mains, sewers and other surface or sub-surface utilities and structures are not guaranteed. Before starting work, the exact location of all such utilities and structures should be confirmed and Stantec assumes no liability for damage to them.

The conclusions are based on the site conditions encountered by Stantec at the time the work was performed at the specific testing and/or sampling locations, and conditions may vary among sampling locations. Factors such as areas of potential concern identified in previous studies, site conditions (e.g., utilities) and cost may have constrained the sampling locations used in this assessment. In addition, analysis has been carried out for only a limited number of chemical parameters, and it should not be inferred that other chemical species are not present. Due to the nature of the investigation and the limited data available, Stantec does not warrant against undiscovered environmental liabilities nor that the sampling results are indicative of the condition of the entire site. As the purpose of this report is to identify site conditions which may pose an environmental risk; the identification of non-environmental risks to structures or people on the site is beyond the scope of this assessment.

Should additional information become available which differs significantly from our understanding of conditions presented in this report, Stantec specifically disclaims any responsibility to update the conclusions in this report.

This report was prepared by Kyla Fisher, EIT., and Sundar Premasiri, Ph.D., P.Eng., and was reviewed by Sheldon Smith, MES., P.Geo.

Respectfully Submitted,

STANTEC CONSULTING LTD.

Kyla Fisher, EIT
Junior Water Resources Engineer

Sundar Premasiri, Ph.D., P.Eng.
Senior Hydrotechnical Engineer

Sheldon Smith, MES., P.Geo.
Principal, Environmental Services

7.0 REFERENCES

Aivek Stantec Limited Partnership (Stantec), 2012, Marine Study – Hopedale Harbour, Hopedale, Labrador, May 2012, Prepared for Newfoundland and Labrador, Department of Environment and Conservation.

Aivek Stantec Limited Partnership (Stantec), 2014, Freshwater and Marine Sampling in Support of the Marine Study – Years 2 and 3, Former U.S. Military Site, Hopedale, NL, April 2014, Prepared for Newfoundland and Labrador, Department and Environment and Conservation.

Edinger, J.E. and Buchak, E.M., 1980, Numerical Hydrodynamics of Estuaries in Estuarine and Wetland Processes with Emphasis on Modeling, (P.Hamilton and K.B. Macdonald, eds.), Plenum Press, New York, pp. 115-146.

Edinger, J.E. and Buchak, E.M., 1985, Numerical Waterbody Dynamics and Small Computers, Proceedings of ASCE 1985 Hydraulic Division Specialty Conference on Hydraulics and Hydrology in the Small Computer Age, Lake Buena Vista, FL.

ERM, 2006. GEMSS-HDM Hydrodynamic and Transport Module, Technical Documentation, GEMSS Development Team, Surface Water Modeling Group (SMG), ERM Inc.

ERM, 2006. GEMSS-STM Sediment Transport Module, Technical Documentation, GEMSS Development Team, Surface Water Modeling Group (SMG), ERM Inc.

ERM, 2006. User Guide – GEMSS – GridGen, GEMSS Development Team, Surface Water Modeling Group (SMG), ERM Inc.

NATECH, 2013. Presentation of Field Test Results Hopedale Harbour, NL, September 2012, Prepared for Stantec Consulting Ltd.

Okubo, A. 1971. Oceanic Diffusion Diagrams, Deep Sea Research, Vol.18, pp.789-802.

Van Rijn, L.C., 1984 a. Sediment Transport, Part I: Bed Load Transport, Journal of Hydraulic Engineering, ASCE, Vol. 110, No. 10, pp.1431-1456.

Van Rijn, L.C., 1984 b. Sediment Transport, Part II: Suspended Load Transport, Journal of Hydraulic Engineering, ASCE, Vol. 110, No. 10, pp.1613-1641.